Union College
Union | Digital Works

Honors Theses | Student Work

6-2023

Characterization of Stream Turbidity in the Catskills, New York: Insights into Environmental Controls

Christine Marie Swanson
Union College - Schenectady, NY

Follow this and additional works at: https://digitalworks.union.edu/theses

Recommended Citation

Swanson, Christine Marie, "Characterization of Stream Turbidity in the Catskills, New York: Insights into Environmental Controls" (2023). *Honors Theses*. 2747.
https://digitalworks.union.edu/theses/2747

This Open Access is brought to you for free and open access by the Student Work at Union | Digital Works. It has been accepted for inclusion in Honors Theses by an authorized administrator of Union | Digital Works. For more information, please contact digitalworks@union.edu.

Characterization of Stream Turbidity in the Catskills, New York: Insights into Environmental Controls

By

Christine M. Swanson

****

Submitted in partial fulfillment

of the requirements for Honors in the

Environmental Science, Policy, and Engineering Program

UNION COLLEGE

June, 2023

ABSTRACT

SWANSON, CHRISTINE M. Characterization of Stream Turbidity in the Catskills, New York: Insights into Environmental Controls. Environmental Science, Policy, and Engineering Program, Union College, Schenectady, New York, June 2023.

ADVISOR: Mason Stahl

Elevated turbidity poses a threat to water quality, which is especially problematic in unfiltered water supply systems such as New York City's (NYC). The Catskills Region of New York, which supplies NYC with the majority of its drinking water, is especially prone to chronically elevated turbidity due to the erosion of glacial till in Catskill streams. Here, we characterize turbidity and streamflow in the Catskills to understand the drivers of turbidity in this region. To accomplish this, we examined over a decade's worth of observed turbidity and streamflow data (2010-2022, n = 88,255) at 20 United States Geological Survey (USGS) monitoring sites. We investigated the seasonal and temporal trends in turbidity and streamflow, as well as the potential underlying causes for extreme turbidity events. Our results indicate that turbidity peaks during January through April across sites, which suggests that earlier timings of spring snow melt may contribute to elevated turbidity during these months. The turbidity baseline conditions also differ across sites, along with several sites frequently exceeding the Environmental Protection Agency (EPA) turbidity regulatory limit of 5 NTU, suggesting that certain areas of the Catskill Watershed are more susceptible to higher turbidity. Examination of extreme floods in the Catskills, such as a severe flood in December 2020 that affected the entire region, reveals that there is a characteristic process that can explain turbidity dynamics after severe flooding in this region. The December 2020 flood elevated turbidity above baseline conditions for approximately three months at several Catskill sites. There was an intermediate

flood in March 2021 that could flush the easily erodible sediment that had been deposited in the channels as a result of the first flood event. However, this intermediate flood did not produce enough energy to overwhelm the system and keep turbidity above baseline conditions. Overall, our analysis proposes potential mechanisms to explain elevated turbidity events throughout the watershed and highlights the extent of the turbidity problem in the Catskills, which has important implications for water resources management of this water supply system.

ACKNOWLEDGEMENTS

I would like to thank my thesis advisor and mentor, Dr. Mason Stahl, for his guidance and support throughout my project and during my time at Union College. I am so grateful to have had the opportunity to work with him for three years. He has fueled my passion for scientific research and taught me tremendously about the research process; I do not believe I would be the researcher and scientist I am today without his support. He has shaped my career and passion for hydrology and data analytics, which is largely why I am pursuing my PhD in Environmental Engineering at Cornell University to explore the fields of water resources management, hydrology, and systems analysis. I greatly look forward to continuing this project with him after I graduate from Union. Additionally, thank you to my lab mates, Jacob Abbott and Grace Levins, for providing me thoughtful feedback throughout various stages of my project. This research was funded by the NASA NY Space Grant; special thanks to Professor Rebecca Koopmann, NASA PI. Thank you to Union College for allowing me to conduct research for the past two summers as well.

I would also like to thank the professors who have made a significant impact on me during my time at Union, especially Dr. John Garver (Geosciences), Dr. Donald Rodbell (Geosciences), Dr. Shou-Ping Liu (Music), and Dr. Leila Khatami (Mathematics). I have learned so much from taking your classes and want to thank you all for always supporting me both inside and outside the classroom. Lastly, thank you to my friends and family for supporting me along the way. To my parents, I know you are extremely proud of how far I have come. To my friends, thank you for always being by my side and making my time at Union so special.

TABLE OF CONTENTS

1. Introduction

1.1 TURBIDITY PROBLEM BACKGROUND

High suspended sediment loads in surface waters pose threats to water quality. Characterizing surface water quality is important not only to preserve aquatic ecosystems, but also to ensure the sustainability of freshwater resources intended for human use. Stream turbidity, which is a measure of the cloudiness of water due to the light scattering from fine suspended sediments in the water column (Davies-Colley and Smith, 2001), is one parameter often examined in water quality investigations. Measuring and analyzing turbidity is important because in highly turbid waters, suspended sediments can permit the attachment of pollutants to these particles, which poses health concerns when this water is used for human consumption (Tessier, 1992). In addition to health impacts, there are several other reasons why it is important to measure turbidity. For instance, elevated turbidity affects water treatment processes, light transmission through water which affects water temperatures, among other factors (Mukundan et al., 2018). Thus, elevated turbidity levels are of high concern in water supply systems, especially when filtration treatments are not implemented (Gelda et al., 2009).

In this research, I use a case study of the Catskills Region of New York to examine the turbidity conditions in this region. The Catskills was chosen as a case study for this research because it is an important supplier of water to the 9 million residents of New York City (NYC), as the Catskill/Delaware Watersheds contribute to 90% of NYC's daily water needs (Watershed Agricultural Council, 2022). The Catskill Watershed alone contributes to approximately 40% of NYC's daily water needs, whereas the Delaware Watershed contributes the rest of the water supply (National Academies of Sciences, Engineering, and Medicine, 2020). The NYC Water

Supply System (NYCWSS), which is one of the largest unfiltered surface water supplies in the world, overall supplies NYC with approximately 1.1 billion gallons of drinking water per day; this water supply is entirely collected and transported by gravity (National Academies of Sciences, Engineering, and Medicine, 2020). The nature of the sources of turbidity in the Catskills are largely caused by the steep topography of the region, which allows for highly erodible sediments to generate turbidity (Mukundan et al., 2013). Therefore, it is important to understand where and when elevated turbidity is being generated in the Catskills system, as well as what factors (e.g., environmental or climatic) are most influential in generating turbidity. In this study, I characterize turbidity in this region and investigate which factors are most influential in generating turbidity within this water supply system. This research has important implications for better informing policy and engineering solutions with respect to protecting the sustainability of NYC's water supply system.

1.2 TURBIDITY THEORY AND MEASUREMENT

Turbidity, being dependent on the suspended sediment load in a water body, represents the optical properties of a liquid that cause light to be scattered or absorbed (rather than transmitted) by these particles in a sample (ASTM International, 2003). Thus, the greater the intensity of the light scattering, the higher the turbidity will be for a given water sample (ASTM International, 2003). However, turbidity is not an inherent property of the water; rather, it is an indicator of the environmental health of water bodies (Anderson, 2005). Thus, turbidity is not an absolute scientific quantity (Davies-Colley and Smith, 2001). Moreover, turbidity only has a relative measure of light scattering compared to arbitrary standards, meaning this parameter has

no intrinsic environmental significance unless it is calibrated to a scientific quantity, such as suspended sediment concentration (SSC) or water clarity (Davies-Colley and Smith, 2001).

To define turbidity more thoroughly, it is necessary to discuss parameters that are related to turbidity, such as light attenuation and water clarity. Light attenuation is reduced light transmission through water, and it indicates lower water clarity (Davies-Colley and Smith, 2001); however, there is a distinction between water clarity and turbidity. Water clarity is a representation of how deep in the water column light can penetrate, often measured with a Secchi disk, whereas turbidity is closely related to the suspended sediment load and characteristics (e.g., particle size and shape) of the suspended sediment load (New Jersey Sea Grant Consortium, 2014). In terms of light attenuation, total light attenuation is caused by both absorption and scattering of light (Davies-Colley and Smith, 2001). For example, there are several paths photons can take when passing through a clear container of water. Some photons may disappear in the water column as their energy is dissipated as heat, which is known as the process of absorption (Davies-Colley and Smith, 2001). Other photons may abruptly change direction in the water column, meaning photons are not absorbed, which is known as the process of scattering (Davies-Colley and Smith, 2001). However, light absorption is considered to be negligible when measuring turbidity, which differentiates light attenuation from turbidity (Kitchener et al., 2017).

Turbidity is measured through two distinct methodologies: turbidimetry and nephelometry (Kitchener et al., 2017). Turbidimetry represents the degree of light *transmission*, whereas nephelometry represents the degree of light *scattering* (Kitchener et al., 2017). As nephelometry is directly related to light scattering, nephelometry will be the methodology that will be considered when interpreting measurements of turbidity within this study. Within a water sample, nephelometers – one of the two main types of turbidimeters – detect light scattering at an

angle of 90 degrees to the incident light beam (Davies-Colley and Smith, 2001) (Figure 1). Turbidimeters, once having obtained the amount of light scattering at a specific angle, such as at 90 degrees, can then convert this light scattering to a turbidity measurement (Fondriest, 2014).

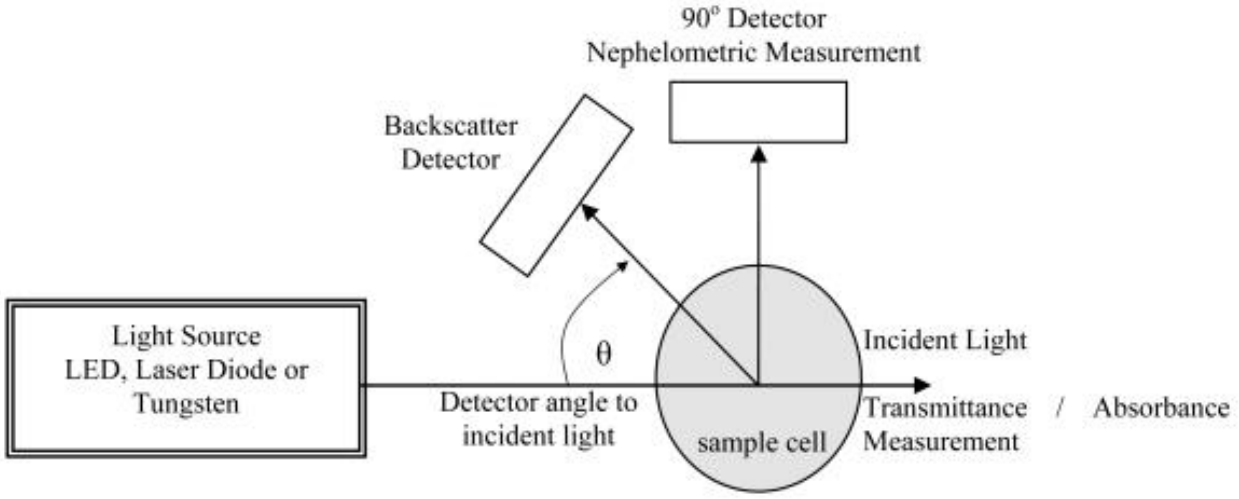

Figure 1. Techniques for measuring turbidity (Omar and MatJafri, 2009).

In surface water bodies, several factors can affect turbidity. Such factors include streamflow, precipitation and storm events, suspended and dissolved sediment load (including clay, silt, fine organic matter, plankton and other microscopic organisms, organic acids, and dyes) (ASTM International, 2003), and particle size and composition (Minnesota Pollution Control Agency, 2008). Land use change, topography, resuspension of sediments, point-source pollution, and erosional connectivity are also factors capable of affecting stream turbidity. For example, particularly after peak precipitation events, increased streamflow can affect turbidity as a result of the transport of sediments into streams from the surrounding land. The resuspension of sediment in streams can allow light to be scattered by more particles, thus increasing turbidity. Additionally, during periods of high streamflow, stream velocity increases, which can further

erode the stream bed and bank (National Academies of Sciences, Engineering, and Medicine, 2020).

In addition to outlining the factors affecting turbidity, it is also important to discuss the different applications of using turbidity data. Turbidity data can be used across a variety of contexts, including, but not limited to, regulating and monitoring the quality of drinking water, characterizing water clarity for aquatic ecosystems, determining watershed conditions, inferring other parameters of interest (such as SSC), examining the effects of land development and other anthropogenic influences, and determining contaminant transport from suspended solids (Gray and Glysson, 2003). In this study, the application of using turbidity data for monitoring the quality of drinking water is most pertinent.

1.3 PREVIOUS TURBIDITY RESEARCH

Previous studies have examined turbidity for the application of monitoring drinking water quality. LeChevallier et al. (1981) examined the relationship between turbidity and the efficiency of chlorination of drinking water at six watersheds in western Oregon. By measuring the decrease in the number of bacteria at different turbidity values and varying levels of added chlorine, they found that high-turbidity water (13 NTU) reduced the bacteria count by only 20%, whereas low-turbidity water (1.5 NTU) had undetectable levels of bacteria (LeChevallier et al., 1981). Thus, their study showed that turbidity was found to interfere with chlorine disinfection in drinking water. Their results have important implications for maintaining the water quality of surface water sources that are not filtered prior to disinfection, such as the NYCWSS. More recently, a study by Huey and Meyer (2010) used turbidity as an indicator of water quality in watersheds located in the Upper Pecos River Basin. From this study, it was determined that the

greatest threat to public health from microbial contamination in the surface waters examined in this study occurred during storm runoff events, which can result in high turbidity.

Specific to the Catskills, several studies have examined various streams and watersheds in this region for the purpose of monitoring water quality in the NYCWSS. For example, in a USGS report by McHale and Siemion (2014), SSCs and turbidity in the upper Esopus Creek watershed were measured for 2 to 3 years at 14 monitoring sites. They concluded that one site, Stony Clove Creek, had higher SSCs and turbidity than other Esopus Creek tributaries. Future research directions from this study are to develop predictive models of reservoir-turbidity input to better understand possible future reservoir conditions under different climate change regimes (McHale and Siemion, 2014). Furthermore, Wang et al. (2021) investigated the efficacy of stream sediment turbidity reduction projects (STRPs) in the Stony-Clove sub-basin of the Catskills; results suggest that reductions in SSC and turbidity in the Stony-Clove sub-basin were caused by the implementation of stream restoration best management practices (BMPs) and declining streamflow. Although several studies have been performed on specific streams and watersheds in the Catskills, from my knowledge, a synthesis of the existing turbidity data for the Catskills region has not been conducted.

1.4 RESEARCH QUESTIONS AND OBJECTIVES

The objective of this study is to perform a synthesis of the existing turbidity data in the Catskills, with the goal of answering the following research questions: (1) what are the typical turbidity and streamflow conditions in the Catskills, and how do these conditions vary across monitoring sites? (2) how does the relationship between streamflow and turbidity vary spatially and temporally in the Catskills? and (3) what factors (e.g., environmental or climatic) are the

most influential in generating turbidity in the Catskills? This study is motivated by the importance of more thoroughly understanding the turbidity conditions in the Catskills as well as the factors contributing to elevated turbidity, as there are direct broader implications with respect to the sustainability of the NYCWSS.

1.5 STUDY AREA DESCRIPTION

The entire Catskills region of New York State has a total area of 15,500 km^2, which is inclusive of the following counties: Delaware, Greene, Otsego, Schoharie, Sullivan, Ulster, and part of Albany County (Figure 2). There are three watersheds in the NYCWSS, which are the Catskill, Delaware, and Croton Watersheds (Figure 2). Specifically with reference to the Catskill system, the reservoirs within this watershed, the Ashokan and Schoharie Reservoirs, divert streamflow from the streams that are located in New York State (National Academies of Sciences, Engineering, and Medicine, 2020). The Ashokan and Schoharie Reservoirs are connected via the Shandaken Tunnel, an aqueduct that delivers Schoharie water to the Esopus Creek, which is about 11 miles upstream from the Ashokan Reservoir (McHale and Siemion, 2014) (Figure 2). The Esopus Creek supplies water to the system via the Ashokan Reservoir, and flow is diverted at the east basin of the Ashokan Reservoir by the 92-mile-long Catskill Aqueduct (National Academies of Sciences, Engineering, and Medicine, 2020). Then, the water in the Catskill Aqueduct flows to the Kensico Reservoir in Westchester County, which can then finally enter the Hillview Reservoir in Yonkers to reach the city tunnels located in NYC (National Academies of Sciences, Engineering, and Medicine, 2020) (Figure 2).

Figure 2. Map of the New York City Water Supply System (NYCWSS) (NYC DEP, n.d.).

In addition to presenting how the current NYCWSS operates, it is useful to understand how the NYCWSS began operations and when the Catskills started being used for NYC's water supply. In 1677, the first public well was constructed for Manhattan residents (National Academies of Sciences, Engineering, and Medicine, 2020). But, as population growth accelerated in the 1800s, Manhattan could no longer supply its residents with clean, sufficient water; therefore, in 1834, New York State permitted NYC to expand its water supply outside of the city itself (National Academies of Sciences, Engineering, and Medicine, 2020). The Catskills was chosen to be used for NYC's water supply because it was estimated to be able to supply two and a half times more water than currently available from other sources (as of 1909), according to Engineer Albert Flinn (National Academies of Sciences, Engineering, and Medicine, 2020). As of 1915, the first key components of the Catskill system were constructed, including the Ashokan, Kensico, and Hillview Reservoirs, as well as the Catskill Aqueduct (National Academies of Sciences, Engineering, and Medicine, 2020). The Shandaken Tunnel was put into service in 1928, which led to the completion of the Catskill system during the same year (National Academies of Sciences, Engineering, and Medicine, 2020).

1.6 PROBLEM BACKGROUND IN THE CATSKILLS

Considering that the Catskill/Delaware system, also known as the West-of-the-Hudson (WOH) System, is one of the largest unfiltered surface water supplies in the world (National Academies of Sciences, Engineering, and Medicine, 2020), it is imperative to ensure that the highest quality water possible is being delivered to NYC. Motivating the turbidity problem in the Catskills is that high turbidity episodes in streams are episodic due to extreme streamflow events, which is problematic with respect to maintaining a long-term supply of high quality water for the

NYCWSS (Mukundan et al., 2018). Furthermore, during severe storm events, erosion can lead to excessive turbidity in the Ashokan Reservoir (Riverkeeper, 2022) (Figure 2). Elevated turbidity in the Ashokan Reservoir is especially problematic for communities along the Lower Esopus Creek (which flows from the Ashokan Reservoir to the Hudson River) who receive this turbid water from the reservoir (Riverkeeper, 2022) (Figure 2). Therefore, understanding the turbidity conditions in the Catskills is crucial towards maintaining the water quality of the NYCWSS and protecting downstream communities.

For this study, characterizing turbidity will also be useful for watershed management to better understand the current turbidity conditions in the Catskills, which may provide valuable insights toward efforts to ultimately predict turbidity in this region. Further motivating the turbidity problem in the Catskills, turbidity is a key water quality parameter of interest for the NYCWSS because (1) there is a low regulatory limit for turbidity in streams established by the EPA (5 NTU), (2) the nature of the sources of turbidity in the Catskills, and (3) uncertainty surrounding the resilience of restored stream reaches due to extreme storm events (National Academies of Sciences, Engineering, and Medicine, 2020). From a regulatory standpoint, analyzing turbidity in the Catskills is important in order to remain in compliance with the Safe Drinking Water Act (SDWA) for monitoring NYC's water supply, as well as two State Pollutant Discharge Elimination Systems (SPDES) permits (Cornell Cooperative Extension of Ulster County, 2007). Although the details on the regulation of water quality in the Catskills system will not be discussed in this study, broadly speaking, the SDWA for monitoring NYC's water supply is concerned with the levels of turbidity entering the public water supply system, and the SPDES permits are concerned with monitoring limits on turbidity and other water quality

parameters entering the Esopus Creek from the Shandaken Tunnel (Cornell Cooperative Extension of Ulster County, 2007).

Next, it is important to provide a brief overview of the areas in the Catskill system that are considered to be the most susceptible towards generating turbidity. Within the Catskill/Delaware system, the Catskill Watershed is the primary contributor to turbidity in the NYCWSS (Cornell Cooperative Extension of Ulster County, 2007). Specifically in the Catskill Watershed, streams located in the eastern Catskills are generally more susceptible to high turbidity due to the input of suspended sediment during and following flood events (NYCDEP, 2019). However, due to stream remediation that was conducted in certain stream reaches, especially in the northeastern Catskills, this has led to decreased turbidity in some of these remediated areas (National Academies of Sciences, Engineering, and Medicine, 2020). Furthermore, the areas that drain to the Ashokan Reservoir tend to be associated with the highest turbidity in the system (National Academies of Sciences, Engineering, and Medicine, 2020). This is because the turbidity of the water that enters the Ashokan Reservoir is dependent on both the streamflow and turbidity that comes from the Shandaken Tunnel as well as the Esopus Creek (Figure 2). The Ashokan Reservoir has a settling basin to allow for sediments to settle from within the water column (McHale and Siemion, 2014), which further highlights the issue of elevated turbidity that exists in certain areas of the Catskills.

1.7 GEOLOGY, HYDROLOGY, AND LAND USE OF THE CATSKILLS

Understanding the multitude of factors that can affect stream water quality in the Catskills is important in order to better manage the water supply system. These factors include the geology, hydrology, and land use and land cover of the watershed. In the Catskills, the

geology is the main factor controlling water quality (Cornell Cooperative Extension of Ulster County, 2007). The advance of glaciers over this region during the Pleistocene left behind glacial till (Titus, 1996). The composition of the glacial till is primarily clay and silt from eroded bedrock; as the glacial-ice melted, fine sediments in the meltwater were deposited into pro-glacial lakes (Mukundan et al., 2013). Although the bedrock of the Catskills, being Devonian-aged fluvial sedimentary bedrock (Wang et al., 2021), generally provides high water quality due to its filtration capacity, the geology of the region can also frequently degrade the water quality (Cornell Cooperative Extension of Ulster County, 2007). Specifically, the Pleistocene clay and silt deposits are the main sources of turbidity in streams in the Catskills because during high streamflow events, the stream erodes the fine glacial deposits into the water (thus, mobilizing the deposits), which contributes to the generation of turbidity due to the input of suspended sediment into streams (Mukundan et al., 2018) (Figure 3).

Figure 3. Exposure of glacial till at the stream bank of Fox Hollow. The water is highly turbid due to contact with glacial till (Cornell Cooperative Extension of Ulster County, 2007).

The hydrology and climate of the Catskills are also necessary to consider to better understand how the region may be affected by flood events in the future, which has direct implications on water quality. The climate of the Catskills is characterized by cool summers and cold winters. The lowest amount of precipitation occurs in the northern and western parts of the Catskills; specifically, the total annual precipitation is related to the elevation (National Academies of Sciences, Engineering, and Medicine, 2020). The valleys have an annual median precipitation of ~1,100 - 1,200 mm and mountaintops have an annual median of ~1,500 mm (most falling as snow) in this region (National Academies of Sciences, Engineering, and Medicine, 2020). Overall, both the climate and hydrology of the Catskills are variable, which motivates the importance of having well-informed operations for the NYCWSS (National Academies of Sciences, Engineering, and Medicine, 2020). The need for well-informed operations of the system will especially be important due to the already observed effects of climate change on hydrologic regimes throughout the world. Specifically in the Catskills, these effects have already been recorded – over the past 50 years, there have been increasing trends in mean annual precipitation and streamflow in the region (Burns et al., 2007).

Land use and land cover are factors that are also important to consider when characterizing water quality in the Catskills because they can affect the stability of streams, which has the potential to affect water quality. Although settlement of the Catskills during the 1700s and 1800s was largely associated with agriculture and land clearing, the Catskill Park was established in 1904 to preserve the forested lands (Cornell Cooperative Extension of Ulster County, 2007). Most of the hill-slope land that was cleared for agriculture has grown back as forest, although the agricultural land use today is focused in the valley bottoms (Nagle et al., 2007). Today, forested land is the dominant land cover in the Catskills. From a GIS analysis

using the National Land Cover Database (NLCD) for the Catskill/Delaware Watersheds to characterize land cover from 2001 to 2016, the top three land cover categories in the Catskills were deciduous forests, mixed forests, and hay/pasture (National Academies of Sciences, Engineering, and Medicine, 2020). As of 2001, the Catskill/Delaware Watersheds were approximately 85% forested (McHale et al., 2020). Developed land accounted for roughly 4% of the land cover in the Catskills as of 2016 (National Academies of Sciences, Engineering, and Medicine, 2020). Thus, from the analysis conducted in 2001 to 2016, changes in land use and land cover from forest, farmland, and developed areas in the Catskill/Delaware Watersheds have not been substantial; in fact, these changes have been one-tenth the average change for the entirety of New York State (National Academies of Sciences, Engineering, and Medicine, 2020).

1.8 THESIS OVERVIEW

This thesis is structured as follows. In Chapter 2, I will provide a general overview of the factors and mobilization processes that can contribute to turbidity generation, and then apply this conceptual framework to a few examples in the Catskills. In Chapter 3, I will characterize turbidity and streamflow in the Catskills across 20 monitoring sites, most of which are located above the Ashokan Reservoir. This chapter will not only involve a characterization of streamflow and turbidity across monitoring sites but will also include the examination of seasonal trends in turbidity and streamflow, the streamflow-turbidity relationship across sites, and spatial and temporal variability in turbidity and streamflow. In Chapter 4, I will summarize the key results from this research and outline plans for future work, including the development of a predictive model to understand the key drivers of turbidity in the Catskills.

1.9 References

Anderson, C.W., 2005, Turbidity: v. 1, p. 699–704, doi:10.1016/B978-012370626-3.00075-2.

ASTM International., 2003, D1889–00 Standard test method for turbidity of water, in ASTM International, Annual Book of ASTM Standards, sec. 11.01: West Conshohocken, Pa., p. 6.

Burns, D.A., Klaus, J., and McHale, M.R., 2007, Recent climate trends and implications for water resources in the Catskill Mountain region, New York, USA: Journal of Hydrology, v. 336, p. 155–170, doi:10.1016/J.JHYDROL.2006.12.019.

Cornell Cooperative Extension of Ulster County, 2007, UPPER ESOPUS CREEK MANAGEMENT PLAN Volume III Watershed and Stream Characterization: v. III, p. 225.

Davies-Colley, R.J., and Smith, D.G., 2001, Turbidity, Suspended Sediment, and Water Clarity: A Review: Journal of the American Water Resources Association, v. 37, p. 1085–1101.

Fondriest Environmental, Inc., 2014, Measuring Turbidity, TSS, and Water Clarity. Fundamentals of Environmental Measurements. Web. https://www.fondriest.com/environmental-measurements/measurements/measuring-water-quality/turbidity-sensors-meters-and-methods/ (August 3, 2022).

Gelda, R.K., Effler, S.W., Peng, F., Owens, E.M., and Pierson, D.C., 2009, Turbidity Model for Ashokan Reservoir, New York: Case Study: Journal of Environmental Engineering, v. 135, p. 885–895.

Gray, J. R., & Glysson, G. D., 2003, Synopsis of outcomes from the federal interagency workshop on turbidity and other sediment surrogates. In *Virginia Water Research Symposium 2003*, p. 37.

Huey, G.M., and Meyer, M.L., 2010, Turbidity as an Indicator of Water Quality in Diverse Watersheds of the Upper Pecos River Basin: Water, v. 2, p. 273–284,

doi:10.3390/w2020273.

Kitchener, B.G.B.; Wainwright, J.;Parsons, A.J., 2017, A review of the principles of turbidity measurement: Progress in physical geography, v. 41, p. 620–642.

Lechevallier, M.W., Evans, T.M., and Seidler, R.J., 1981, Effect of Turbidity on Chlorination Efficiency and Bacterial Persistence in Drinking Water: Applied and environmental microbiology, v. 42, p. 159–167.

McHale, M.R., and Siemion, J., 2014, Turbidity and Suspended Sediment in the Upper Esopus Creek Watershed, Ulster County, New York: US Department of the Interior, US Geological Survey, p. 1–42.

McHale, M.R., Siemion, J., and Murdoch, P.S., 2020, The Water Quality of Selected Streams in the Catskill and Delaware Water-Supply Watersheds in New York: US Geological Survey, p. 1999–2009.

Minnesota Pollution Control Agency., 2008, Turbidity: Description, Impact on Water Quality, Sources, Measures – A General Overview. https://www.pca.state.mn.us/sites/default/files/wq-iw3-21.pdf (August 3, 2022).

Mukundan, R., Pierson, D.C., Wang, L., Matonse, A.H., Samal, N.R., Zion, M.S., and Schneiderman, E.M., 2013, Effect of projected changes in winter streamflow on stream turbidity, Esopus Creek watershed in New York, USA: Hydrological Processes, v. 27, p. 3014–3023, doi:10.1002/hyp.9824.

Mukundan, R., Scheerer, M., Gelda, R.K., and Owens, E.M., 2018, Probabilistic Estimation of Stream Turbidity and Application under Climate Change Scenarios: Journal of Environmental Quality, v. 47, p. 1522-1529, doi:10.2134/jeq2018.06.0229.

Nagle, Gregory; Fahey, Timothy; Ritchie, Jerry; Woodbury, P., 2007, Variations in Sediment

Sources and Yields in the Finger Lakes and Catskills Regions of New York: Hydrological Processes, v. 21, p. 828–838, doi:10.1002/hyp.

National Academies of Sciences Engineering and Medicine, 2020, Review of the New York City Watershed Protection Program (2020): Washington, DC, The National Academies Press, 1–401 p., doi:10.17226/25851.

New Jersey Sea Grant Consortium., 2014, Clarity and Turbidity. http://www.njseagrant.org/wp-content/uploads/2014/03/clarity_and_turbidity.pdf (August 3, 2022).

NYC DEP, 2019, Upper Esopus Creek watershed turbidity/suspended-sediment monitoring study: Biennial Status Report.

New York City Department of Environmental Protection, [n.d.], New York City water supply system: New York State Department of Environmental Conservation Web page, accessed August 5, 2022, at https://www.dec.ny.gov/lands/53884.html.

Omar, A.F. Bin, and MatJafri, M.Z. Bin, 2009, Turbidimeter design and analysis: A review on optical fiber sensors for the measurement of water turbidity: Sensors, v. 9, p. 8311–8335, doi:10.3390/s91008311.

Riverkeeper, Ashokan Reservoir: Stop the Mud, 9 Feb. 2022, https://www.riverkeeper.org/campaigns/safeguard/ashokan-reservoir-stop-the-mud/.

Tessier, A., 1992, Environmental Particles.

Titus, R., 1996, The Catskills in the Ice Age. Purple Mountain Press, Fleischmanns, New York, p. 123.

Wang, K., Davis, D., and Steinschneider, S., 2021, Evaluating suspended sediment and turbidity reduction projects in a glacially conditioned catchment through dynamic regression and

fluvial process-based modelling: Hydrological Processes, v. 35, doi:10.1002/hyp.14351.

Watershed Agricultural Council, 2022, Croton & Catskill/Delaware Watersheds. https://www.nycwatershed.org/about-us/overview/croton-catskilldelaware-watersheds/ (July 30, 2022).

2. Factors and Mobilization Processes of Turbidity Generation: An Application in the Catskills, New York, USA

2.1 BACKGROUND AND CHAPTER OVERVIEW

Conceptual models can be useful to simplify complex phenomena. In this chapter, I propose a conceptual model for turbidity to (1) understand the different types of turbidity events that can occur (characterize turbidity events), (2) what may be causing these events (defined as factors and mobilization processes), (3) describe how these events can be partitioned into "stages," and finally (4) apply the conceptual model to a case study in the Catskills. This proposed conceptual model allows us to better understand how turbidity events "operate" with an application in the Catskills. Specifically, I define a "stage" of a turbidity event to being analogous to different periods of time in a storm hydrograph.

In this chapter, first, I outline the factors and mobilization processes of turbidity generation, which are broadly applicable across watersheds both within and outside of the Catskills. Then, I outline the different possible turbidity event types that can occur, such as whether the turbidity event was largely driven by streamflow or not. Next, I separate each of the turbidity event types into stages, and finally apply the proposed conceptual model to a case study in the Catskills located at Stony Clove Creek at Chichester, NY (USGS site number 01362370). This conceptual model derivation has important implications for stream remediation, as different remediation efforts are likely needed for both the turbidity event type as well as the stage of the turbidity event. Thus, there are clear watershed management implications in the Catskills that can be better understood through the application of this proposed conceptual model.

2.2 FACTORS AND MOBILIZATION PROCESSES OF TURBIDITY GENERATION

The conceptual diagram to explain the mobilization processes and factors that can generate turbidity events is shown in Figure 1. From Figure 1, turbidity can be defined by the following function:

$$\text{Turbidity} = \text{f}(\text{sediment source type}, \text{source protection}, \text{energy input}) \quad \text{(Eqn. 1)}$$

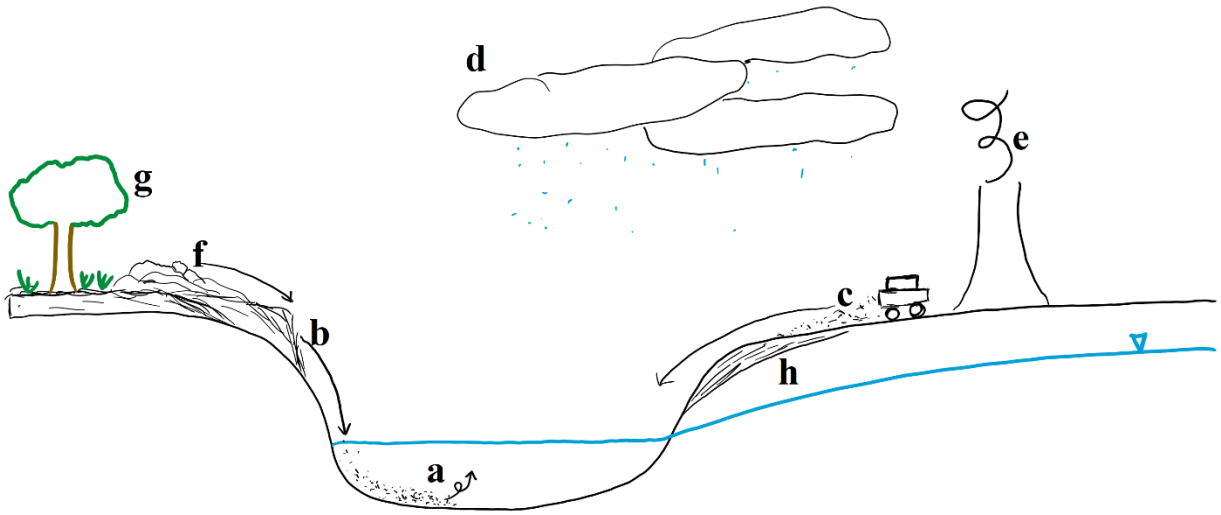

Figure 1. Process diagram to explain the different sources of turbidity across different turbidity event types (Table 1). The letters denote the source of turbidity to the stream and are described as follows: (a) scouring of the stream bed (in-stream suspension from suspended and bed load), (b) mass-wasting of regolith (destabilization of stream bank), (c) anthropogenic influence, (d) climatic regime or biome (affects precipitation and temperature), (e) point-source pollution, (f) land surface erosion, (g) land cover change, and (h) lithology. Note that this process diagram differs across climatic regimes and seasons. For example, ice cover and snowmelt events likely play an important role in regulating turbidity throughout the winter in temperate biomes. This diagram is also not an exhaustive representation of all of the potential contributions or processes leading to the generation of turbidity.

Thus, the main requirements to generate turbidity are a sediment source and energy to mobilize the sediment. Sediment source type refers not only to the sediment type and lithology, but also the grain size and composition of the sediment. We would expect sediments that are

more easily erodible to have a greater impact on turbidity. The source protection refers to the vegetation, land cover, and anthropogenic influences, which can also generate turbidity. The energy input refers to the necessary factors to cause a response in turbidity (i.e., to mobilize the sediment). Such energy inputs include water delivered by precipitation, stream velocity, and snowmelt events. Thus, the energy inputs for contributing to turbidity here are characterized as hydrologic inputs. The energy input can also be defined as the transfer of potential energy to kinetic energy. For example, slope failures and landslides represent this type of energy transfer.

In the following two sections, I define both the factors and mobilization processes affecting turbidity generation; the factors affect turbidity generation processes. Firstly, I outline the factors that contribute to turbidity generation. Then, I outline the processes of turbidity generation (Figure 1) and discuss how the different factors affect turbidity generating processes. Although there may be overlap between factors (e.g., sediment type) and processes (e.g., stream bed scouring) of turbidity generation, it is necessary to distinguish between factors and processes to gain a broader understanding of the controls on turbidity generation across various hydrologic regimes.

2.2.1 Factors of Turbidity Generation

Factors of turbidity generation affect mobilization processes causing turbidity, which will be described in the following sub-section.

(1) Streamflow

High streamflow tends to increase turbidity (Figure 2). High or increased streamflow tends to keep particles suspended, meaning light can be scattered by more particles, thus

increasing turbidity. During periods of high discharge, the stream velocity increases, causing erosion of the stream bank and bed to occur (National Academies of Sciences, Engineering, and Medicine, 2020). This facilitates the downstream transport of these eroded particles (National Academies of Sciences, Engineering, and Medicine, 2020).

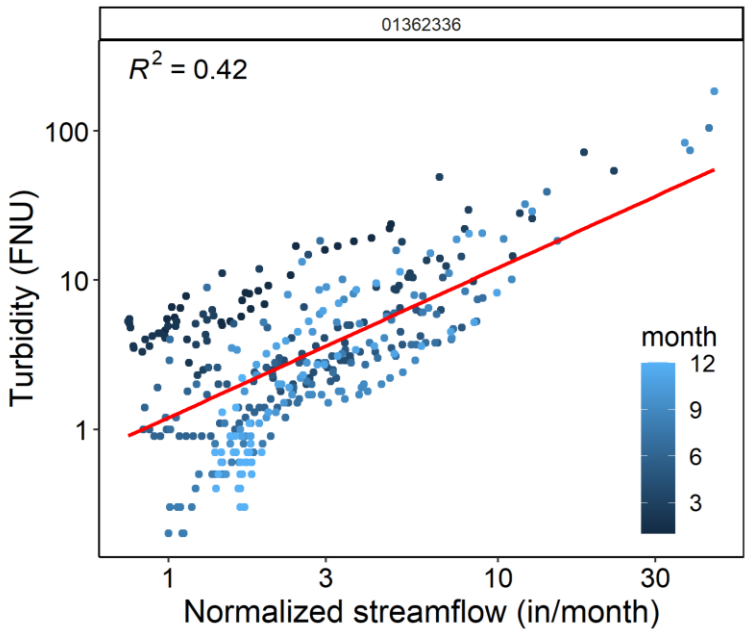

Figure 2. Expected relationship between turbidity and streamflow. Both axes are log scaled. Data are from 2021 at Stony Clove at Lanesville (01362336).

Even though this trend between discharge and turbidity exists, turbidity is nonetheless temporally and spatially variable (e.g., by stream reach) (National Academies of Sciences, Engineering, and Medicine, 2020). This can be explained, for example, by sediment sources differing spatially for a given stream. Thus, such a difference can cause uncertainty in the streamflow-turbidity relationship (e.g., Mukundan et al., 2013). Although streamflow is largely expected to explain the variation in turbidity, there is uncertainty in the streamflow-turbidity relationship, which occurs due to the multiple influences on turbidity in addition to streamflow

(e.g., Mukundan et al., 2013). These additional factors influencing turbidity (e.g., seasonal changes in land cover) will be discussed in this section.

The streamflow-turbidity relationship is also affected by hysteresis (see section 2.4.2). Hysteresis means that the dissolved load and sediment load are path and time dependent rather than solely depending on streamflow (Bierman and Montgomery, 2014). This suggests that the rate of sediment transport differs between the rising and falling limb of the hydrograph (e.g., Mukundan et al. 2013). The preceding streamflow history may also have an effect on turbidity. For example, through time, the more easily scourable or erodible sediments may be removed from the channel. These pulses of sediment mobilization may limit the amount of sediment available to be mobilized later, which can therefore reduce turbidity through time (such as between storm events) as sediments are removed from the channel system.

(2) Source material

The geological source material refers to the sediments and particles that can affect the turbidity of surface waters (either allochthonous or autochthonous, i.e., from the land or the stream channel itself). Specifically, sediment sources can be supplied to channels from surface erosion on slopes, mass wasting, stream banks, and tributaries (Hassan et al., 2005). In small forested streams (such as in the Catskills), the channel is not usually bordered by a well-developed floodplain (Hassan et al., 2005). Thus, mass wasting and bank erosion are the dominant controls on sediment supply to these channels (Hassan et al., 2005).

Suspended or dissolved sediment load: Fine particles, such as clay, silt, inorganic and organic matter, can contribute to suspended or dissolved sediment load, which can affect turbidity. The cloudiness of the water results from light scattering by fine particles, which is the definition of turbidity (Davies-Colley and Smith, 2001) (see Chapter 1). Thus, high suspended

sediment can lead to turbid water. Suspended sediment concentration (SSC) is often used as a proxy for turbidity, and vice versa. Sediment can be transported during storm events, thus generating turbidity. Once the source material on land becomes mobilized (e.g., through erosion), then this source material can be transported to streams, thus affecting the turbidity.

Particle size, composition, and shape: Particle composition changes along the stream reach can indicate changes in sediment sources. The particle size and composition affect the scattering of light, which affects turbidity (Kleizen et al., 1995) (Figure 3). Because the spatial distribution of light scattering is dependent on the ratio of the size of the particle to the wavelength of the incident light, particles that are smaller than the wavelength of the incident light have a relatively equally distributed scattering forward and backward (Hatch, n.d.). Thus, particle size affects the magnitude and direction of light scattering. With larger particles, more forward scattering is expected (Hatch, n.d.). More particles may not directly correlate to greater turbidity because if these particles are closely related spatially, then absorption of light can increase due to multiple scattering occurring by the particles (Hatch, n.d.). There are multiple factors related to the physical properties of particles (size, composition, amount/density, color) that can all affect turbidity, which complicates determining a clear relationship between the physical properties of particles and turbidity.

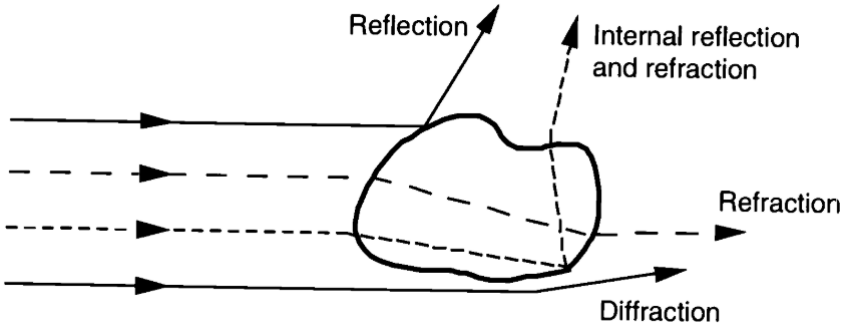

Figure 3. Schematic diagram of the light scattering properties (reflection, refraction, and diffraction) of particles (Davies-Colley and Smith, 2001).

Nonetheless, particles in the size range of 0.2 to 5 μm for minerals and 1 to 20 μm for organic particles have significant controls on the light attenuation in water (Davies-Colley and Smith, 2001). Furthermore, clay particles and small organic particles (e.g., phytoplankton cells) have significant controls on light attenuation in water (Davies-Colley and Smith, 2001).

Lithology and sedimentology: The underlying lithology of a particular stream also affects SSC and turbidity. For example, bedrock streams are less influential in contributing to sediment load of streams (and therefore turbidity) as they are more resistant to erosion than streams incised in unconsolidated deposits. The surficial material on top of bedrock plays a key role in controlling turbidity. In the Catskills, the surficial glacial till deposits are highly erodible, which is a key contributor to turbidity throughout the region.

(3) Land cover and land use

Land use and cover affect the hydrologic regimes of freshwater systems (National Academies of Sciences, Engineering, and Medicine, 2020), deeming it necessary to consider these factors in the context of turbidity generating factors. Land cover refers to the vegetative characteristics of the landscape, whereas land use refers to the application of the land, such as agricultural use by humans. Anthropogenic effects of land use change can affect water quality (Figure 4). Broadly, we would expect forested ecosystems to contribute less to turbidity than cleared land due to two main reasons: (1) the vegetation provides structural support to the soil, and (2) the vegetation can dissipate the energy of raindrops and flowing water, reducing the amount of energy available to erode the sediment.

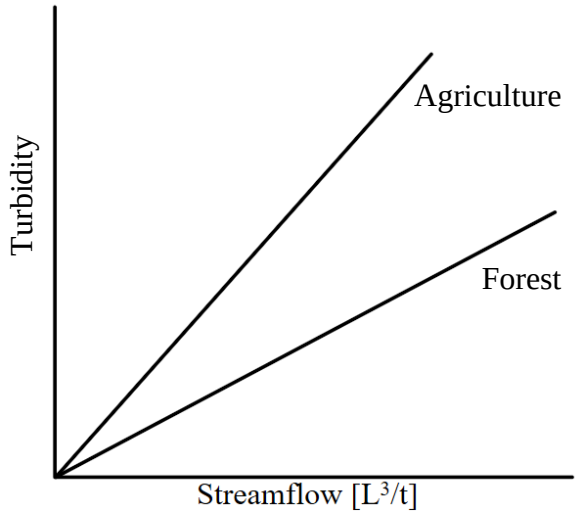

Figure 4. Expected effects of both forested and agricultural land on turbidity.

When sediment gets eroded (e.g., during a flood event), the vegetation can restrict the amount of sediment that can get washed into the stream (i.e., providing structural support). Forests can also reduce turbidity by filtering sediment and other particles (Brauman et al., 2007; Cunha et al., 2016).

Clearing land also primes the sediment to be mobilized during a flood event, as the sediments could accumulate after land clearing and before a soil mobilization event (e.g., flood, landslide). Furthermore, land use changes such as surface compaction can reduce the infiltration capacity of the soil and increase the likelihood and intensity of overland flow, which can increase the transport of pollutants to streams (National Academies of Sciences, Engineering, and Medicine, 2020). Such changes can result from urbanization (e.g., more impervious surfaces). Even if the land cover class does not change (e.g., agricultural use), changing the land and resource use *within* that land cover class (e.g., switching from dairy farming to vegetable production) can impact water quality, including turbidity (National Academies of Sciences, Engineering, and Medicine, 2020). Another example of changing land use within a land class

pertains to timber harvesting. With increased timber harvesting in secondary forests, although this may not drastically change the total forest area, this can nonetheless increase sediment loading to nearby streams (National Academies of Sciences, Engineering, and Medicine, 2020).

Additionally, riparian areas – where aquatic and terrestrial ecosystems meet – are important in controlling the water quality of streams. With land use and land cover change of riparian ecosystems, this has a direct impact on flow regimes and thus water quality. For example, if a riparian area is dominated by overland flow, short residence times, and limited vegetation, then water quality would be expected to degrade (National Academies of Sciences, Engineering, and Medicine, 2020). As riparian areas act as sediment traps by reducing the amount of sediment that may enter a stream (Figure 5), clearing riparian areas can permit soil erosion and degrade water quality.

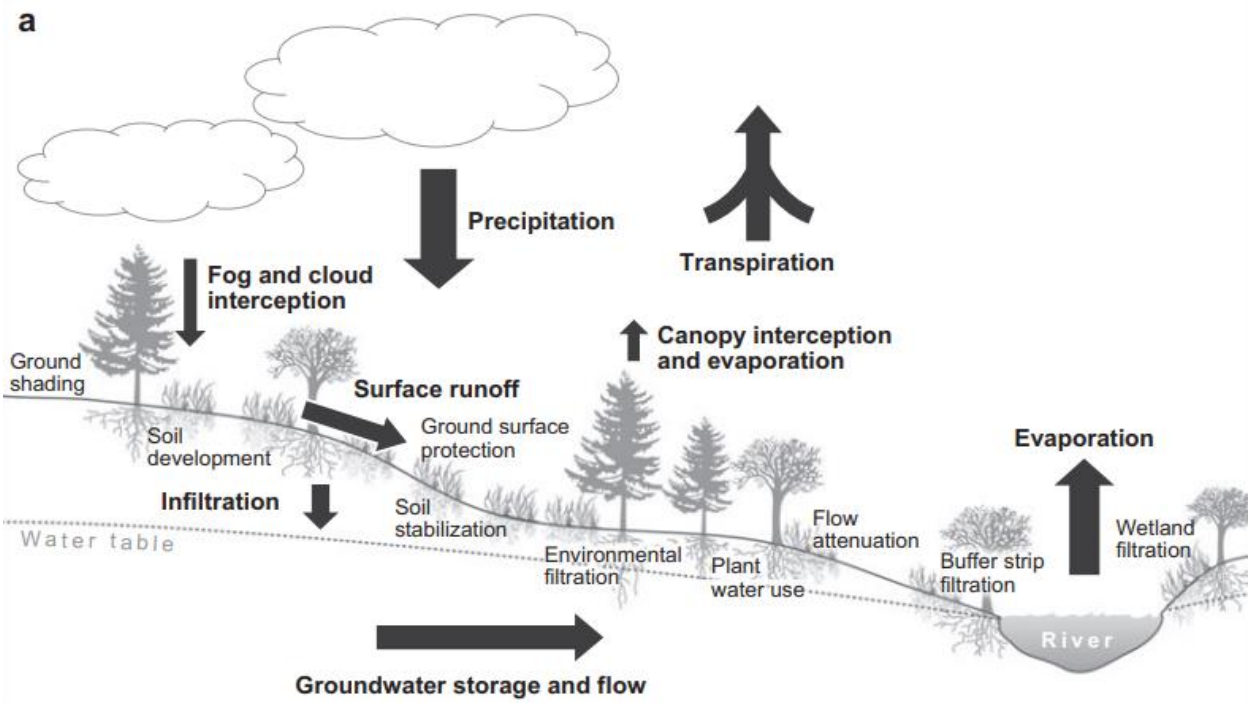

Figure 5. Schematic diagram of how vegetation can regulate turbidity (Brauman et al. 2007).

(4) Topography

Topography differences (e.g., between steep versus shallow slopes) also affect turbidity due to differences in the amount of sediment transport to streams (Figure 6). Greater topographic relief increases the potential for sediment to get transported into streams.

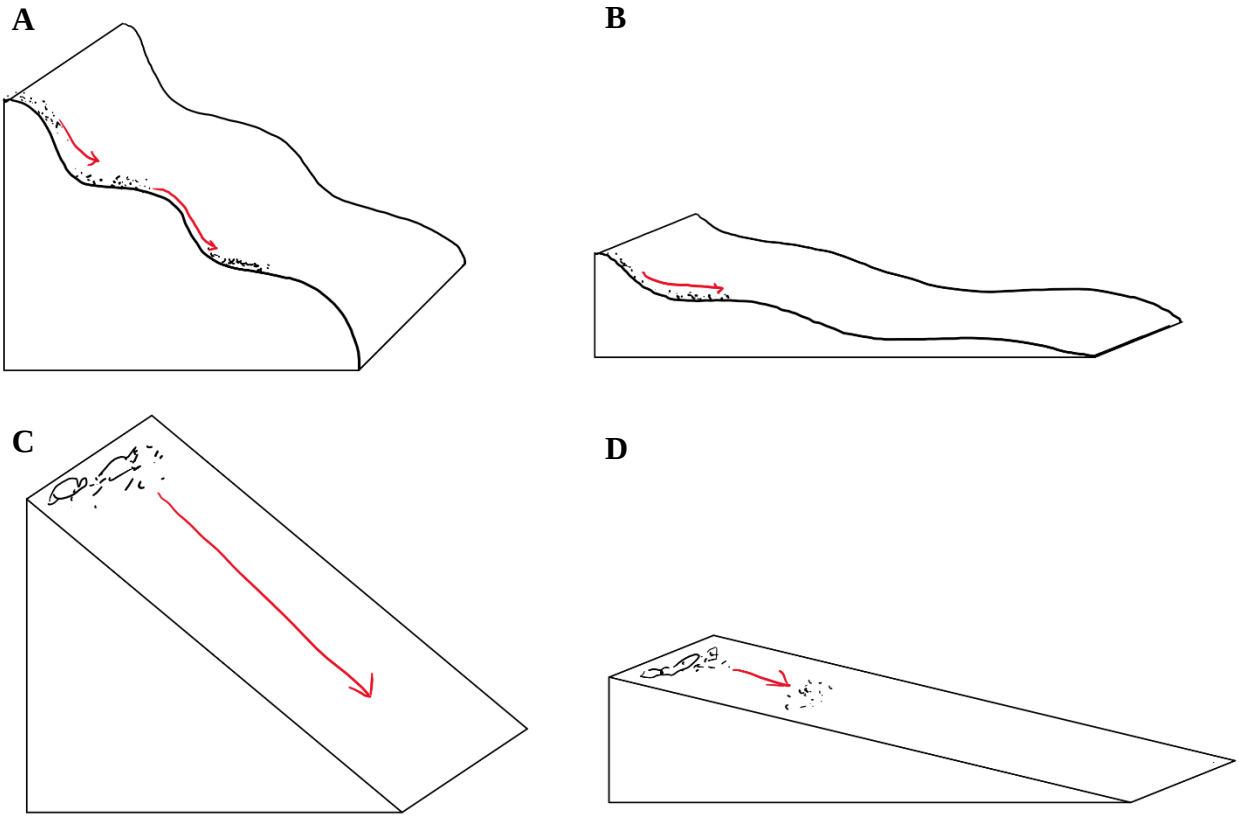

Figure 6. Schematic diagram of the effect of topography on sediment transport to streams: (**A**) steep, depressions; sediment transport to streams is intermediate (limited by sediment capture in depressions), (**B**) shallow, depressions; sediment transport to streams is low (limited by slope gradient), (**C**) steep, depressionless; sediment transport to streams is high, and (**D**) shallow, depressionless; sediment transport to streams is low or intermediate (limited by slope gradient). Steeper, depressionless topography (panel C) is generally expected to be associated with the greatest sediment transport to stream channels through surface erosion on slopes. This influx of sediment can therefore drive turbidity in the stream.

The watershed topography (elevation, basin length, slope) can also affect sediment discharge to streams (Cheng et al., 2017). Topography is dynamic because material is constantly being transported and deposited (Bierman and Montgomery, 2014). Thus, steeper slopes allow for

faster rates of downslope transport of sediments (Bierman and Montgomery, 2014), which can ultimately get transported to streams. But, convergent topography can focus sediment transport (Bierman and Montgomery, 2014). Convergent topography coupled with steep slopes, however, may affect the amount of sediment load transported to streams because sediment can get deposited in low-lying topography (e.g., valleys and concave depressions in the landscape) rather than being transported directly to streams (Figure 6).

(5) Climate and meteorology

Climatic conditions influence erosion, such as the intensity, amount, and frequency of rainfall, which also affects turbidity.

Rainfall characteristics: With more or frequent rainfall, more runoff is expected, thus increasing the potential for erosion. Rainfall can influence erosion because more rainfall can mobilize more sediment, which can get transported to streams and rivers. Because rainfall drives soil erosion, this impacts the separation of soil particles and thus the transport of eroded sediment (Meng et al., 2021). The frequency or duration of rainfall also affects the transport of sediment to streams. For example, moderate rainfall characterized by low intensity and long duration often results in interflow (Meng et al., 2021). However, storms that are characterized by high intensity events can initiate runoff and thus transport sediment into streams. Therefore, the conditions that are most conducive to the mobilization of sediment to streams include rainfall patterns that are described as being high intensity, short duration, and high frequency (Meng et al., 2021). This influx of sediment, as previously discussed, has the potential to elevate turbidity in streams.

Seasonal dynamics: Changes in vegetation cover throughout the year affect the influx of sediment to streams and thus turbidity. Turbidity is expected to increase in streams when there is

less vegetation stabilizing the soil. Such increases in turbidity may occur during the late winter, fall or early spring when there is less vegetation. The late winter may also be more susceptible to wind-driven re-suspension of sediments along streams, which can contribute to turbidity. During the winter months, less sediment can be mobilized by stream channels because, in general, streamflow and stream velocity decrease (Beltaos and Burrell, 2021). However, substantial erosion and sediment transport can occur if the streamflow is channeled by deposits of slush or under a solid ice sheet (Beltaos and Burrell, 2021). Thus, the breakup of river ice can be a significant contributor to erosion (Beltaos and Burrell, 2021), which can affect turbidity.

Additionally, there may be different mechanisms driving peaks in turbidity in the winter and summer seasons. For example, ice jams during the winter can drive streamflow and thus turbidity to peak (Figure 7).

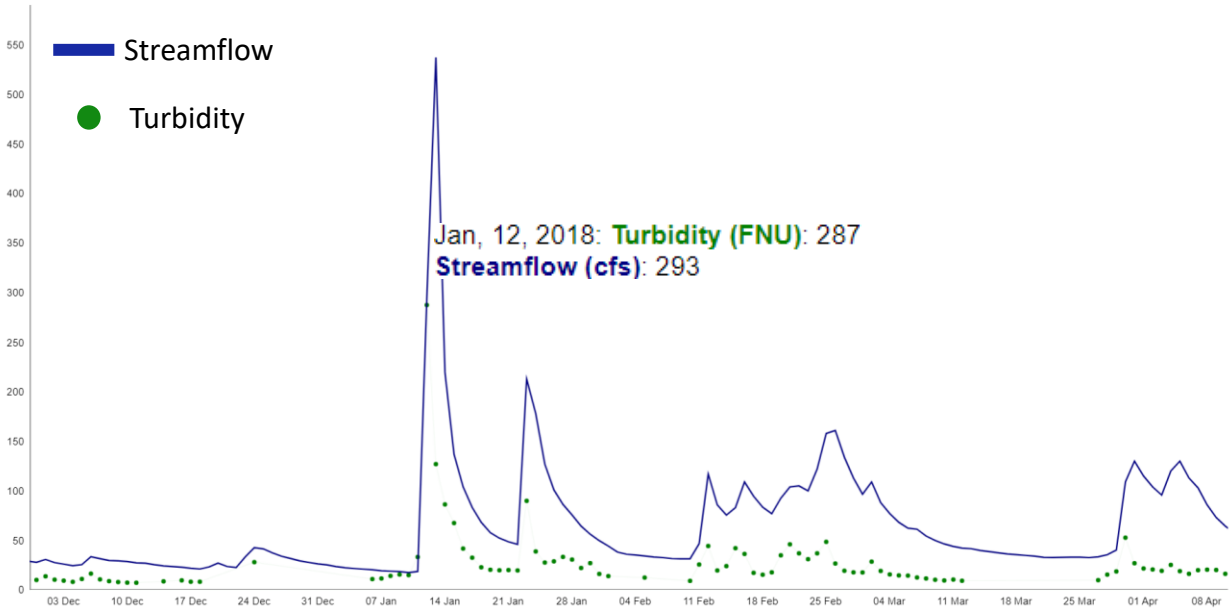

Figure 7. Ice jam event on 12 January 2018, documented at Woodland Creek at Phoenicia, NY (site 0136230002). Green dots are daily average turbidity and blue line is daily average streamflow. The ice jam event was likely caused by thawing and rain on 12 January 2018, as a similar event was observed in the lower Mohawk River on the same day (Garver, 2018).

Furthermore, storms of equal size occurring in different seasons (e.g., late fall and summer) also likely have differing effects on turbidity. This is due to the confounding effects of changes in temperature, precipitation, and vegetative cover across seasons.

Temperature: In the context of climate change, it is important to consider the effects of significant fluctuations of climatic variables, such as temperature, on turbidity. The effect of precipitation on turbidity is also influenced by temperature. Temperature controls the form of precipitation (e.g., snow, sleet, rain) as well as soil permeability. With frozen soils, less erosion would be expected compared to thawing soils.

(6) Disturbances

Disturbances, such as floods, plowing fields, and forest fires can also affect turbidity. In this sub-section, I list some of the possible effects of disturbances on turbidity – this list is not exhaustive, as only a few possible examples are outlined.

Storm events and floods: Storm events and floods affect turbidity because during peak rain events, solid particles can be washed into surface water bodies from the surrounding land, increasing turbidity. Also, precipitation increases stream volume and thus the streamflow; this can resuspend sediment that became settled in the steam and erode riverbanks.

Plowing fields and forest harvest: Plowing fields and cutting down trees can prime sediment to be mobilized by increasing the sediment that is available to be mobilized (see previous section on land use change). That is, when fields are continuously plowed, this can accumulate the amount of sediment available that can ultimately get transported to streams and rivers. Plowing fields clears the vegetation away, which, as previously discussed, can increase erosion and sediment transport to streams, therefore increasing turbidity. Plowing also breaks

apart soil aggregates, which increase the potential for these soils to become more erodible. Drainage systems in croplands can also increase erosion in streams due to the force of the draining water.

Fires: Wildfires, when coupled with other disturbances such as logging, can lead to increased overland flow, soil erosion, and sediment transport (National Academies of Sciences, Engineering, and Medicine, 2020). Fires can affect stream water quality by leading to greater rates of mass movement on hillslopes (National Academies of Sciences, Engineering, and Medicine, 2020). This process can be explained by soil moisture increasing after wildfires due to decreased evapotranspiration, which can trigger mass movement events such as landslides (Helvey, 1980). This increased soil moisture storage can remain high years after severe fires, making watersheds more vulnerable to changes in water input (e.g., snowmelt or rainfall) (Helvey, 1980). Such an effect after a forest fire was observed in North Central Washington, USA, where a creek within the affected watershed experienced increased annual water yield following the forest fire compared to before the fire occurred (Figure 8) (Helvey, 1980).

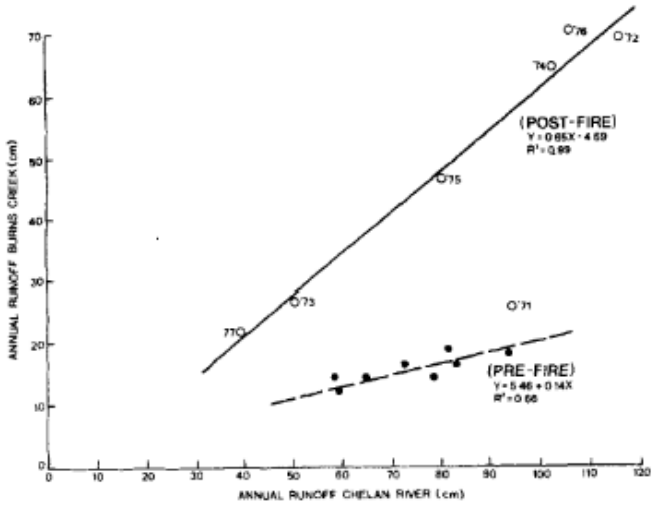

Figure 8. Difference between pre- versus post-fire annual water yield from a North Central Washington creek and river, from Helvey (1980).

Roots can also be destroyed following forest fires, which can reduce the stability of soil and thus result in hillslopes being more prone to failure.

Another important component of wildfires is the significant quantities of ash that are generated from them. The rapid conveyance of ash to surface waters can impair surface water quality. Wildfires change watersheds because they burn the vegetation and leaf litter on the forest floor, causing more rainfall to fall onto the surface of the soil ("How Wildfires Threaten U.S. Water Supplies", n.d.). Moreover, soil heating makes the soil less porous, which permits overland flow to occur more intensely ("How Wildfires Threaten U.S. Water Supplies", n.d.). The intense overland flow can pick up wildfire ash and sediment along the way to streams, thus affecting turbidity ("How Wildfires Threaten U.S. Water Supplies", n.d.).

Dam construction: Dams and reservoirs can allow for sediment to be trapped where the dams and reservoirs and being constructed, which can have significant impacts on sediment load downstream. Dams tend to decrease turbidity downstream because water flow can slow behind the dam, which allows sediment to settle out rather than remaining in suspension in the stream channel. Thus, deposition processes can occur upstream, reducing the sediment concentration downstream. For example, the Gilboa Dam, which impounds the Schoharie Reservoir at its northern point, plays a key role in regulating the sediment supply and transport throughout the Catskill Water Supply System.

(7) Biota

Biota in streams can have differing effects on turbidity. That is, some biota can enhance turbidity, while others can reduce it. For example, bioturbation, which is the disturbance of sediment by living organisms, can scour sediment from stream channels, thus elevating turbidity.

Algal growth can also affect turbidity; with increased nutrient concentrations, there will be more phytoplankton, which can increase turbidity. However, biota can also have a stabilizing effect on the bottom sediments in surface waters; for example, ribbed mussels can slow erosion by attaching to plant roots, thus stabilizing ecosystems like marshes (Moran, 2022). This stabilization has an effect on water quality as well, which is important in the context of monitoring turbidity.

(8) Stream restoration efforts

Stream restoration efforts can include bank stabilization to full channel restoration projects (i.e., creating new channels and floodplains) (see Chapter 1 for further description on stream restoration in the Catskills) (National Academies of Sciences, Engineering, and Medicine, 2020). Unstable stream reaches are sources of turbidity to the stream channel (Figures 9, 10).

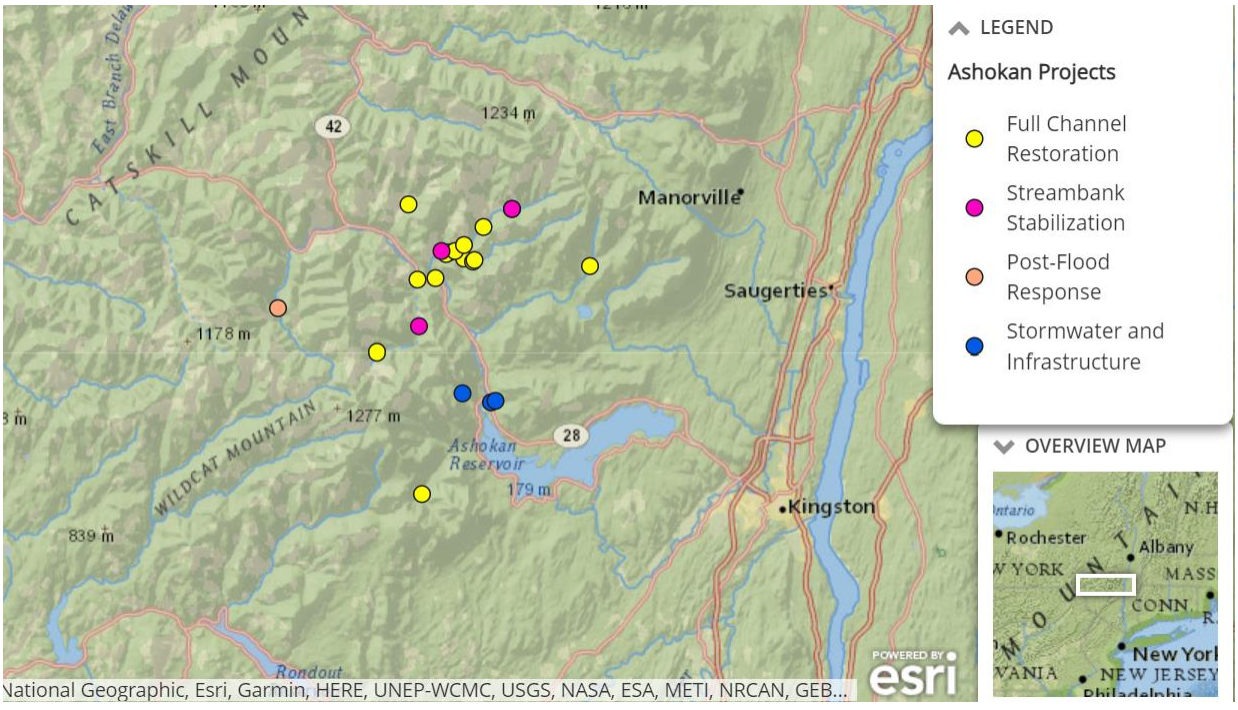

Figure 9. Map of stream restoration projects by the Stream Management Program (SMP) in the Esopus Watershed. From Stream Management Program Projects (Catskill Streams, 2020).

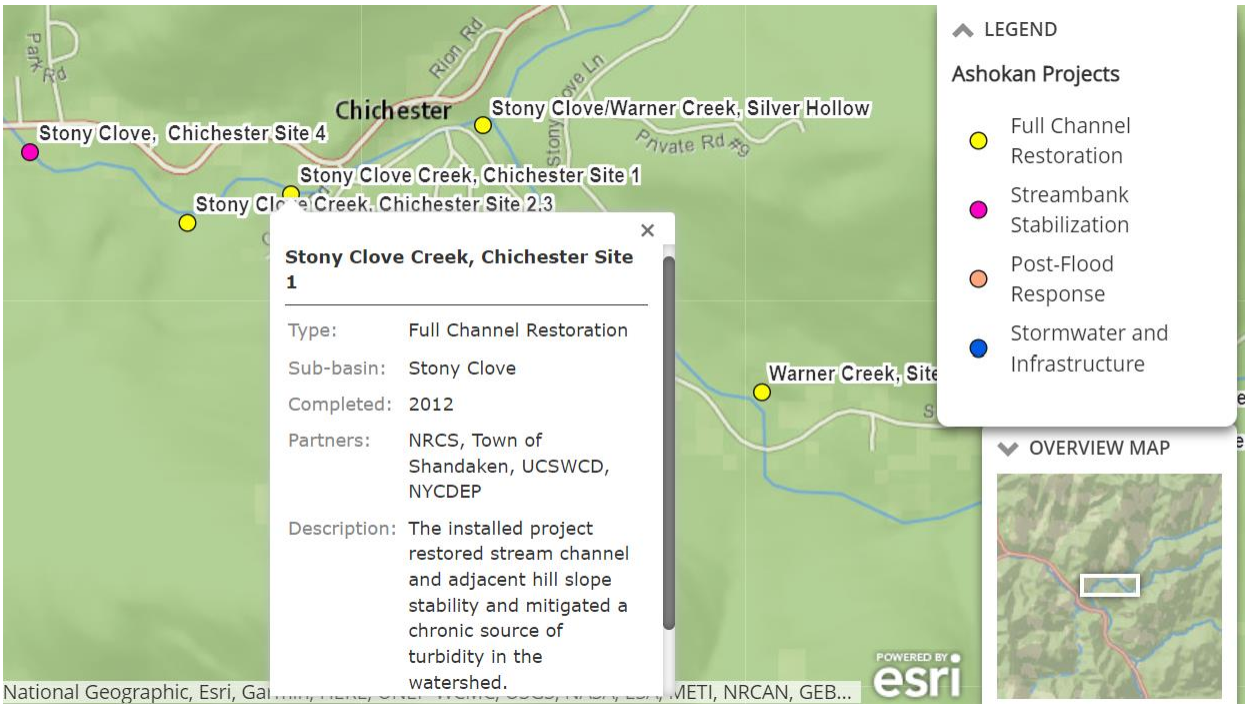

Figure 10. One stream restoration project conducted along a stream reach at Stony Clove at Chichester by the SMP. From Stream Management Program Projects (Catskill Streams, 2020).

As a result, the Stream Management Program (SMP) has implemented stream management projects in the Catskill and Delaware Watersheds to reduce fine sediment in the WOH system, and these practices aim to determine the origin(s) of the sediment (Figures 9, 10) (National Academies of Sciences, Engineering, and Medicine, 2020).

2.2.2 Mobilization Processes of Turbidity Generation

Turbidity mobilization processes are affected by the factors outlined in section 2.2.1. Here, I briefly outline some of the potential mobilization processes that can generate turbidity.

(1) Scouring of the stream bed

Scouring of the stream bed relates most directly to the aforementioned factor of streamflow (it provides the energy for scouring), but also to the factors of source material and

biota. When the source material is deposited in the stream channel, it can be mobilized in-stream through processes such as erosion and bioturbation. Scouring of the stream bed also can contribute to generating baseline turbidity, or the sediments already suspended in the stream before a peak turbidity event. Stream scouring occurs when the armor layer becomes mobile, allowing sediments to be released into the streamflow (Bierman and Montgomery, 2014).

(2) Mass wasting of regolith and destabilization of stream banks

Mass wasting and destabilization of stream banks are mobilization mechanisms that most directly relate to the factors of climate and meteorology, source material, topography, land cover and land use, and disturbances. For climate and meteorology, a mass wasting event may be more likely to occur following a precipitation event because the soil moisture will be higher, thus increasing the weight of the soil and decreasing effective stress, making the soil more prone to slumping. With the source material available, topography can influence mass wasting events as steep topography can permit sediment transport down hillslopes. Land clearing and other disturbances can accelerate erosion in steep terrain by removing roots, which destabilizes the soil. Mass wasting is an important mobilization mechanism of sediment for streamflow-independent turbidity events (see section 2.3).

(3) Anthropogenic influences

Anthropogenic influences can mobilize sediment and ultimately generate turbidity, as humans have increased sediment loading to rivers through time. Such factors that relate directly to this mobilization mechanism include land cover and land use and disturbances. For example, mining, agricultural activities, and poorly managed drainage projects can increase solid

discharge by streams that is beyond their natural capabilities. Point-source pollution is a factor that also contributes to turbidity by increasing sediment loading and wastewater inputs to rivers. Organic matter from sewage discharge can contribute to turbidity as well.

(4) Land surface erosion

Related to the mobilization process of anthropogenic influences, land surface erosion is a key mobilization process in the Catskills that contributes to turbidity. Land surface erosion can be driven by all of the previously mentioned factors; as long as there is sediment available to be mobilized and the necessary energy to mobilize it (e.g., a storm event), then erosion can occur and thus contribute to turbidity. Land surface erosion is an important mobilization mechanism of sediment for streamflow-dependent turbidity events (see section 2.3).

2.3 TURBIDITY EVENT TYPES

After outlining the factors and mobilization processes affecting turbidity generation, I propose different possible turbidity event types that can occur. Understanding the possible different turbidity event types has important implications for proper stream management efforts, as certain streams may be more susceptible to certain turbidity event types. In this section, the three overarching types of turbidity event types I describe are (1) streamflow-independent events, (2) streamflow-dependent events, and (3) partially streamflow-dependent events.

2.3.1 Streamflow-Independent Events

The first turbidity event type, called streamflow-independent, is characterized by a decoupling between the streamflow-turbidity relationship (Table 1).

Table 1. Characterization of turbidity events as part of the turbidity conceptual model. There are three main types of turbidity events described here in the conceptual model, which are classified as either streamflow-independent, streamflow-dependent, or partially streamflow-dependent.

Turbidity Event Type	**Turbidity Event Type Name**	**Characteristics of the Turbidity Event Type**
1	Streamflow-independent	Complete decoupling of the streamflow-turbidity relationship. Streamflow is not the cause of the turbidity event.
2	Streamflow-dependent	The peak in turbidity observed in the event is largely caused by a peak in streamflow.
3	Partially streamflow-dependent (Mixed)	Only partial decoupling of the streamflow-turbidity relationship. Streamflow explains some of the variation observed in turbidity.

That is, streamflow cannot explain the variation in turbidity for the given turbidity event. This could possibly happen during periods of low streamflow and when another variable (such as land cover change that induces an extreme event like a landslide) has a larger influence on turbidity than streamflow. These types of events are likely infrequent as we would expect streamflow to have a dominant control on turbidity, especially when streamflow is high.

2.3.2 Streamflow-Dependent Events

The second turbidity event type, called streamflow-dependent, is characterized by a strong dependency or coupling between streamflow and turbidity. That is, streamflow can explain most of the variation in turbidity during streamflow-dependent events (Table 1). These types of events are most likely to occur when streamflow is high, as streamflow would be exerting a larger control on turbidity. Most turbidity events are characterized as streamflow-dependent.

2.3.3 Partially Streamflow-Dependent Events

The third turbidity event type, called partially streamflow-dependent, is characterized by a partial dependence on streamflow for a given turbidity event. Thus, streamflow can explain some of the variation in turbidity. These mixed turbidity events may occur when streamflow has a moderate influence on a stream, or when other variables besides streamflow exert a control on the system, such as erosional connectivity with sediment.

2.4 PARTITIONING TURBIDITY EVENTS INTO STAGES

The turbidity event types described in section 2.3 can be separated into "stages," or segmented by various points in time for each of the events. Here, I break down hypothetical turbidity events for both streamflow-independent and streamflow-dependent turbidity events. Then, this approach will be applied specifically to the Catskills in a later section. Note that the stages defined in the following sub-sections are not discrete from one another; the different stages help inform the progression of various turbidity events.

2.4.1 Partitioning Streamflow-Independent Events

In some cases under certain hydrologic and geologic regimes, streamflow-independent events can occur as a result of streamflow-dependent events. That is, streamflow-dependent events can prime the system so sediment can be mobilized on the falling limb of the hydrograph. For both streamflow-independent and streamflow-dependent events, these events can start with low streamflow and turbidity (stage 1). A streamflow-dependent event that mobilizes sediment can cause a rapid increase in turbidity (after a critical shear stress is surpassed), which is coupled with streamflow (stage 2). Later on, as streamflow decreases, a mobilization event of sediment

can occur, such as the destabilization of a hillslope (stage 3). This instability of the hillslope may result because of the available energy (of hydrologic origin) produced during the streamflow-dependent event. Although streamflow-dependent events can initiate streamflow-independent events, this may not always occur depending on the hydrologic and geologic regimes of the system. For example, a streamflow-independent event may not occur immediately after a streamflow-dependent event if all of the available energy produced to cause the turbidity peak is dissipated after this streamflow-dependent event. Thus, this energy would no longer be available in the system to initiate a streamflow-independent event, resulting in a return to baseline turbidity on the falling limb of the hydrograph.

Additionally, it is important to note that the lag-time between streamflow-dependent and streamflow-independent turbidity events is variable. That is, the segment of time separating streamflow-dependent from streamflow-independent events is not constant across turbidity events. This lag between turbidity event types can be explained, for example, by the rate at which a hanging block of sediment by the stream bank falls into the stream channel. If the rate the block falls is on the order of magnitude of a few hours or days, then the lag time between the streamflow-dependent event and streamflow-independent event will decrease. But, if it takes a long time for the sediment to become mobilized into the stream channel, on the order of magnitude of several weeks, then this will increase the lag time between streamflow-dependent and streamflow-independent events.

2.4.2 Partitioning Streamflow-Dependent Events

During a typical streamflow-dependent event, we would expect to observe an initial peak in suspended sediment in the system as a result of high streamflow (stage 2). This mobilization of the bed sediment occurs once a critical shear stress is exerted on the bed (Figure 11).

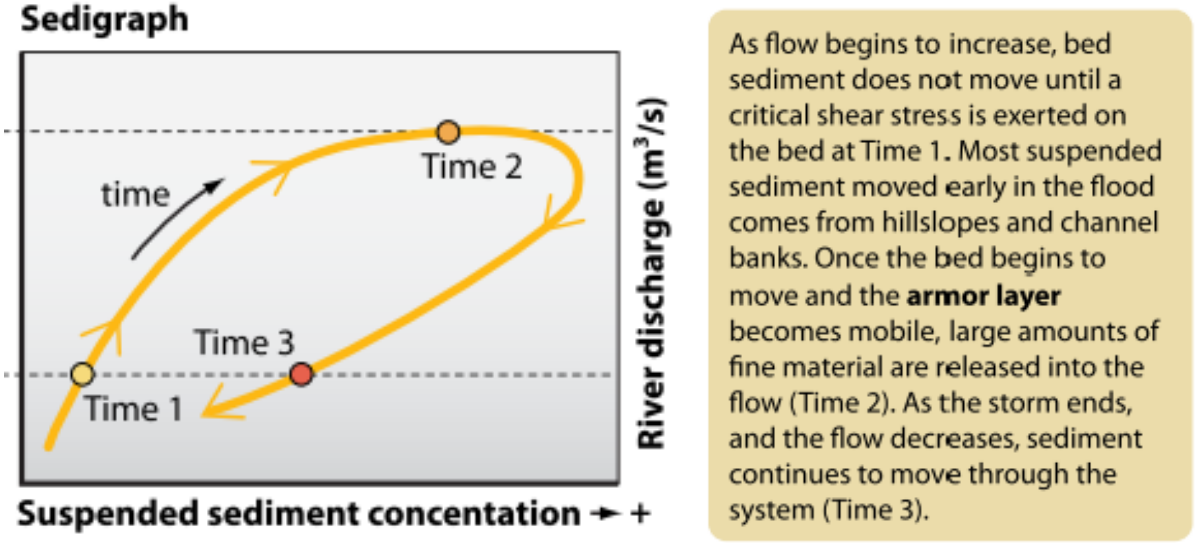

Figure 11. Sedigraph of a typical streamflow-dependent event (Time 2), which can possibly initiate a streamflow-independent event (Time 3). From Bierman and Montgomery (2014).

Then, this sediment gets released into the streamflow (stage 3); on the falling limb of the hydrograph as streamflow decreases, sediment load can return to baseline conditions (stage 4).

However, when the stage of the stream increases, this this can wet more of the stream bank (i.e., the sides of the stream channel between which streamflow is confined). Different sections of the stream bank likely have different sediment source types (e.g., gravel near the base of the stream bank and silts and sands near the top of the stream bank), and these sediment source types have different erosive capacities. For example, silt located near the top of the stream bank would be more erosive than the gravel located near the bottom of the stream bank. Thus, increasing the stage of the stream has important implications on the rates of erosion and turbidity

that occur within the stream channel for a given streamflow-dependent event, as increasing the stage of the stream channel increases the shear stress exerted on the stream bed, inducing weathering on different parts of the stream bank, which have different erosive indices.

Finally, hysteresis is important to consider when characterizing or classifying streamflow-dependent events. Hysteresis is caused by many factors, one likely including the differences in erosion at the same shear stress in the channel. That is, the suspended sediment concentration (SSC) at a given level of streamflow during the rising limb differs from the falling limb due to time lags in the streamflow and SSC curve (Mukundan et al., 2013). For example, for turbidity and streamflow rating curves, on the rising limb, turbidity may be higher than on the falling limb for the same value of streamflow (Seeger et al., 2004). Thus, we can partition the contributions to turbidity and suspended sediment, such as from in-channel suspension or land surface erosion, by examining the difference between turbidity on both the rising and falling limb (Figure 12).

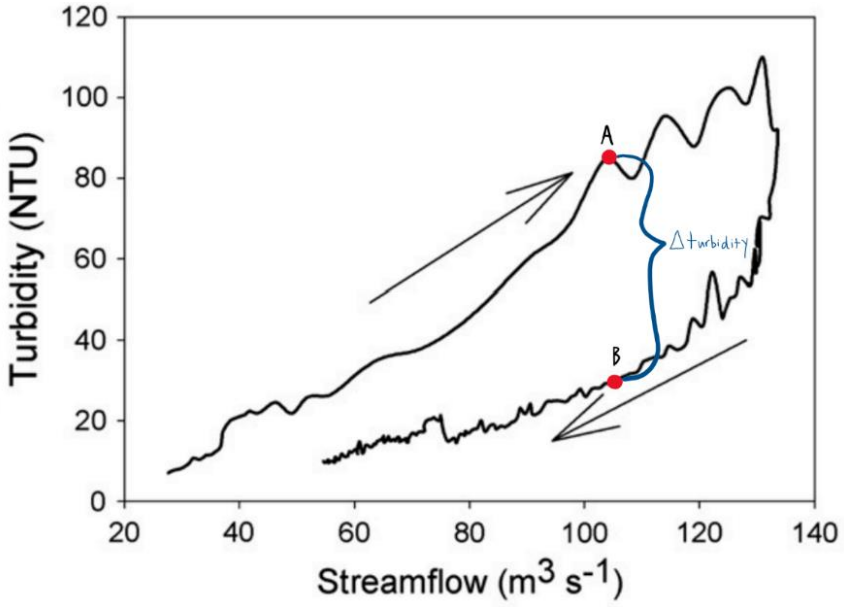

Figure 12. Hysteresis patterns in turbidity-discharge relations. Data are from streams part of the New York City Water Supply System in the Catskills, adapted from Mukundan et al., 2013. Points A and B are hypothetical points in time, representing differences in turbidity for the same streamflow value. The difference between points A and B represents the change in turbidity attributable to hysteresis.

Seasonal differences in hysteresis also likely play a significant role in driving hysteresis patterns across turbidity events. Examination of turbidity-streamflow rating curves to partition hysteresis patterns will be discussed further in a later chapter.

2.5 TURBIDITY EVENTS AND STAGES: CASE STUDY OF STONY CLOVE CREEK

After examination of the contributions and factors controlling turbidity in general and the different turbidity event types, then examples of the possible turbidity events and stages can be examined in the case of Stony Clove Creek (01362370). Here, the years of 2015 ("typical" turbidity year) and 2021 ("anomalous" turbidity year) will be examined. Note that this is a conceptual model, so any given event may not be perfectly described by the model. Nonetheless, the model helps to delineate the overall nature of the turbidity events in the Catskills by allowing us to explicitly characterize certain events.

2.5.1 Streamflow-Independent Event in the Catskills

In the example of Stony Clove Creek, a streamflow-independent event occurred on 3 November 2015 at 7:30 PM to 4 November 2015 at 12:45 AM (Figure 13). There is a peak in turbidity on 3 November 2015 at 9 PM (turbidity = 130 FNU, Q = 77.4 cfs), which occurred in the absence of a peak in streamflow. In fact, streamflow was relatively low and had been falling for several days prior to this turbidity event. This suggests that although streamflow is one variable that can explain variation in turbidity, there are in fact other variables (e.g., precipitation, land cover) besides streamflow that are responsible for causing variation in turbidity. Even if other variables are not directly responsible, then this suggests that there may be lag effects in the streamflow-turbidity relationship causing discrepancies between their associated values (i.e., why streamflow and turbidity do not always correspond to one another).

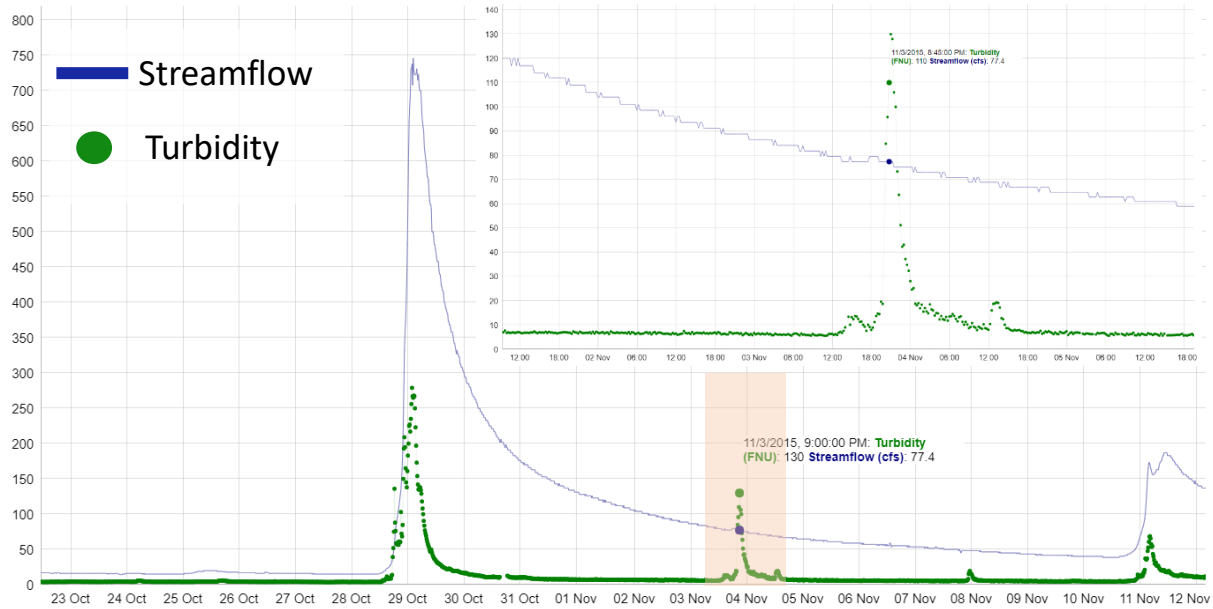

Figure 13. Time series of 15-minute turbidity and streamflow recorded at Stony Clove Creek (01362370) in 2015. The streamflow-independent event is highlighted in light orange and expanded in the upper-right panel of the graph. The y-axis represents either streamflow (cfs) or turbidity (FNU); the green dots are 15-minute turbidity, and the blue lines are 15-minute streamflow.

For the event on 3 November 2015, perhaps there was an influx of sediment from the land surface that caused turbidity to spike, such as a landslide or destabilization of the hillslope or stream bank (Figure 13). This is a plausible scenario because this influx of sediment to the stream could occur independently of streamflow, which explains why the spike in turbidity may have occurred due to streamflow being relatively constant at this time. For example, starting at 3 November 2015 at 2:00 PM, turbidity was at its baseline conditions (turbidity = 9 FNU, Q = 77.4 cfs). However, perhaps the influx of sediment from the destabilization of the stream bank initiated around 7:30 PM, causing turbidity to peak shortly after around 9:00 PM (Figure 13). Then, after the destabilization of the stream bed ended and the influx of sediment into the stream stabilized, then this allowed turbidity to return to its baseline conditions once again the following day (4 November 2015), around 4:00 PM (Figure 13).

2.5.2 Streamflow-Dependent Event in the Catskills

According to Figure 13, a streamflow-dependent event occurred on 28 October 2015 at 5:30 PM to 29 October 2015 at 10:15 AM (Figure 13). Turbidity peaked on 29 October 2015 at 2:00 AM (turbidity = 279 FNU, Q = 738 cfs). Thus, there was a coupling between both the streamflow and turbidity data during this event.

Starting in the afternoon on 28 October 2015, it is likely that there was a storm event (e.g., high precipitation) that initiated the peak in streamflow at this time. This is a possible explanation for the progression of this event because right after the peak in streamflow, turbidity also peaked. Thus, the storm event allowed the sediment in the stream to cross a critical shear threshold, causing turbidity to increase (Figure 13). Then, after the peak in turbidity, both the turbidity and streamflow decreased at approximately the same pace, allowing both streamflow and turbidity to temporarily return to their respective baseline conditions.

2.5.3 Partitioning Turbidity Events in the Catskills: Watershed Contributions

The various watershed contributions to turbidity can be hypothesized for each of the different stages of the turbidity event types described in sections 2.4.1 and 2.4.2. Here, I present potential watershed contributions for the progression of these two events by outlining the most influential areas of the watershed toward contributing to turbidity.

(a) Streamflow-independent event watershed contributions in the Catskills

From these different stages of the streamflow-independent event shown in Figure 13, we can hypothesize what the contributing areas of the watershed were to turbidity at each of the stages of the event. For example, before the destabilization of the stream bank, the baseline

turbidity was likely generated from the sediment already present in the stream (i.e., in-stream suspension) (Figure 14). But, at peak turbidity during the event, the watershed contribution to turbidity was likely from both in-stream suspension (bank and bed erosion) and the sediment influx from the mass wasting land contribution. Thus, we can separate the components contributing to turbidity at different stages of turbidity events by understanding the potential watershed dynamics contributing to an increased sediment load in the stream (Figure 14).

Figure 14. Watershed delineation from the headwaters of the drainage basin for Stony Clove Creek. The red dot is site number 01362370 (Stony Clove Creek at Chichester, NY). A plausible area of the watershed that could be contributing to turbidity during the first stage of the streamflow-independent event at Stony Clove Creek in 2015 is shown in blue (only the stream is highlighted, as the main source of turbidity at this stage is most likely from in-stream suspension). The second main stage of the event is the peak turbidity, where the potential source contributions to turbidity are from the influx of sediment from the mass wasting event and in-stream scouring. Hypothetical source contributions to turbidity near site 01362370 from land surface erosion at this stage can come from anywhere upstream. The source could be confirmed by comparing upstream and downstream gauges to one another for their respective turbidity values.

(b) Streamflow-dependent event watershed contributions in the Catskills

From the streamflow-dependent event shown in Figure 13, the baseline turbidity from 23 October to 28 October could have been generated from either in-stream suspension or land surface erosion, as it is difficult to definitively partition the relative contributions from the watershed during baseline conditions for this streamflow-dependent event. However, during the peak turbidity for the streamflow-dependent event shown in Figure 13, this peak was likely driven by both land surface erosion and in-stream scouring or suspension (Eqn. 2).

$$\text{Peak turbidity} = \text{land surface erosion} + \text{instream scouring or suspension} \qquad \text{Eqn. (2)}$$

Thus, the main difference between the watershed contributions for streamflow-dependent and streamflow-independent events is streamflow-independent events do not have source contributions coming from in-stream scouring, while streamflow-dependent events do.

2.6 CONCLUSIONS

In this chapter, I outline a conceptual framework describing the different factors and processes that can affect turbidity, in and outside the Catskills. I also discussed different turbidity event types, with a case study of the Catskills. Although there are many factors that can affect turbidity, the factor of streamflow will be examined the most in depth in the following chapter. Nonetheless, it is important to recognize that the multitude of factors capable of affecting turbidity exist and may be present to varying extents throughout the Catskills and other regions. This framework is useful to better contextualize the turbidity dynamics in the Catskills by allowing for the consideration of the many factors and processes that affect it, which has

important implications for watershed management and stream restoration efforts. In the next chapter of this thesis, I will explore the turbidity and streamflow characteristics in the Catskills and will also examine the relationship between turbidity and streamflow across Catskill sites in the context of this conceptual framework.

2.7 References

Beltaos, S., and Burrell, B.C., 2021, Effects of River-Ice Breakup on Sediment Transport and Implications to Stream Environments: A Review: Water, v. 13, p. 2541, https://doi.org/10.3390/w13182541.

Bierman, P.R., and Montgomery, D.R., 2014, Key Concepts in Geomorphology: New York, W.H. Freeman and Company Publishers, p. 1–494.

Brauman, K.A., Daily, G.C., Duarte, T.K., and Mooney, H.A., 2007, The Nature and Value of Ecosystem Services: An Overview Highlighting Hydrologic Services: Annual Review of Environment and Resources, v. 32, p. 67–98, doi:10.1146/annurev.energy.32.031306.102758.

Catskill Streams, 2020, Stream Management Projects, Retrieved November 7, 2022, https://catskillstreams.org/stream-management-program/project-maps/

Cheng, N.N., He, H.M., Yang, S.Y., Lu, Y.J., and Jing, Z.W., 2017, Impacts of topography on sediment discharge in Loess Plateau, China: Quaternary International, v. 440, p. 119-129, doi:10.1016/j.quaint.2016.12.005.

Cunha, D., Sabogal-Paz, L., and Dodds, W., 2016, Land use influence on raw surface water quality and treatment costs for drinking supply in São Paulo State (Brazil): Ecological Engineering, v. 94, p. 516–524, doi:10.1016/j.ecoleng.2016.06.063.

Davies-Colley, R.J., and Smith, D.G., 2001, Turbidity, Suspended Sediment, and Water Clarity: A Review: Journal of the American Water Resources Association, v. 37, p. 1085–1101.

Garver, J.I., 2018, Ice Jam flooding on the lower Mohawk River and the 2018 mid-winter ice jam event Ice Jam flooding on the lower Mohawk River and the 2018 mid-winter ice jam event: Proceedings from the 2018 Mohawk Watershed Symposium, v. 10, p. 12–18.

Hassan, M.A., Church, M., Lisle, T.E., Brardinoni, F., Benda, L., and Grant, G.E., 2005, Sediment transport and channel morphology of small, forested streams: Journal of the American Water Resources Association, v. 41, p. 853–876, doi:10.1111/j.1752-1688.2005.tb03774.x.

Hatch., n.d., Turbidity, Retrieved November 7, 2022, https://www.hach.com/parameters/turbidity

Helvey, J.D., 1980, Effects of a North Central Washington Wildfire on Runoff and Sediment Production: Journal of the American Water Resources Association, v. 16, p. 627–634.

How Wildfires Threaten U.S. Water Supplies, labs.waterdata.usgs.gov/visualizations/fire-hydro/index.html#/. Accessed 17 May 2023.

Kleizen, H.H., Putter, A.B., M., B., and Huynink, S.J., 1995, Particle concentration, size and turbidity: Particle Concentration and Size Analysis, v. 32, p. 897–901.

Meng, X., Zhu, Y., Yin, M., and Liu, D., 2021, The impact of land use and rainfall patterns on the soil loss of the hillslope: Scientific Reports, v. 11, p. 1–10, doi:10.1038/s41598-021-95819-5.

Moran, Barbara. *How A Little Mussel Could Help Save a Merrimack River Salt Marsh*, 19 Oct. 2022, www.wbur.org/news/2022/10/19/salt-marsh-erosion-ribbed-mussels.

Mukundan, R., Pierson, D.C., Schneiderman, E.M., Donnell, D.M.O., Pradhanang, S.M., Zion, M.S., and Matonse, A.H., 2013, Factors affecting storm event turbidity in a New York City

water supply stream: Catena, v. 107, p. 80–88, doi:10.1016/j.catena.2013.02.002.

National Academies of Sciences Engineering and Medicine, 2020, Review of the New York City Watershed Protection Program (2020): Washington, DC, The National Academies Press, 1–401 p., doi:10.17226/25851.

Seeger, M., Errea, M.P., Beguería, S., Arnáez, J., Martí, C., and García-Ruiz, J.M., 2004, Catchment soil moisture and rainfall characteristics as determinant factors for discharge/suspended sediment hysteretic loops in a small headwater catchment in the Spanish pyrenees: Journal of Hydrology, v. 288, p. 299–311, doi:10.1016/j.jhydrol.2003.10.012.

3. Characterization of Streamflow and Turbidity in the Catskills

3.1 BACKGROUND AND CHAPTER OVERVIEW

In this chapter, I characterize streamflow and turbidity across 20 monitoring sites in the Catskills. The key research questions I address in this chapter are as follows:

1. What are the typical streamflow and turbidity conditions in the Catskills, and how do these conditions vary across monitoring sites?
2. How does the relationship between streamflow and turbidity vary spatially and temporally in the Catskills?
3. What factors (e.g., environmental or climatic) are the most influential in generating turbidity in the Catskills?

To answer these questions, I first provide background on the site characteristics to motivate future analyses. I outline the characteristics of each site, data availability at each site, and then provide a map of the watersheds examined in this study. Then, I present the streamflow characteristics across sites in the Catskills. After performing the streamflow characterization, I characterize turbidity in the context of streamflow. This chapter was organized in this manner because streamflow is a driver of turbidity; the analyses on turbidity can then be examined in the context of the streamflow data. In the next sub-section of this chapter, I then discuss the streamflow-turbidity relationship in the Catskills, and how this relationship varies spatially and temporally. Finally, I end with the main conclusions from this chapter.

Before proceeding to the methods, it is necessary to provide background information required to interpret analyses presented later in this chapter. Specifically, in section 3.3.2.1 on the temporal and seasonal trends in streamflow, I discuss the concepts of seasonality indices and

seasonality concentrations. These metrics are useful to better understand seasonal cycles apparent in various data sets. Here, I utilized the metrics of the Seasonality Index (SI) and Seasonality Concentration (SC) after Markham (1970). The SI describes how uniformly a given variable is distributed across months (Stahl, 2022). The SI ranges from 0 to 1, where 0 represents an even spread across the months and 1 represents that the variable is concentrated within a given month. The SC describes the time of the year when the values are most concentrated. The SC represents an angular direction that ranges from 0 to 360, where a value of 0 represents most concentration in the month of January and a value of 180 represents most concentration in the month of June. From the Markham (1970) approach, there is some overlap between months (i.e., the regime centered in January overlaps with the last week of December and the first week of February). The mathematical approach to calculate the SI and SC (Stahl, 2022) are outlined in the methods section of this thesis.

3.2 METHODS

3.2.1 Data Acquisition

For this study, I obtained daily average turbidity and streamflow data for 20 monitoring sites located in the Catskills from 2010 to 2022 (n = 88,255) by querying the National Water Information System (NWIS) web service. The dataRetrieval package in R (De Cicco et al., 2021) was used to obtain these data. The USGS parameter codes used to obtain these data are listed in Table 1. The level of granularity of the turbidity and streamflow data is USGS Site ID and Date. These monitoring sites in the Catskills, most of which are located above the Ashokan Reservoir, have turbidity and streamflow data recorded at the same gage location. The turbidity data I obtained are classified as unfiltered, light source of monochrome near infra-red LED light at

wavelength range of 780-900 nm, and a detection angle of 90 ± 2.5 degrees, reported in formazin nephelometric units (FNU). Three sites located near the Mohawk River were also obtained to compare to the Catskill sites. All data acquisition, analysis, and visualization was performed in the statistical programming language R (R Core Team, 2020).

Table 1. List of the USGS parameter and statistic codes used to obtain the turbidity and streamflow data.

Variable Name	USGS Parameter Code	USGS Statistic Code	USGS Statistics Code Short Name
Turbidity (FNU)	63680	00003	Daily mean
Discharge (cfs)	00060	00003	Daily mean

Table 2. Description of the data sources used in this study in addition to streamflow and turbidity. For more information, see the Model My Watershed Technical Documentation.

Variable(s)	Data set	Additional information
Climate (precipitation and temperature)	PRISM Climate Group AN81m	- Mean monthly precipitation and temperature covering the conterminous US - Period of record: 1981-2020
Land cover	USGS National Land Cover Database (NLCD)	- Land coverage grids - NLCD 2019 was used
Soil group	Gridded Soil Survey Geographic (gSSURGO) 2016	- Database for the conterminous US - Hydrologic Soil Groups is one gSSURGO soil category, based on water infiltration rates during wet, saturated conditions. Low infiltration rate soils translate to high runoff potential.
Stream length and channel slope	National Hydrography Dataset (NHD) plusV2	- Continental US Medium Resolution Stream Network from NHDplusV2 Medium Resolution (1:100,000-scale) NHDFlowlines
Basin slope	NHDplusV2 NED Snapshot DEM	- Slope grids are visualized based on NHD plus National Elevation Data Snapshot Digital Elevation Model
Watershed boundaries	NHDplusV2	- USGS sub basin unit of the eight-digit level (HUC-8), averaging 700 square miles

In addition to the turbidity and streamflow data, I also obtained data on other variables that describe the site characteristics and also can affect turbidity (Table 2). These variables that I obtained data for include climate, land cover, soil group, stream characteristics (e.g., channel slope), and the watershed boundaries for each monitoring station (Table 2). These data were

queried from the Model My Watershed website[1], but the individual data sources for each variable are shown in Table 2.

3.2.2 Data Cleaning and Preparation

Before performing the data analysis, I cleaned and prepared the data. The main components required to prepare the data were to normalize both the streamflow and the turbidity data. Normalization of the turbidity, but especially the streamflow data, was necessary to allow for valid comparisons to be made across monitoring sites. To area normalize the streamflow data, for each monitoring site, I divided the streamflow data (cfs) by the drainage area (ft^2), which was then converted to units of in/month. To normalize the turbidity data, I grouped the data by site and year, and then took the ratio of the median turbidity to the maximum of the median turbidity (Table 3). Unless otherwise specified, the observed turbidity (i.e., unnormalized) data was used throughout my analyses.

Table 3. Method used to normalize the turbidity data.

Calculation of normalized turbidity	Purpose
$\frac{\text{median(Turbidity)}}{\text{max(median(Turbidity))}}$	- Grouped by site and year - Ratio of median turbidity to the maximum median turbidity, assuming the minimum median turbidity is small or negligible.

3.2.3 Computing the SI and SC

The mathematical approach to compute the SI and SC are shown below (Stahl, 2022):

$$SI = \frac{(V_x^2 + V_y^2)^2}{V_{tot}}$$

$$SC = \tan^{-1}\left(\frac{V_y}{V_x}\right) * \frac{180}{\pi} + \alpha$$

[1] https://modelmywatershed.org/

where:

$$\alpha = \begin{cases} 180, \text{when } V_x \leq 0 \\ 0, \text{when } V_x > 0 \text{ and } V_y > 0 \\ 360, \text{when } V_x > 0 \text{ and } V_y \leq 0 \end{cases}$$

where:

V_x represents the x directional component of monthly precipitation; $V_x = \sum V_i * \cos(\theta_i)$

V_y represents the y directional component of the monthly precipitation; $V_y = \sum V_i * \cos(\theta_i)$

V_{tot} represents the sum of the monthly precipitation, where $V_{tot} = \sum V_i$; V_i represents the monthly precipitation for month i, and θ_i is the monthly angle for month i (i.e., January = 15 degrees, February = 45 degrees,…).

Although Markham (1970) implemented the seasonality indices in the context of precipitation, these metrics can be applied to any data set with a seasonal component.

3.2.4 Field Site Visits

Although this study is focused on analyzing existing data on turbidity and streamflow in the Catskills, I visited a few sites in the Catskills during October 2022 to gain an understanding of the geomorphology and extent of stream restoration at some of the sites. For sites located in the Catskills, I visited the Panther Kill stream restoration site, which is shown in Figure 1.

Figure 1. Panther Kill Stream Restoration Site in Woodland Valley. The Panther Kill sediment turbidity reduction project (STRP) is one of a dozen in the Catskills that have been constructed since 2012. The STRP at Panther Kill was near completion in the fall of 2022. Photo taken by C. Swanson on October 28th, 2022.

3.3 RESULTS AND DISCUSSION

3.3.1 Site Characteristics

A description of the watershed characteristics at each site is shown in Table 4. The longest stream with the largest drainage area is the Esopus Creek at Mount Marion, which makes sense because this stream is further from the Esopus Creek Headwaters (Esopus Creek at Big Indian) (Table 4). The watershed for the Esopus Creek at Mount Marion also extends below the Ashokan Reservoir. The streams with the highest mean basin slopes are Myrtle Brook, the Stony Clove at Lanesville sites, and the two Hollow Tree Brook sites. The Hollow Tree Brook and Myrtle Brook sites are primary Stony Clove tributary streams (NYC DEP, 2022).

Table 4. Watershed characteristics at the 20 monitoring sites in this study. USGS station ID is the USGS streamgaging station number. The stream length is the total length of the stream upstream of the gage. The mean channel slope is the first order stream value for each channel. The dominant soil group is the hydrologic soil group distribution with the greatest percent coverage for each monitoring station's watershed. The mean annual precipitation and temperature are the annual average for the available data at each monitoring station.

Stream name	USGS Station ID	Drainage area (mi^2)[1]	Stream length (km)[2]	Mean basin slope (%)[3]	Mean channel slope (%)[2]	Dominant soil group[4]	Mean annual precipitation (cm)[5]	Mean annual temperature (°F)[5]
Esopus Creek Below Lost Clove Rd at Big Indian	0136219503	29.6	12.47	31.4	3.1	Very Slow Infiltration	138	41.6
Birch Creek at Big Indian	013621955	12.5	10.26	24.9	4.2	Very Slow Infiltration	120	42.6
Esopus Creek at Allaben	01362200	63.7	33.46	30.4	3.6	Very Slow Infiltration	129.6	42.3
Panther Kill at Woodland Valley Rd Nr Phoenicia	01362297	3.5	4.97	38.4	8.1	Very Slow Infiltration	140.4	42.9
Woodland Creek Above Mouth at Phoenicia	0136230002	20.6	14.46	34.9	4.6	Very Slow Infiltration	147.6	42.5
Myrtle Brook at State Hwy 214 at Edgewood	01362322	1.8	4.42	40.1	2.5	Slow Infiltration	142.8	43.2
Stony Clove Creek Near Lanesville	01362330	7.5	5.22	39.5	2.5	Slow Infiltration	142.8	43.2
Stony Clove Creek at Wright Rd Near Lanesville	01362332	8.1	5.66	39.4	2.5	Slow Infiltration	142.8	43.2
Stony Clove Cr at Janssen Rd at Lanesville	01362336	9.2	7.25	38.5	2.5	Slow Infiltration	141.6	43.5
Hollow Tree Brook at Lanesville	01362342	2	7.29	39.3	2.5	Slow Infiltration	140.4	43.6
Hollow Tree Brook at St Hwy 214 at Lanesville	01362345	4.6	7.29	39.3	2.5	Slow Infiltration	140.4	43.6
Warner Creek at Silver Hollow Rd Nr Chichester	01362356	8.6	11.46	33.5	4.8	Very Slow Infiltration	134.4	45
Warner Creek Near Chichester	01362357	8.7	11.67	33.4	4.8	Very Slow Infiltration	134.4	45
Ox Clove Near Mouth at Chichester	01362368	3.8	23.94	35.4	3.7	Moderate Infiltration	136.8	44.6
Stony Clove Creek Blw Ox Clove at Chichester	01362370	30.9	23.94	35.8	3.7	Moderate Infiltration	136.8	44.6
Beaver Kill at Mount Tremper	01362487	25	8.87	25.6	6.5	Very Slow Infiltration	135.6	45.3
Little Beaver Kill at Beechford Near Mt Tremper	01362497	16.5	8.32	18.5	0.7	Very Slow Infiltration	127.2	47
Esopus Creek at Coldbrook	01362500	192	103.55	29.8	4.2	Very Slow Infiltration	133.2	43.8
Esopus Creek Near Lomontville	01363556	279	149.51	25.5	3.8	Very Slow Infiltration	132	44.8
Esopus Creek at Mount Marion	01364500	419	201.53	20.9	3.7	Slow Infiltration	127.2	45.7

[1]Source: USGS National Water Information System (NWIS) [2]Source: National Hydrography Dataset Plus (NHDPlusV2)
[3]Source: National Hydrography Dataset Plus (NHDPlusV2 NEDSnapshot DEM) [4]Source: United States Department of Agriculture (USDA) Gridded Soil Survey Geographic (gSSURGO) 2016 Database [5]Source: PRISM (Parameter-elevation Regressions on Independent Slopes Model) Climate Group 30-Year Normals

The stream with the lowest mean basin slope is the Little Beaver Kill. Panther Kill has the highest mean channel slope compared to the other streams (Figure 1), whereas Little Beaver Kill has the lowest mean channel slope. As evidenced by the steep slope of Panther Kill, the channel is actively incising, which means it is important to stabilize the channel bed and the toe of the slope (Figure 1). Hence, the Panther Kill STRP has been implemented to limit erosional contact with the glacial legacy sediment and thus minimize the effects of elevated suspended-sediment concentrations (SSCs) in the stream channel. Most sites examined in this study (18 out of 20) have a dominant soil group of either "Very Slow Infiltration" or "Slow Infiltration," with the exception of the Ox Clove and Stony Clove at Chichester sites, which have "Moderate Infiltration" as their dominant soil group. It is expected that most sites have slow soil infiltration because the soils in the region have developed in glacial till, which generally has low porosity due to compression under glacial ice (Earle, 2015).

In terms of the climate data, Woodland Creek at Phoenicia has the highest average annual precipitation, whereas Birch Creek at Big Indian has the lowest average annual precipitation. The range on the average annual precipitation across all monitoring sites is 27.6 cm; mean annual precipitation ranged from a low of 120 cm/yr at Birch Creek at Big Indian to a high of 147.6 cm/yr at Woodland Creek at Phoenicia. The average annual temperature for each monitoring site exhibits a small range in values, encompassing a range of 5.4˚F across all the sites. The mean annual temperature ranged from a low of 41.6˚F at Esopus Creek at Big Indian to a high of 47˚F at the Little Beaver Kill. Although there may be seasonal trends underlying the differences in the climate data aggregated as averages across sites, the results from Table 4 nonetheless highlight the watershed characteristics across monitoring sites examined in this study.

In addition to presenting the site characteristics, the data availability at each site is shown in Table 5. All the monitoring sites have turbidity data available, but some sites are missing streamflow data (Table 5). The sites with missing streamflow data include two of the Stony Clove sites, one of the Hollow Tree Brook sites, and one of the Warner Creek sites. Table 5 also reveals a data quantity issue at one site in the Catskills, Panther Kill, as this site only has turbidity and streamflow data from 2021 to 2022 ($n_{turbidity}$ = 228, $n_{streamflow}$ = 231). This result on the data availability at Panther Kill was expected, considering that the STRP at Panther Kill neared completion in the fall of 2022. The site with the greatest number of turbidity measurements is Warner Creek near Chichester (01362357). Most sites have sufficient streamflow data, with the exception of Panther Kill. The monitoring sites with the longest turbidity periods of record are the two Beaver Kill sites (Beaver Kill and Little Beaver Kill), Esopus at Allaben, and Stony Clove at Chichester. Most sites, with the exception of Panther Kill, Esopus at Big Indian, Myrtle Brook, Stony Clove at Lanesville (01362336), and Ox Clove near Chichester, have streamflow measurements since 2013 (or earlier) and onward. Also, it is important to note that each site that has both turbidity and streamflow data available has more streamflow measurements on record compared to turbidity measurements.

The watersheds examined in this study are shown in Figure 2. The Stony Clove Creek is the largest tributary to the Esopus Creek, and it serves as an experimental sub-basin to examine suspended sediment (SS) and turbidity dynamics at the reach to sub-basin scale (NYC DEP, 2021). The Stony Clove sub-basin monitoring stations are examined for five streams: Stony Clove Creek, Ox Clove Creek, Warner Creek, Hollow Tree Brook, and Myrtle Brook (Table 5).

Table 5. Data availability for each monitoring site. Streamflow (Q) data are available before 2010 from NWIS, but all analyses on streamflow were performed from 2010 onward.

Stream name	USGS Station ID	Start of turbidity record	End of turbidity record	Number of turbidity measurements	Start of Q record	End of Q record	Number of Q measurements
Birch Creek at Big Indian	013621955	10/1/2016	6/1/2022	1763	9/30/1998	7/20/2022	4561
Esopus Creek at Allaben	01362200	11/23/2010	7/20/2022	2208	10/1/1963	7/20/2022	4561
Woodland Creek Above Mouth at Phoenicia	0136230002	11/23/2011	7/20/2022	2424	8/1/2003	7/20/2022	4561
Hollow Tree Brook at Lanesville	01362342	12/14/2011	7/20/2022	2402	10/1/1997	7/20/2022	4561
Stony Clove Creek Blw Ox Clove at Chichester	01362370	11/23/2010	7/20/2022	3304	2/1/1997	7/20/2022	4561
Little Beaver Kill at Beechford Near Mt Tremper	01362497	11/17/2010	7/20/2022	2640	10/1/1997	7/20/2022	4561
Esopus Creek at Coldbrook	01362500	10/1/2016	7/20/2022	1743	10/1/1931	7/20/2022	4561
Esopus Creek at Mount Marion	01364500	11/9/2013	7/20/2022	2934	4/4/1907	7/20/2022	4561
Beaver Kill at Mount Tremper	01362487	11/17/2010	7/20/2022	3372	9/30/2010	7/20/2022	4289
Warner Creek Near Chichester	01362357	5/30/2012	7/20/2022	3416	5/29/2012	7/20/2022	3682
Esopus Creek Near Lomontville	01363556	11/8/2013	7/20/2022	2953	11/8/2013	7/20/2022	3154
Esopus Creek Below Lost Clove Rd at Big Indian	0136219503	11/15/2016	7/20/2022	1977	10/12/2016	7/21/2022	2085
Stony Clove Cr at Janssen Rd at Lanesville	01362336	11/5/2016	7/20/2022	1874	11/15/2016	7/21/2022	2051
Ox Clove Near Mouth at Chichester	01362368	11/23/2016	7/20/2022	1888	12/15/2016	7/21/2022	2016
Myrtle Brook at State Hwy 214 at Edgewood	01362322	11/15/2016	7/20/2022	1721	11/14/2016	7/20/2022	2002
Panther Kill at Woodland Valley Rd Nr Phoenicia	01362297	9/16/2021	7/20/2022	228	10/23/2021	7/20/2022	231
Stony Clove Creek Near Lanesville	01362330	4/11/2014	6/2/2022	2167	NA	NA	NA
Stony Clove Creek at Wright Rd Near Lanesville	01362332	12/11/2014	6/2/2022	2090	NA	NA	NA
Hollow Tree Brook at St Hwy 214 at Lanesville	01362345	12/21/2016	7/19/2022	1920	NA	NA	NA
Warner Creek at Silver Hollow Rd Nr Chichester	01362356	9/30/2014	6/2/2022	2359	NA	NA	NA

The Esopus Creek is important to monitor in terms of SS and turbidity dynamics because it has glacially derived sources of clay and silt, which are key factors in generating turbidity in the

Ashokan Reservoir (NYC DEP, 2021). Within the upper Esopus Creek (UEC) basin, McHale and Siemion (2014) found that the Stony Clove Creek, Beaver Kill, Woodland Creek, and Birch Creek sub-basins contributed the most to SSC and turbidity, respectively. The UEC watershed is defined by the Esopus Creek at Coldbrook (01362500) monitoring station, which is located approximately 0.6 miles upstream from the Ashokan Reservoir (McHale and Siemion, 2014). The Esopus Creek near Lomontville and Mount Marion sites were included in this study to compare to the results from the UEC basin.

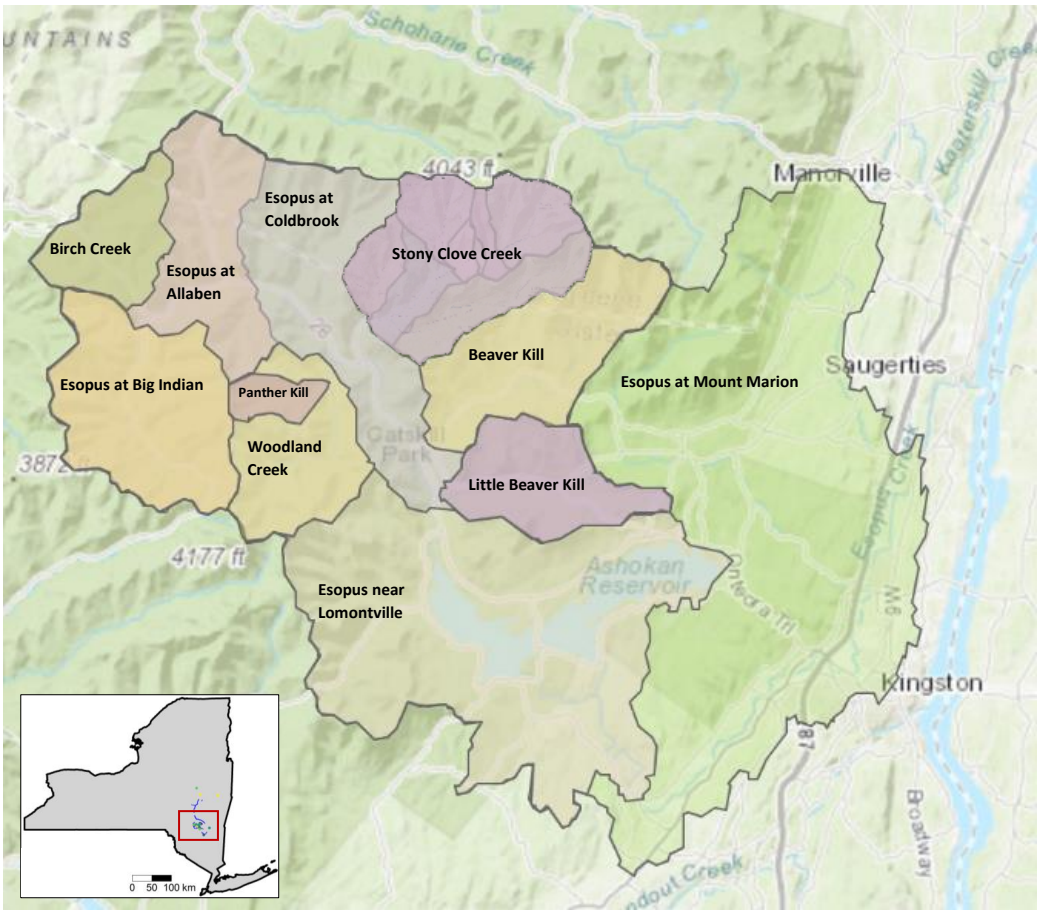

Figure 2. Map of the watershed study area for each monitoring station. The Esopus at Big Indian is the Esopus Creek Headwaters (Wang et al., 2021).

3.3.2 Streamflow Characteristics

In this section, I present the streamflow characteristics for the monitoring sites located in the Catskills before presenting the turbidity characteristics. The summary statistics for the area normalized streamflow at each site are shown in Table 6.

Table 6. Summary statistics for the daily normalized streamflow (Q) data by site. The normalized streamflow values are converted to units of in/month. Note that four sites in the Catskills are missing streamflow data (Table 5); thus, there are only 16 monitoring stations shown in this table. Data are aggregated based on the full period of record (2010 – 2022).

Stream name	USGS Station ID	Mean Q (in/month)	Median Q (in/month)	Minimum Q (in/month)	Maximum Q (in/month)	Standard deviation of Q (in/month)
Esopus Creek at Coldbrook	01362500	4.04	2.7	0.16	170.85	5.63
Woodland Creek Above Mouth at Phoenicia	0136230002	3.53	1.97	0.14	219.64	6.24
Hollow Tree Brook at Lanesville	01362342	3.48	2.02	0.12	168.22	6.31
Stony Clove Creek Blw Ox Clove at Chichester	01362370	3.39	1.93	0.15	189.99	6.7
Stony Clove Cr at Janssen Rd at Lanesville	01362336	3.38	2.12	0.19	105.65	5.13
Myrtle Brook at State Hwy 214 at Edgewood	01362322	3.36	2.1	0.17	84.37	4.47
Panther Kill at Woodland Valley Rd Nr Phoenicia	01362297	3.25	2.51	0.87	29.38	2.53
Esopus Creek Below Lost Clove Rd at Big Indian	0136219503	3.01	2.12	0.08	95.15	4.52
Esopus Creek at Allaben	01362200	2.99	1.83	0.15	176.86	5.06
Warner Creek Near Chichester	01362357	2.93	1.78	0.05	136.36	4.96
Ox Clove Near Mouth at Chichester	01362368	2.75	1.75	0.01	88.01	3.97
Beaver Kill at Mount Tremper	01362487	2.72	1.38	0.03	96.37	4.89
Little Beaver Kill at Beechford Near Mt Tremper	01362497	2.7	1.36	0.04	88.43	5.09
Birch Creek at Big Indian	013621955	2.66	1.73	0.19	67.14	3.31
Esopus Creek at Mount Marion	01364500	1.65	0.75	0.05	48.32	2.59
Esopus Creek Near Lomontville	01363556	1.05	0.25	0.01	24.97	1.68

The top four sites in the Catskills by their mean area normalized streamflow are the Esopus at Coldbrook (01362500), Woodland Creek at Phoenicia (0136230002), Hollow Tree Brook at Lanesville (01362342), and Stony Clove Creek at Chichester (01362370) (Table 6). These results generally correspond to results obtained by the NYC DEP (2022), who found that during a study period from October 2016 to September 2021, the highest mean annual runoff (MAR) (i.e., area normalized streamflow) was observed at Woodland Creek (0136230002) and Stony Clove Creek (01362370), respectively. The Esopus at Coldbrook had the largest mean normalized streamflow compared to all other sites in the Catskills; the Esopus at Coldbrook is the outlet of the Esopus Creek watershed (NYC DEP, 2008) and has streamflow contributions from the Shandaken Tunnel (Table 6). The Woodland Creek site (0136230002) having the second highest mean normalized streamflow can partly be explained by this site having the greatest mean annual precipitation across all sites (Table 4). The sub-basins part of the lower Esopus Creek watershed, Esopus Creek at Mount Marion and Lomontville, had the smallest mean normalized streamflow values for the examined period of record. These low mean normalized streamflow values at these sites can be explained by the segmented nature of the lower Esopus Creek watershed; the watershed transitions from a steeply sloping, fast moving channel reach to a wider and slower stream located at Lomontville (NYC DEP, 2020). However, there are sources of suspended sediment to the lower Esopus Creek that come from the sub-basins that drain to the lower Esopus Creek, so although the influence of streamflow from the Ashokan Reservoir decreases further downstream (NYC DEP, 2020), it is nonetheless important to monitor turbidity and SSCs in both the upper and lower Esopus Creek watersheds.

Additionally, although Panther Kill has the highest mean channel slope (Table 4), it does not have the highest mean normalized streamflow across all sites (Table 6). This observation can

be explained by the stream gradient being only one factor contributing to water flow within a stream; the stream channel geometry also contributes to water flow (Earle, 2015). In addition to stream channel geometry, the normalized streamflow can be affected by precipitation, basin slope, land cover, geology, and storage (NYC DEP, 2022). This observation at Panther Kill may also be explained by the limited data availability at this site (Table 5). The highest normalized streamflow value ever recorded within the period of record was at Woodland Creek at Phoenicia (Q = 219.64 in/month), which occurred on 28 August 2011 as a result of Hurricane Irene.

After presenting the streamflow characteristics at each site, it is useful to examine the spatial distribution of the mean normalized streamflow values across sites (Figure 3).

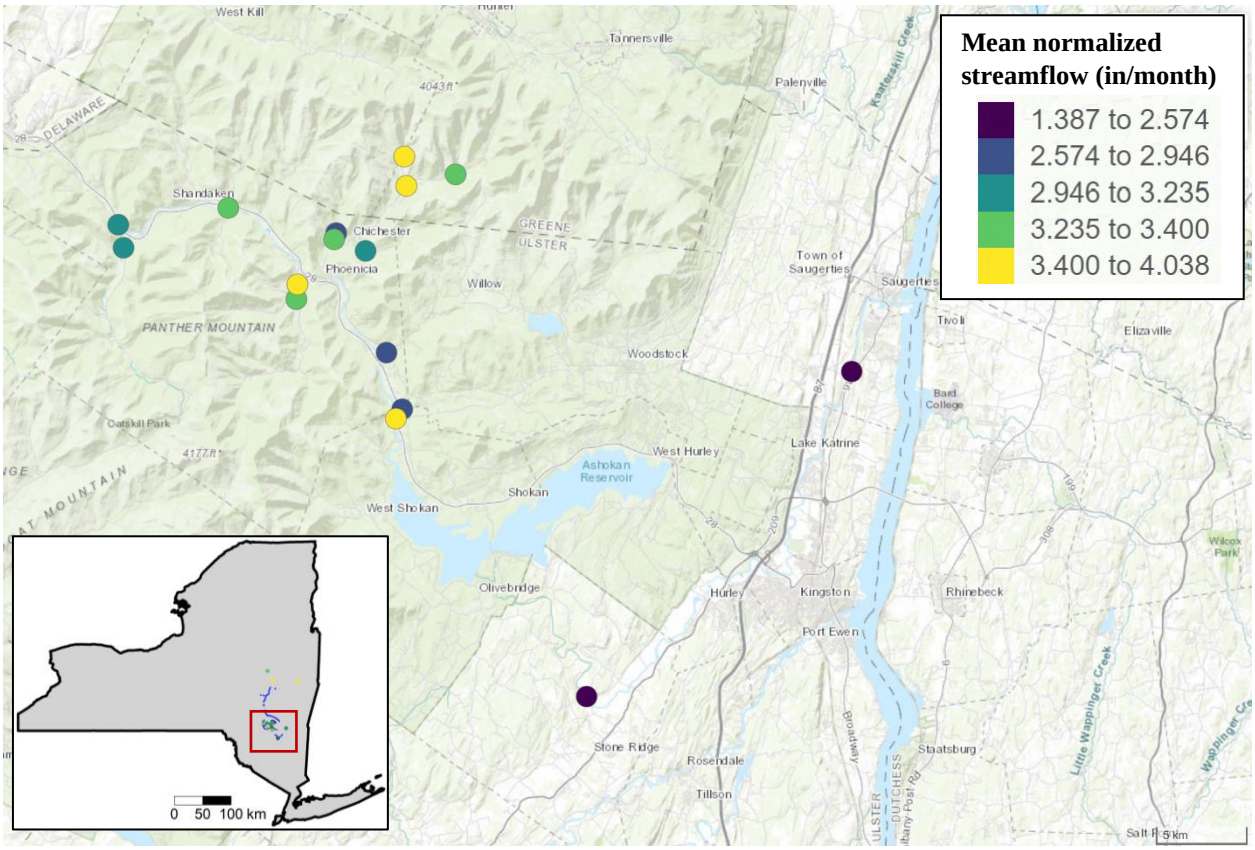

Figure 3. Map of the mean normalized streamflow by site in the Catskills. Data are binned by quantiles. The period of record shown is from the beginning of 2017 to July 2022. This period of record was chosen to select the most amount of normalized streamflow data that are overlapping across monitoring sites, which helps to examine differences in the underlying watershed characteristics rather than confounding both the spatial and temporal trends in the data.

Spatially, there is a statistical difference in mean normalized streamflow across monitoring sites (ANOVA, $P < 0.05$); this result suggests that there may be various controls on streamflow that may differ across sites, such as their average annual precipitation and stream channel gradients (Table 4). The sites with the highest mean normalized streamflow values tend to be located in the northeastern Catskills (Figure 3). Specifically, these sites correspond to the Stony Clove sites and Hollow Tree Brook. This result corresponds to results from McHale and Siemion (2014), who found that streamflow was generally higher during 2010 to 2012 than the previous 10 years, especially at Hollow Tree Brook. Although McHale and Siemion (2014) used an earlier period of record than this study, the results from Figure 3 suggest that the Hollow Tree Brook and Stony Clove sites may be more susceptible to elevated normalized streamflow, which is a potential driver of turbidity.

However, the results on the broad spatial trends for mean normalized streamflow in the Catskills are somewhat unexpected; we generally would expect streamflow to be higher at the headwaters (e.g., Esopus at Big Indian) due to greater stream gradients. But, this trend is not the case according to Figure 3. These results likely cannot be explained by the spatial variability in stream channel gradients, as the headwaters tend to have the highest mean basin slopes in the Catskills, which is to be expected (Table 4). Additionally, the contributions from baseflow can affect the observed streamflow at each site; with lower baseflow contributions, then lower streamflow would be observed, regardless of the stream gradient. Thus, further investigation is required to understand other potential reasons why the spatial variability exists in the mean normalized streamflow across the monitoring sites.

3.3.2.1 Temporal and seasonal trends in streamflow

In this sub-section, I present the temporal (annual changes) and seasonal (monthly changes) in the streamflow data in the Catskills. These fluctuations in streamflow are important to quantify in order to better interpret the seasonal and temporal trends in turbidity. Additionally, these trends are important to discern in order to better characterize the differences in watershed characteristics, as differences in streamflow across sites are confounded by both spatial and temporal factors. Firstly, examination of the temporal trends, specifically with respect to the mean annual normalized streamflow across sites, is shown in Figure 4. The mean annual normalized streamflow across sites appears to follow a similar trend though time, but the magnitudes in the mean normalized streamflow differ across sites (Figure 4).

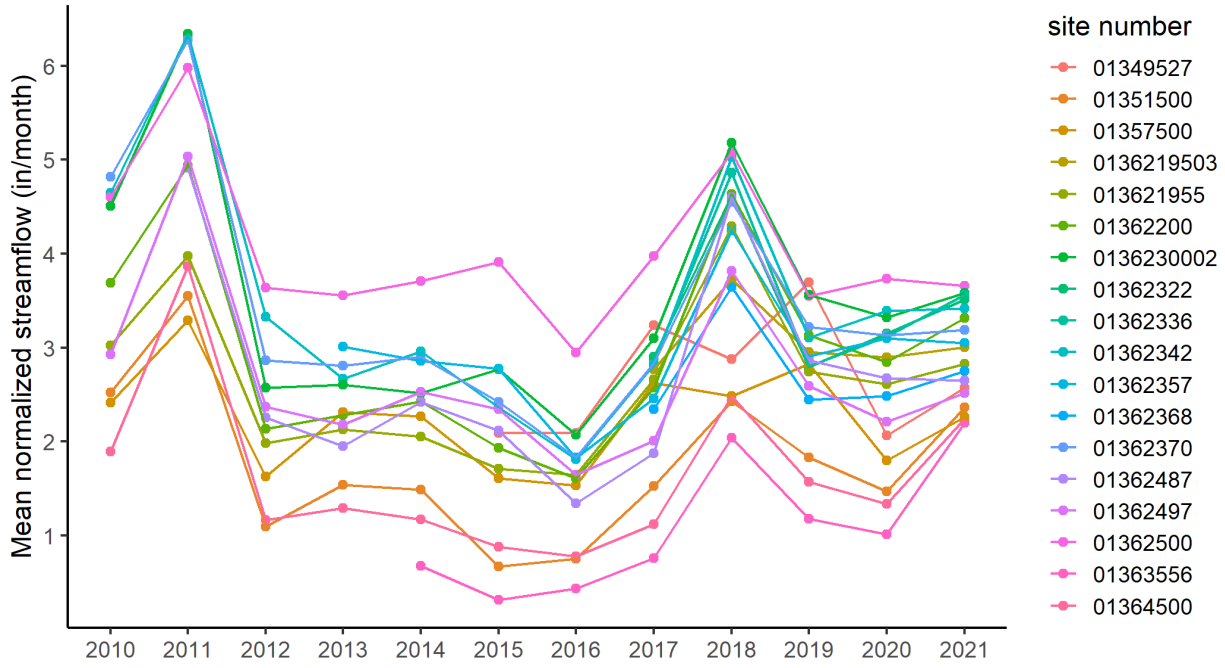

Figure 4. Mean annual normalized streamflow by site for the 2010-2021 period. Lines are colored by site number (Table 4). For each year at each site, I removed the data point if the number of flow measurements in that year for that site was less than 350 to ensure that each year had sufficient data (n = 365 represents a full year's worth of data).

The range of the average annual normalized streamflow across all years and sites is 0.316 in/month to 6.34 in/month. The typical (50th percentile) mean normalized streamflow across all years and sites is approximately 2.8 in/month (Figure 4). There are also clear dips and peaks in the mean normalized streamflow across years. For example, 2011, 2018, and 2021 had extreme mean normalized streamflow across most sites relative to the rest of the years in the study period. This result makes sense because there were large hurricanes during these years (Irene in 2011, Florence in 2018, and Henri in 2021). Contrarily, 2016 appears to have a dip in the mean normalized streamflow across most sites, which can be explained by this year being an anonymously dry year in terms of its mean annual precipitation. Additionally, Hollow Tree Brook (01362342) has one of the highest mean normalized streamflow across years for all the sites included in the study area (Figure 4), which corresponds to the results from Figure 3.

After examination of the temporal trends in the mean normalized streamflow data, seasonality analysis can be useful to indicate whether there are seasonal patterns in the normalized streamflow data, such as when the peaks and dips occur (Table 7). Performing this analysis reveals that across all years and all sites in the study period (2010 – 2022), the mean normalized streamflow was highest in April, March, and December in the Catskills (Table 7). April has the greatest mean normalized streamflow compared to the rest of the months, which makes sense considering that snow melt is likely to occur in this month. The months with the lowest mean normalized streamflow values across all years and sites were June, July, and August (Table 7). This result makes sense considering that the summer months are likely to have the lowest streamflow in the Catskills. This is because although precipitation is relatively aseasonal, temperature is very seasonal in the region. Thus, these months have precipitation similar to the rest of the year, but they are warmer and have more active vegetation.

Table 7. Summary statistics for the seasonal trends in the mean monthly normalized streamflow across all monitoring sites. Data are from 2010 – 2022. The number of flow measurements (count field) are generally consistent across all months. February and September have the most sparse flow data out of all the months on record.

Month	Mean normalized Q (in/month)	Median normalized Q (in/month)	Minimum normalized Q (in/month)	Maximum normalized Q (in/month)	Standard deviation normalized Q (in/month)	Count
1	2.8	2.06	0.1	92.61	3.45	5969
2	2.48	1.69	0.07	57.37	2.97	5439
3	3.75	2.48	0.06	93.71	5.37	6008
4	5.07	3.98	0.06	49.77	4.56	5818
5	3.04	2.24	0.04	77.15	3.71	6017
6	1.72	1.13	0.05	40.86	2.22	5788
7	1.5	0.71	0.04	59.67	2.79	5456
8	1.97	0.61	0.03	219.64	7.08	5456
9	2.01	0.57	0.02	71.75	4.96	5279
10	2.51	1.23	0.01	158.87	5.64	5541
11	2.73	1.97	0.03	45.47	3.16	5447
12	3.65	2.34	0.09	153.75	6.62	5690

Therefore, evapotranspiration demand is high, which means less runoff is generated during these months. The greatest variance in the normalized streamflow occurs in August across all sites. This result can be explained by the maximum normalized streamflow occurring in August, where there may have been a large storm one year during this month. Although examining summary statistics across years in the study period provides useful information for when the normalized streamflow peaks, it does not provide information with respect to how this trend varies across sites. Thus, seasonality indices and seasonality concentrations computed for each monitoring site in the Catskills can be used to address this question (Figure 5).

The monitoring sites in the Catskills show a relatively even spread in the mean monthly normalized streamflow, which is indicated by the SI being close to zero across all sites (Figure 5). But, Birch Creek (013621955) has the greatest SI, meaning this site has its mean normalized streamflow most concentrated in a select number of months relative to the rest of the sites in the

Catskills (Figure 5). Contrarily, Stony Clove at Janssen at Lanesville (01362336) has the smallest SI, suggesting this site has the most even spread in its mean normalized streamflow across months. Nonetheless, this result suggests that the mean normalized streamflow is relatively evenly spread across all months throughout the Catskills.

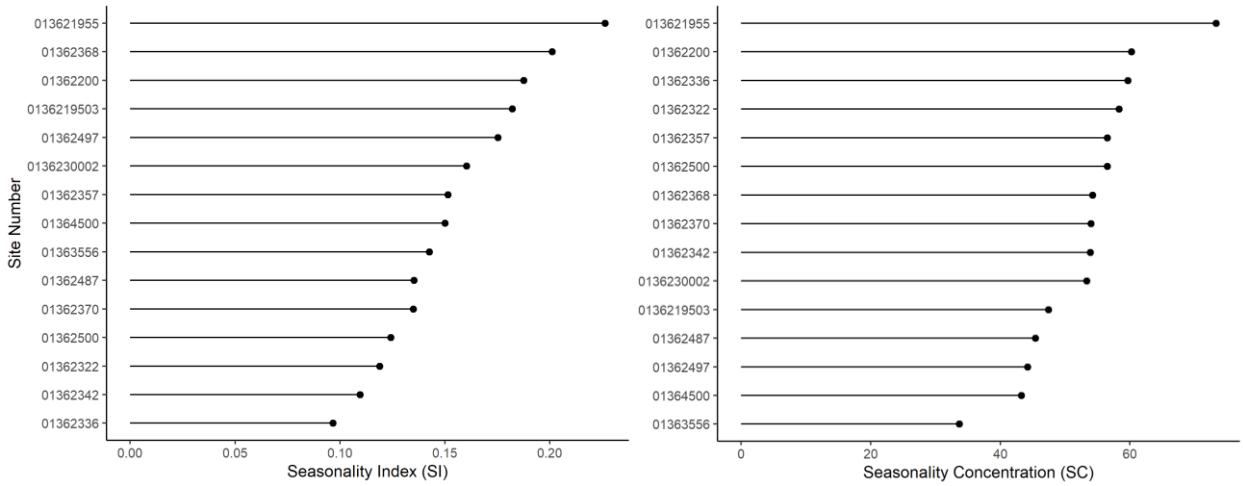

Figure 5. Markham (1970) Seasonality Indices (SI) and Seasonality Concentrations (SC) computed on the mean monthly normalized streamflow data for each site in the Catskills. Sites shown on the graphs were filtered to only include site and year combinations that exceeded a count of 350 observations. This data filtering approach was undertaken to ensure that the SI and SC at each site were not artificially skewed to favor certain months solely based on their data availability.

Examination of the SC for each site in the Catskills reveals that the Esopus Creek near Lomontville (01363556) has its mean normalized streamflow most focused in late January to early February (SC ≈ 33) (Figure 5). For sites upstream of the Ashokan Reservoir, the Little Beaver Kill (01362497) has its mean normalized streamflow most focused in February (SC ≈ 44), whereas Birch Creek (013621955) has its mean normalized streamflow most focused in March (SC ≈ 73). These results suggest that the normalized streamflow is relatively evenly

concentrated throughout the monitoring sites in the Catskills, with the greatest concentration within the months of February and March (Figure 5).

Although the previous analyses regarding seasonal and temporal changes are informative, it is also useful to examine temporal and seasonal trends simultaneously for sites in the Catskills. For data with both seasonal and long-term components, cycle plots can be effective in representing these data (Figure 6). For Birch Creek (013621955), the seasonal and long-term trends in the average monthly normalized streamflow are evident (Figure 6).

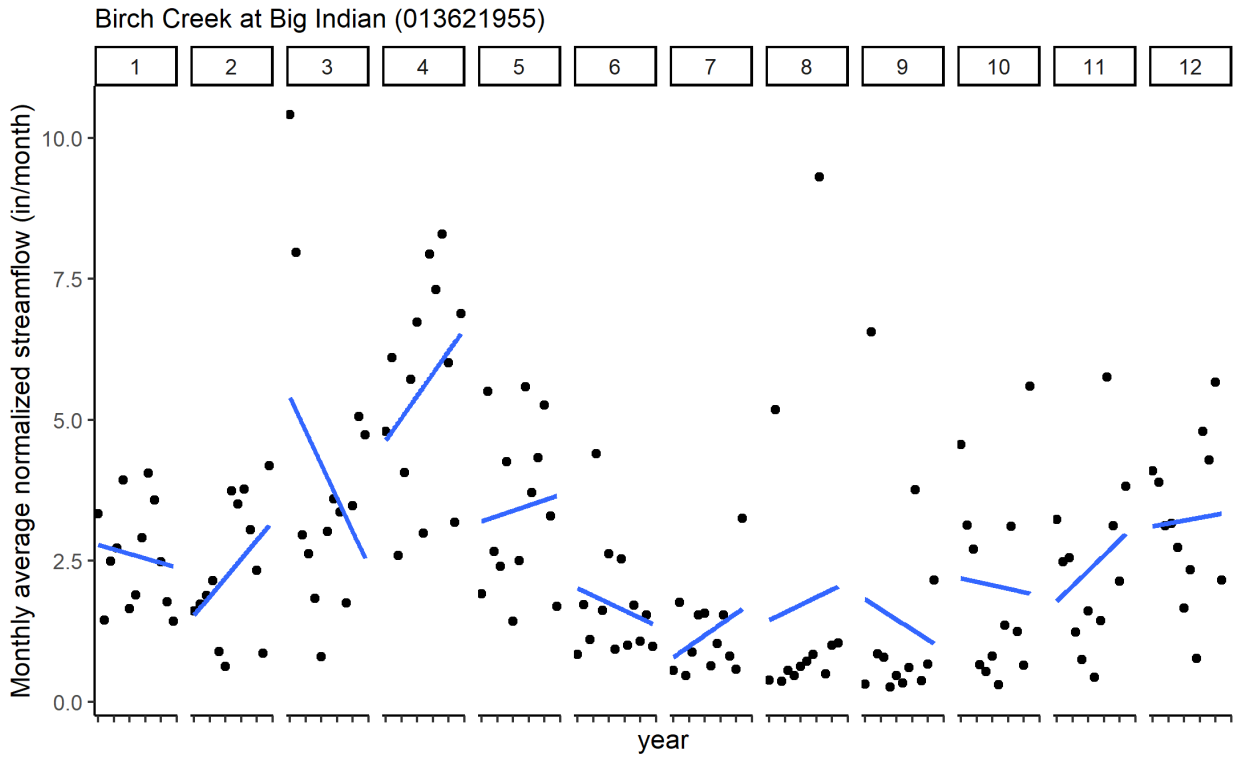

Figure 6. Cycle plot for one site, Birch Creek (013621955). The period of record shown is from 2010 to 2022. The top row of the figure represents each month (1-12), whereas each tick at the bottom of the x-axis represents an increment of every 2 years, starting at 2010 all the way to 2022. This site was selected as an example to demonstrate both the seasonal and long-term trends in the normalized streamflow data because it had the highest SI out of all the Catskill sites (Figure 5). Linear regression is shown for each month (computed across all years in that month) as a solid blue line.

April overall appears to have the highest mean normalized streamflow across all months at Birch Creek (Figure 6). The month of April has also been receiving greater mean normalized streamflow through time (from 2010 to 2022), as evidenced by the blue regression line (Figure 6). This result can perhaps be explained by earlier timings of spring snow melt in the Catskills, which corresponds to expected results by Burns et al. (2007), who predict for this region reduced snowfall and earlier timings of snow melt-driven runoff as a result of higher mean annual air temperatures over a 50-year period. After performing this analysis across all sites in the Catskills, 8 out of the 15 sites (≈ 53%) (with the exception of Panther Kill, as this site only has two years of data available) experienced greater normalized streamflow in April through time (i.e., across years). Thus, it is difficult to predict whether more frequent extreme normalized streamflow events will occur in the Catskills during April based on this result alone. Nonetheless, these predicted shifts resulting in streamflow in earlier months as shown at Birch Creek have important implications for projected changes in stream turbidity (e.g., Mukundan et al., 2013), which will further be discussed in the next section of this thesis.

3.3.3 Turbidity Characteristics in the Context of Streamflow

In this section, I present the turbidity characteristics for the monitoring sites in the Catskills, which will complement the results from the streamflow characteristics. The summary statistics for turbidity at each site are shown in Table 8. The site with the highest mean turbidity is Panther Kill (01362297) (Table 8). However, Panther Kill only has two years of available data, which can impact the results. With the exception of Panther Kill, the top four sites by their mean turbidity from 2010 to 2022 are Hollow Tree Brook (1362345), Stony Clove at Chichester

(1362370), Woodland Creek (0136230002), and Ox Clove (1362368) (Table 8). These results partially correspond to the findings by McHale and Siemion (2014).

Table 8. Summary statistics for the turbidity data by site. Data are aggregated based on the full period of record (2010 – 2022). Data are sorted in descending order based on the mean turbidity. The turbidity data are unnormalized.

Stream name	USGS Station ID	Mean turbidity (FNU)	Median turbidity (FNU)	Minimum turbidity (FNU)	Maximum turbidity (FNU)	Standard deviation of turbidity (FNU)
Panther Kill at Woodland Valley Rd Nr Phoenicia	01362297	41.39	32.9	7.7	346	33.79
Hollow Tree Brook at St Hwy 214 at Lanesville	01362345	25.70	4.9	1.0	866	65.13
Stony Clove Creek Blw Ox Clove at Chichester	01362370	20.36	6.0	1.1	1190	47.19
Woodland Creek Above Mouth at Phoenicia	0136230002	16.32	7.9	0.8	782	29.93
Ox Clove Near Mouth at Chichester	01362368	15.89	8.3	1.4	336	23.52
Birch Creek at Big Indian	013621955	15.06	6.9	0.9	916	35.96
Esopus Creek at Coldbrook	01362500	13.51	6.5	0.4	1000	36.15
Warner Creek Near Chichester	01362357	12.96	6.5	0.2	441	19.61
Esopus Creek at Allaben	01362200	12.64	5.2	0.5	912	36.69
Beaver Kill at Mount Tremper	01362487	11.49	2.8	0.0	1010	33.47
Esopus Creek at Mount Marion	01364500	9.97	4.5	0.7	338	21.49
Warner Creek at Silver Hollow Rd Nr Chichester	01362356	9.93	5.1	0.0	158	14.34
Esopus Creek Near Lomontville	01363556	8.29	2.6	0.0	237	21.05
Stony Clove Cr at Janssen Rd at Lanesville	01362336	5.24	2.6	0.2	210	11.85
Esopus Creek Below Lost Clove Rd at Big Indian	0136219503	5.05	1.7	0.3	634	20.33
Stony Clove Creek at Wright Rd Near Lanesville	01362332	3.81	2.2	0.2	347	9.88
Stony Clove Creek Near Lanesville	01362330	2.82	1.3	0.0	337	10.19
Little Beaver Kill at Beechford Near Mt Tremper	01362497	2.45	1.4	0.0	120	5.50
Myrtle Brook at State Hwy 214 at Edgewood	01362322	2.27	1.5	0.1	112	5.11
Hollow Tree Brook at Lanesville	01362342	0.82	0.6	0.0	28.9	1.34

Although McHale and Siemion (2014) examined a period of record before this study (2009-2012), they concluded that turbidity values and SSCs rarely were high at the headwater site on the Esopus main channel at Olivera, Hollow Tree Brook (01362342), and Little Beaver Kill. However, McHale and Siemion (2014) only examined the Hollow Tree Brook site number 01362342, which in fact was found to have the lowest mean turbidity according to Table 8. Thus, the results for Hollow Tree Brook (01362342) correspond to the study by McHale and Siemion (2014). However, the results from Hollow Tree Brook (01362345) starkly contrast to Hollow Tree Brook (01362342); the difference in their mean turbidity is 24.88 FNU (Table 8). Perhaps these results can be explained by more frequent bank failures only experienced at Hollow Tree Brook (01362345), but not at Hollow Tree Brook (01362342). This can serve as a possible explanation because McHale and Siemion (2014) stated that Hollow Tree Brook (01362342) serves as a reference tributary because it did not have any significant bank failures or contain any chronic sources of suspended sediment.

Additionally, note the high standard deviation in turbidity at Hollow Tree Brook (01362345) (Table 8). Although Hollow Tree Brook (01362345) has the highest recorded standard deviation across all sites in the Catskills, Hollow Tree Brook (01362342) has the lowest recorded standard deviation across all sites (Table 8). I initially thought this could be due to a discrepancy in data quantity (e.g., one site having much more data than the other, thus leading to higher variance), but this is not necessarily the case (Table 5). Although Hollow Tree Brook (01362342) has more data (n_turb = 2402) than Hollow Tree Brook (01362345) (n_turb = 1920), I would not expect data quantity alone to affect the standard deviation this drastically for the turbidity. Thus, differences in the frequency of bank failures at each Hollow Tree Brook site is a plausible hypothesis to explain these results. However, the underlying mechanisms to explain

why the frequency of these bank failures may differ at each site at Hollow Tree Brook remains unclear. Also, note that the site closest to Hollow Tree Brook (01362345), Stony Clove at Lanesville (01362336), has a relatively low standard deviation of turbidity relative to Hollow Tree Brook (01362345) (Table 8). Thus, further investigation is required to determine what may explain the differences (e.g., differences in the frequency of geomorphic processes) in the results at the Hollow Tree Brook sites.

The results from the mean turbidity from Stony Clove Creek (01362370) and Woodland Creek (0136230002) from this study correspond to results from McHale and Siemion (2014). They concluded that Stony Clove produces more sediment per hectare than any other tributary that they examined in their study; Woodland Creek also was consistently high in terms of sediment production, but not as high as Stony Clove Creek. Stony Clove Creek served as a chronic source of suspended sediment to the Esopus Creek (McHale and Siemion, 2014). However, the turbidity production at Stony Clove Creek was reduced following the STRPs implemented at Stony Clove Creek since 2012. The potential effectiveness of the STRPs at Stony Clove Creek will further be examined later in this thesis (Figure 9).

Relating the summary statistics on turbidity to the normalized streamflow data, Woodland Creek (0136230002) and Stony Clove Creek at Chichester (01362370) were ranked in the top four sites based on their mean normalized streamflow (Table 6). Thus, as these two sites were also ranked as having high mean turbidity during the study period, normalized streamflow can in fact explain some of the variation in turbidity at these sites.

Similar to the analyses conducted for the normalized streamflow data, examining the spatial distribution of the median turbidity values across sites is useful, especially in the context of the normalized streamflow data (Figure 7). However, for examining the spatial relationships

in the turbidity data across sites, I filtered the data to only include site and year combinations where the number of turbidity measurements exceeded 350 (where 365 measurements would represent a complete years' worth of data).

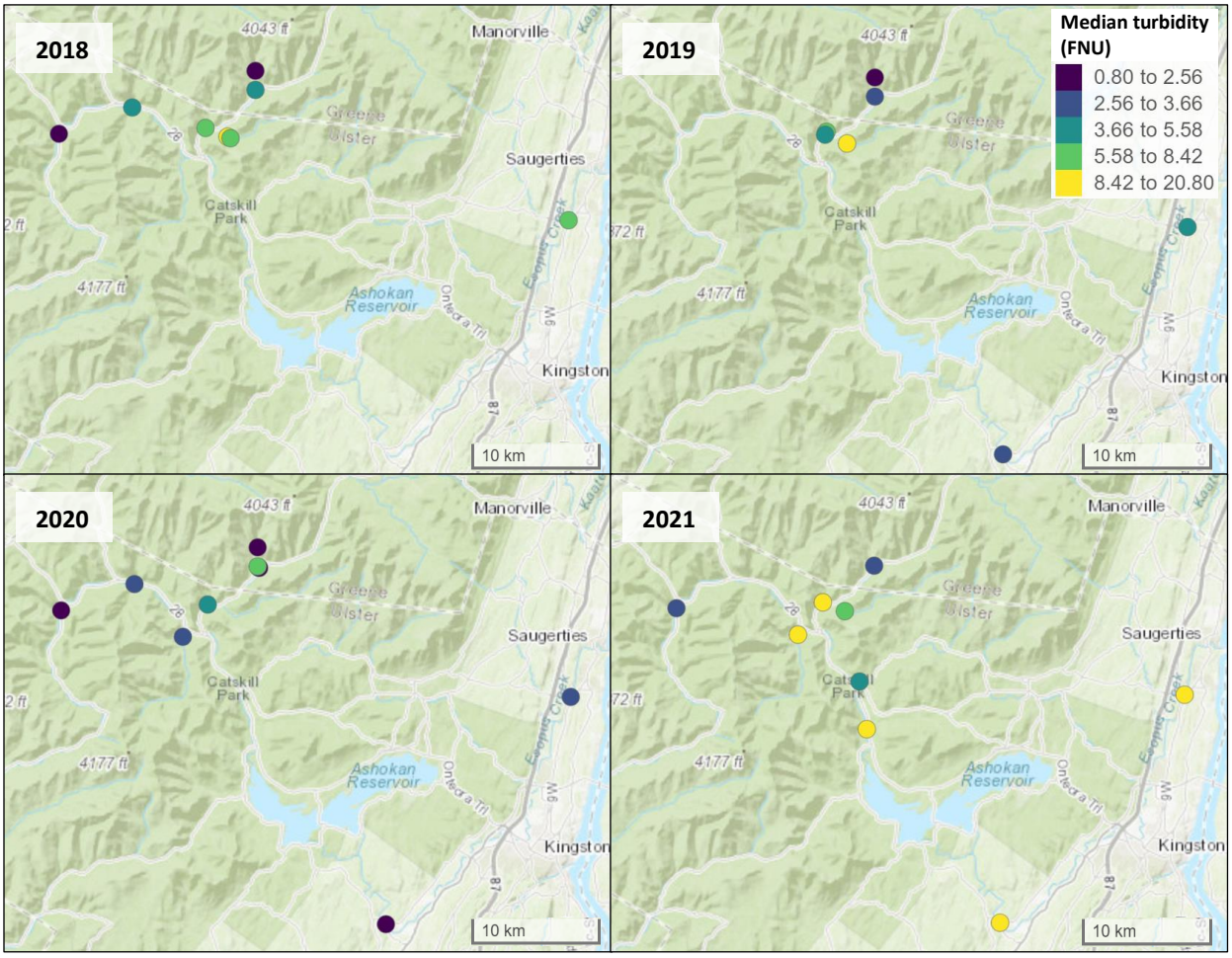

Figure 7. Maps of the median turbidity by monitoring site from 2018 to 2021. The data availability for each year and site combination was filtered to only include 350 turbidity measurements to limit temporal influences on the underlying spatial data (i.e., differences in data availability across years driving the differences in turbidity across sites rather than the site characteristics themselves). The years 2018 to 2021 are only shown because these years have the most amount of data for each site and year combination. Note that every site may not appear across different years due to these filtering criteria. Data are binned by quantiles.

Additionally, to examine the most amount of data with overlapping years across sites, I examined the count of turbidity measurements in each year for each site; the greatest number of

turbidity measurements occurred in the years from 2018 to 2021. After implementing these filtering criteria, the median turbidity results by site for the years 2018 to 2021 are shown in Figure 7. Spatially, there is a statistical difference in the mean turbidity across monitoring sites (ANOVA, $P < 0.05$). This result may suggest that there are various mechanisms that may control turbidity across sites in the Catskills, such as differences in topography, land use, and the extent of stream remediation efforts.

To understand the typical turbidity conditions in the Catskills, summarizing the data at each monitoring site with sufficient data reveals that the median turbidity values for sites in the Catskills from 2018 to 2021 ranged from 0.8 to 20.8 FNU (Figure 7). Specific sites can be pinpointed that typically have elevated turbidity values during the time period of 2018 to 2021, which include Warner Creek (01362357), Ox Clove (01362368), and Stony Clove at Chichester (01362370) (Figure 7). These results only correspond to the study by McHale and Siemion (2014) with respect to the Stony Clove results. Interestingly, Woodland Creek (0136230002) experienced the greatest median turbidity (20.8 FNU) during 2018 to 2021 for site and year combinations with greater than 350 measurements. In fact, the next highest site by median turbidity grouped within the fifth quintile[2] across the years of 2018 to 2021 had a value of 12.25 FNU, which occurred at Warner Creek (01362357) during 2018. Although this observation from Woodland Creek only represents a single year of data, its corresponding median turbidity from 2021 is much higher than the other values from each site across a time span of four years. Thus, Woodland Creek should undergo continual monitoring (turbidity and streamflow) to examine whether it experiences elevated turbidity in the future.

[2]A quintile is a statistical value of a data set representing 20% of a given population. Hence, the first quintile is the lowest fifth of the data (1% to 20%), whereas the fifth quintile is the highest fifth of the data (81% to 100%). Note that quantiles cut points by splitting the range of a probability distribution into continuous intervals each with equal probabilities. Thus, the observations in the sample are divided in the same way. Also note that quantiles may be misleading when very different values are placed in the same grouping category. Quantiles should also be considered with the underlying distribution of the data in mind (i.e., Gaussian or non-Gaussian distribution). For more information on quintiles, see https://www.investopedia.com/terms/q/quintile.asp.

Understanding the underlying mechanism(s) that may have caused the elevated median turbidity in 2021 at Woodland Creek are also imperative to determine what factors or mobilization processes (see Chapter 2) that may contribute the greatest to elevated turbidity at this site in the future.

Furthermore, 2021 experienced elevated turbidity across most monitoring sites, which is likely an artifact of the severe December 2020 flood reported in the Catskills. The Catskills were hit by a severe flood from snowmelt and rain on December 25th, 2020. The elevated turbidity in 2021 can likely be explained by the December 2020 flood because the lower Esopus Creek sites (Lomontville and Mount Marion) experienced elevated turbidity during 2021. These lower Esopus sites typically have lower median turbidity relative to the other sites in the Catskills (Figure 7). Although there remain uncertainties with respect to the potential mechanisms to explain the spatial differences in turbidity in the Catskills, these results highlight the need for more rigorous examination of the field sites to better explain the discrepancies in turbidity on a spatial scale, specifically with consideration of the time component of the data.

3.3.3.1 Temporal and seasonal trends in turbidity

In this sub-section, I highlight the temporal and seasonal trends in turbidity in the Catskills in the context of streamflow. Understanding how the turbidity data relates to the streamflow data through time is important in order to hypothesize which underlying mechanisms may be dominant in controlling the various responses in turbidity (e.g., streamflow-independent versus streamflow-dependent events; see Chapter 2). Firstly, for the temporal trends, I chose to examine Woodland Creek (0136230002) to determine why the median turbidity during 2021 was so high relative to the other Catskill sites, as well as to introduce the relationship between

streamflow and turbidity. An example time series for streamflow and turbidity at Woodland Creek is shown in Figure 8. The December 2020 flood is clearly shown; turbidity peaked at 782 FNU, with an associated streamflow of 1460 cfs (Figure 8).

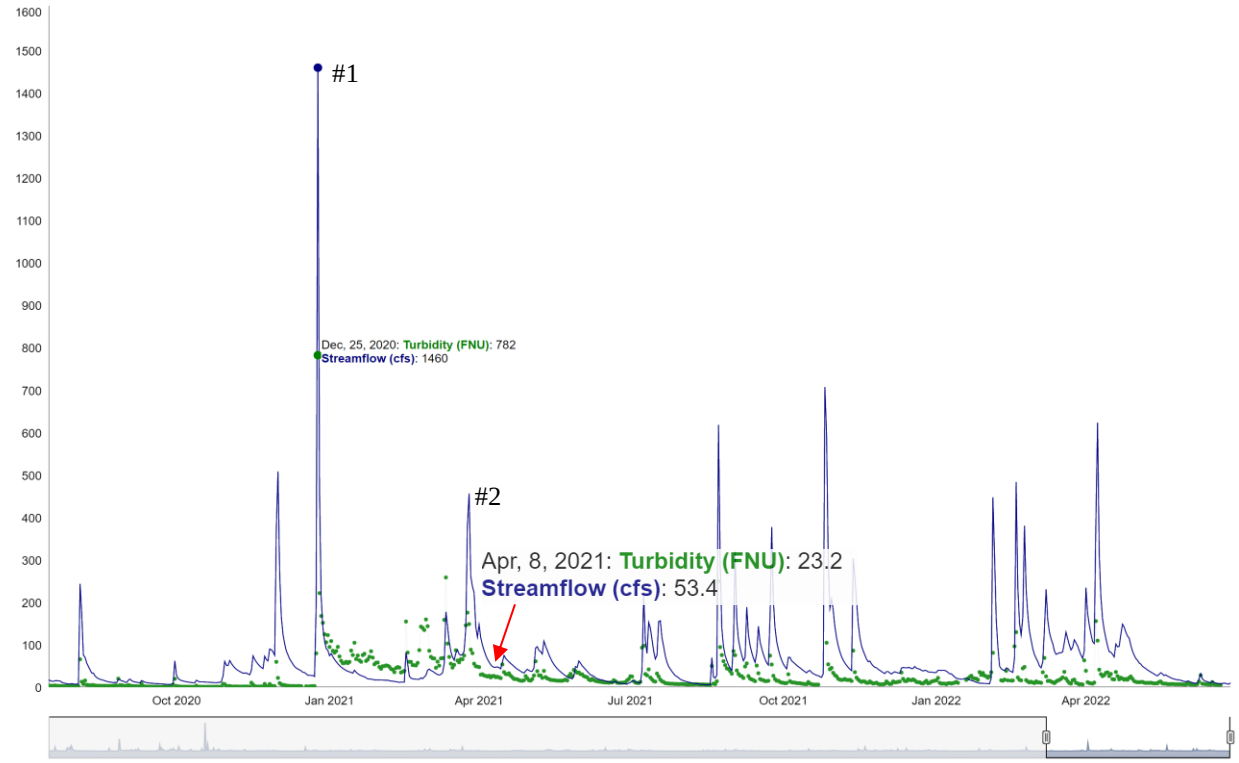

Figure 8. Time series of the daily average streamflow and turbidity at Woodland Creek in Phoenicia (0136230002) from late 2020 to mid-2022. The y-axis represents the associated values for either the streamflow or turbidity. The green dots represent turbidity, whereas the blue line represents streamflow. This time period of the time series was selected to understand why the high median turbidity value in 2021 at Woodland Creek may have occurred (Figure 7). Data are not plotted on logarithmic scale; this approach was chosen to highlight when streamflow-dependent and streamflow-independent turbidity events may occur, as well as to examine when turbidity returns back to baseline conditions after a disturbance (e.g., an extreme flood event). The red arrow represents approximately when turbidity returned to baseline conditions after the December 2020 flood. Baseline conditions here refer to the median turbidity at Woodland Creek from 2021, which was 20.8 FNU. The "#1" and "#2" refer to the primary and secondary streamflow events that likely contributed to turbidity being elevated and then ultimately returning to baseline conditions.

Examination of the December 2020 flood event at Woodland Creek allows for determination of the time taken to return to baseline turbidity after extreme flood events (Figure 8). Here, the baseline turbidity being used is the median turbidity at Woodland Creek from 2021 (20.8 FNU). We can deduce that the approximate time taken for turbidity to return to baseline conditions after the December 2020 flood was 103 days, or over three months (Figure 8). This result for the return to baseline turbidity conditions has important management implications with respect to how STRPs may need to be implemented at sites in the Catskills, such as at Woodland Creek.

Furthermore, examining the conditions that led to the return to turbidity baseline conditions at Woodland Creek after the December 2020 flood can provide key insights into how turbidity may respond to factors such as streamflow after extreme flood events. After the December 2020 flood (labeled #1 on Figure 8), a second large streamflow event (labeled #2 on Figure 8) occurred on March 26th, 2021, where streamflow peaked at 457 cfs. I hypothesize that this second relatively large streamflow event flushed the easily erodible sediments that had been deposited as a result of the original large flood from the channel. That is, this intermediate streamflow event produced enough energy to resuspend the easily erodible sediment that had been deposited in the channel as a result of the first flood event (at least where the turbidity data was being monitored), but not enough energy to overwhelm the system and keep the turbidity above baseline conditions. This response was also observed at other sites in the Catskills, including Stony Clove Creek (01362370) and Warner Creek (01362357); a second intermediate streamflow event also occurred on March 26th, and baseline turbidity was reached at these sites shortly after. Thus, the hypothesis explaining the mechanism of the return to baseline turbidity outlined above can apply to multiples sites in the Catskills, and therefore it can be considered as a characteristic process in the Catskills. These geomorphic responses at the end of 2020 through

2021 that occurred at multiple sites in the Catskills, including Woodland Creek, Stony Clove Creek, and Warner Creek, can provide key insights into the underlying mechanisms responsible for controlling turbidity dynamics in the Catskills. These results have important implications for stream restoration and management of the Catskill water supply system.

Examination of the temporal trends in turbidity can also be accomplished across all sites and years with available data. Figure 9 is a raster plot that shows both regional and site-specific trends for the normalized turbidity data.

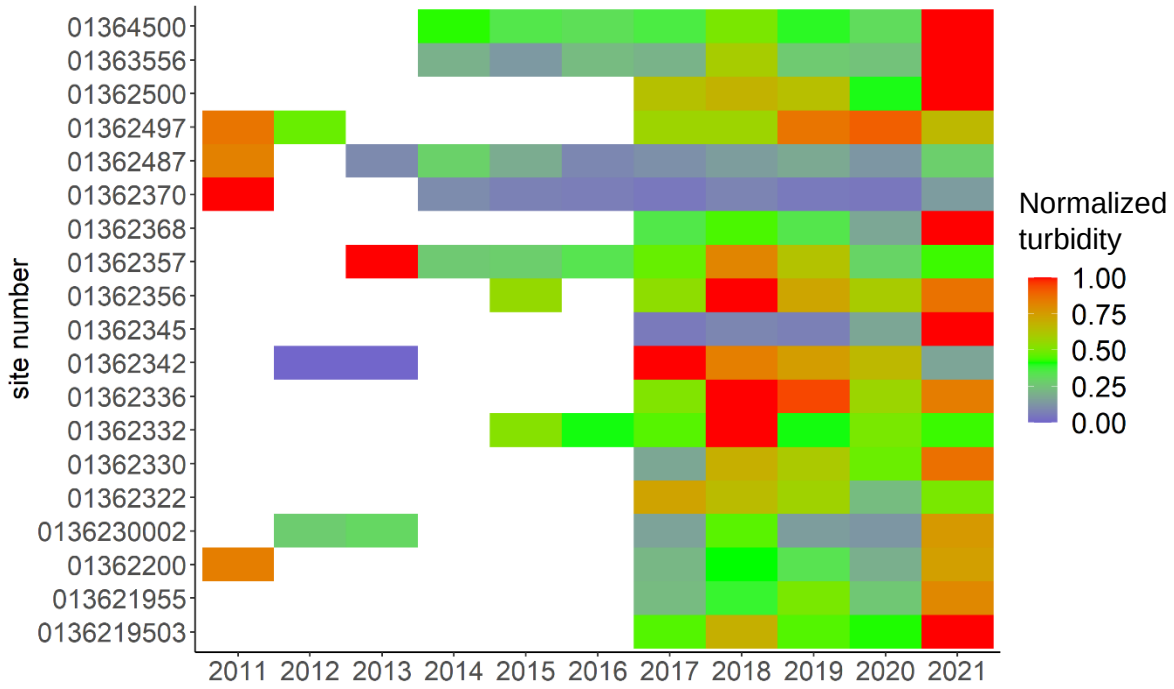

Figure 9. Raster plot of the normalized turbidity data through time at each site in the Catskills. To ensure data quantity was not confounding the results, the data for each year and site combination was filtered to include only site-year combinations with more than 200 turbidity measurements. The white spaces indicate no data (i.e., the filtering criteria removed those year and site combinations from the data set). The turbidity data were normalized through the method outlined in Table 3. Note that the normalized turbidity computed through this method is unitless.

The regional trends, such as trends in the data that are broadly observed throughout the Catskills, are shown vertically as columns of the raster plot, whereas site-specific trends are shown

horizontally as rows of the raster plot. An example of a regional event in the Catskills is the December 2020 flood; 70% (14 out of 20) of the sites in the Catskills had elevated normalized turbidity during 2021, as shown by the orange and red cells in the matrix (Figure 9). Thus, this result confirms the effects on turbidity from the December 2020 flood.

In addition to examining regional trends, site-specific trends can be discerned through time in the Catskills (Figure 9). For example, the high mean turbidity shown in Table 8 at Hollow Tree Brook (01362345) can partly be explained from Figure 9. This site at Hollow Tree Brook most likely had a high mean turbidity as a result of the December 2020 flood, as other years at this site had low normalized turbidity (represented as blue cells in the matrix). This result can also explain the high standard deviation at Hollow Tree Brook (01362345) (Table 8); all years except 2021 had relatively low normalized turbidity, so the red cell in 2021 increases the standard deviation of the turbidity data at this site across all years. Additional site-specific trends can be found at Stony Clove Creek (01362370). Considering that stream remediation was conducted at this Stony Clove site since 2012, the raster plot highlights that these remediation efforts were likely effective. This can be inferred because the cell for this site in 2011 is red, but all subsequent years have cells that are blue (Figure 9). Thus, the normalized turbidity at this Stony Clove site decreased though time. The specific locations where STRPs were conducted in the Stony Clove and Warner Creek watersheds are shown in Figure 10 (Siemion et al., 2016). Nonetheless, the raster plot allows for a better understanding of the typical turbidity conditions at each monitoring site in the Catskills; we can see how certain sites responded to extreme flood events like the December 2020 flood, and we can also deduce site-specific trends through time.

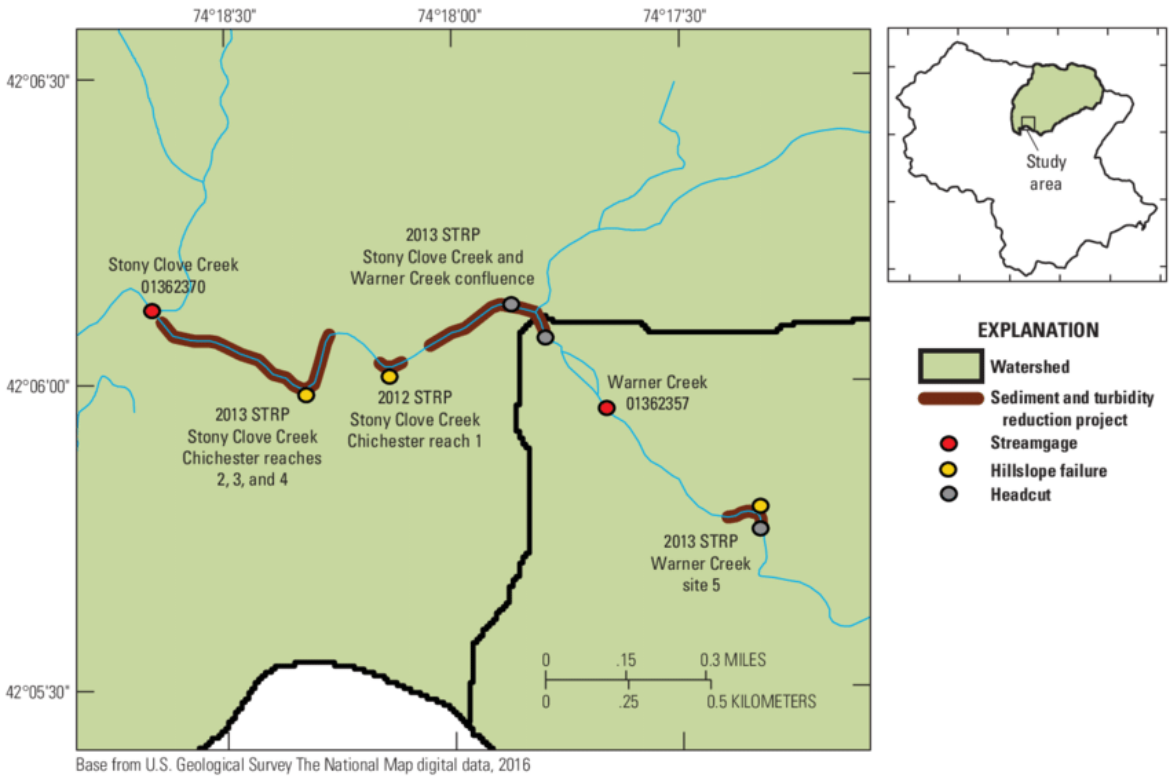

Figure 10. Map of streamgages, hillslope failures, and the extent and locations of STRPs in the Stony Clove and Warner Creek watersheds (modified from Siemion et al., 2016).

An understanding of the typical turbidity and streamflow conditions in the Catskills can also be deduced from turbidity and streamflow exceedance plots (Figures 11 and 12). Exceedance probability plots are often made in the field of hydrology to address specific questions related to flood frequency analysis. This concept can be applied in this study to both streamflow and turbidity to understand the percent of time a given streamflow or turbidity value was equaled or exceeded. For example, the 1% exceedance represents the streamflow or turbidity value that was equaled or exceeded one percent of the time. From the streamflow exceedance probability curve, around 50% of the time, a streamflow value of approximately 20 cfs was exceeded by half (8 out of 16) of the sites in the study area (Figure 11). Specific sites can also be pinpointed for their typical streamflow conditions.

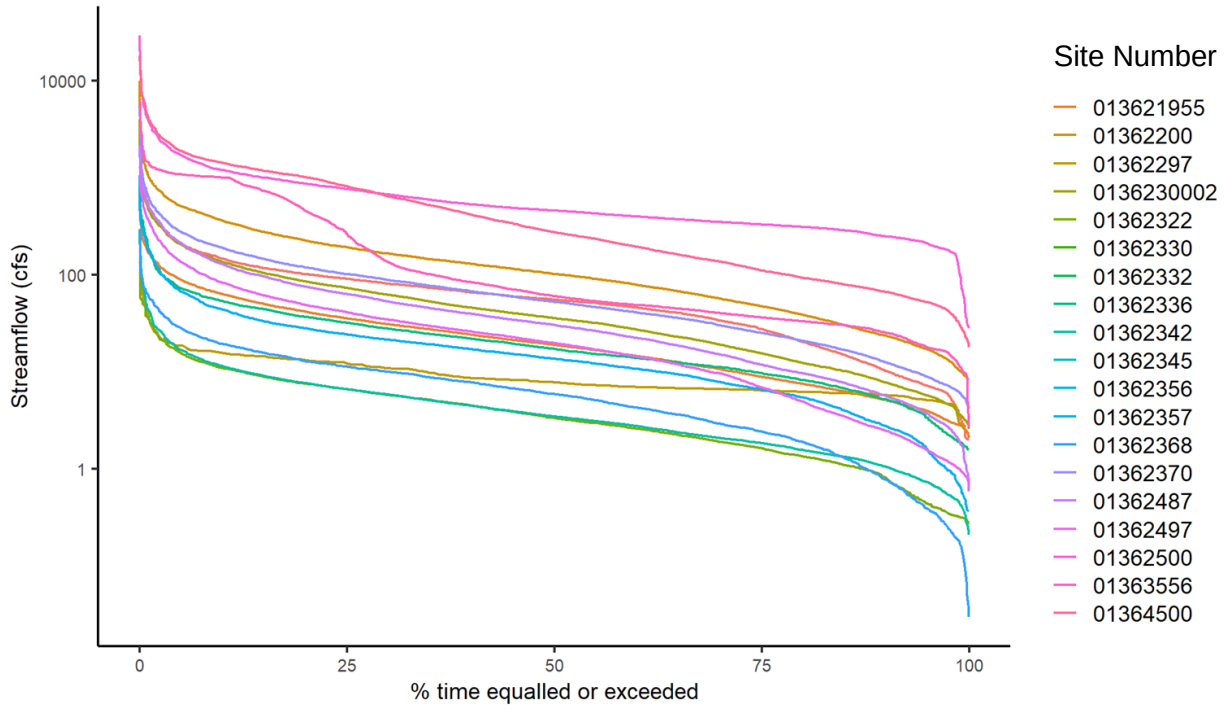

Figure 11. Streamflow exceedance probability plot for all sites in the Catskills. The data are not normalized by drainage area.

For example, at Esopus at Coldbrook (01362500), for 50% of the time, a streamflow value of around 460 cfs was exceeded. Contrarily, at Myrtle Brook (01362322), for around 50% of the time, a streamflow value of 3.4 cfs was exceeded. Although this exceedance plot was computed based on the unnormalized streamflow data, it allows for comparisons to be made in terms of the typical streamflow values across sites in the Catskills.

Applying the concept of exceedance probabilities to the turbidity data, the turbidity exceedance plot can provide useful insights not only on the baseline turbidity conditions at each site (examining the flat part of the curve for each site), but also for each exceedance value, how the sites compare to one another (Figure 12). Examining a specific site, for example, Hollow Tree Brook at Lanesville (01362342), for 25% of the time, a turbidity value of around 1 FNU was exceeded, which suggests this site has a low baseline turbidity relative to the other Catskill

sites (Figure 12, Table 8). But, for Warner Creek (01362356), for 25% of the time, a turbidity value of around 10 FNU was exceeded, which suggests that this site has a higher baseline turbidity than the Hollow Tree Brook site. More generally, for 50% of the time, a turbidity value of around 4.5 FNU or higher was exceeded by 11 sites in the study area (Figure 12). This result suggests that the median turbidity for around half of the sites in the Catskills is close to or above the EPA regulatory limit of 5 NTU for regulating turbidity in stream water that enters a water-supply system (EPA, 2020). Moreover, for 25% of the time, 10 sites in the study area equaled or exceeded a turbidity value of 10 FNU (Figure 12).

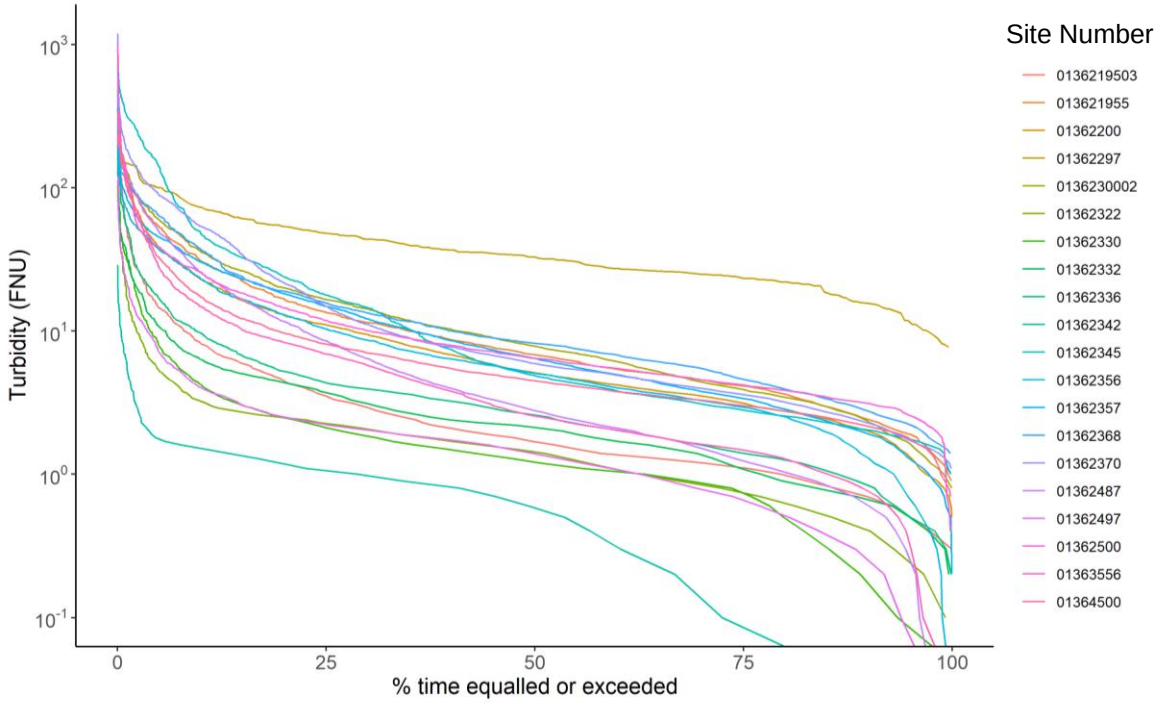

Figure 12. Turbidity exceedance probability plot for all sites in the Catskills.

Although FNU and NTU are not directly equivalent units, as the reporting units are only considered equivalent when measuring a calibration solution (Anderson, 2005), this suggests that there are certain sites in the Catskills susceptible to higher turbidities, including two Warner

Creek sites, two Esopus Creek sites, Birch Creek at Big Indian, Stony Clove at Chichester, Ox Clove at Chichester, Woodland Creek, Hollow Tree Brook, and Panther Kill (Figure 12). These results have important implications for mitigation efforts in terms of responding to elevated turbidity in Catskill streams.

In addition to the temporal trends, examination of the seasonal trends in the turbidity data is useful to relate to the normalized streamflow data. The summary statistics for the seasonal trends in the monthly turbidity data are presented in Table 9. The months with the top median turbidity are January through April (Table 9). These results generally correspond to the seasonality of the normalized streamflow data (Table 7). April has the highest mean normalized streamflow across sites, which also is the month with the highest median turbidity (Table 9).

Table 9. Summary statistics for the seasonal trends in the mean monthly turbidity across all monitoring sites. Data are from 2010 – 2022. February has the most sparse data compared to the rest of the months.

Month	Mean turbidity (FNU)	Median turbidity (FNU)	Maximum turbidity (FNU)	Standard deviation turbidity (FNU)	Count
1	15.3	5.6	394	30.2	4437
2	17.5	5.6	582	39.0	4037
3	17.8	5.9	866	41.8	4605
4	16.3	6.9	674	31.4	4768
5	9.0	4.4	1090	23.9	4985
6	8.3	3.6	1210	26.8	4763
7	8.8	3.3	776	24.8	4331
8	9.3	3.2	1010	31.8	4294
9	8.0	2.4	441	21.7	4151
10	10.6	2.8	916	35.8	4334
11	10.9	4.6	920	25.5	4414
12	13.8	4.6	1190	45.8	4649

Thus, the snow melt that is generated during April can be interpreted as a driver of elevated turbidity throughout the Catskills. The months with the lowest median turbidity are September and October. This result contrasts with the seasonality of the normalized streamflow data, which

suggests that there may be other factors besides streamflow affecting turbidity during the months of September and October. Furthermore, the month with the greatest standard deviation for turbidity is December; this month also had the second highest recorded turbidity value in the data set (1190 FNU). Although turbidity is primarily event-based, useful insights can nonetheless be obtained from examining the turbidity trends across all monitoring sites.

To visualize the differences in turbidity across monitoring sites and years, plotting the percent rank of turbidity by site and year combinations across months can be informative (Figure 13). Figure 13 shows how turbidity at different sites varies by month and year.

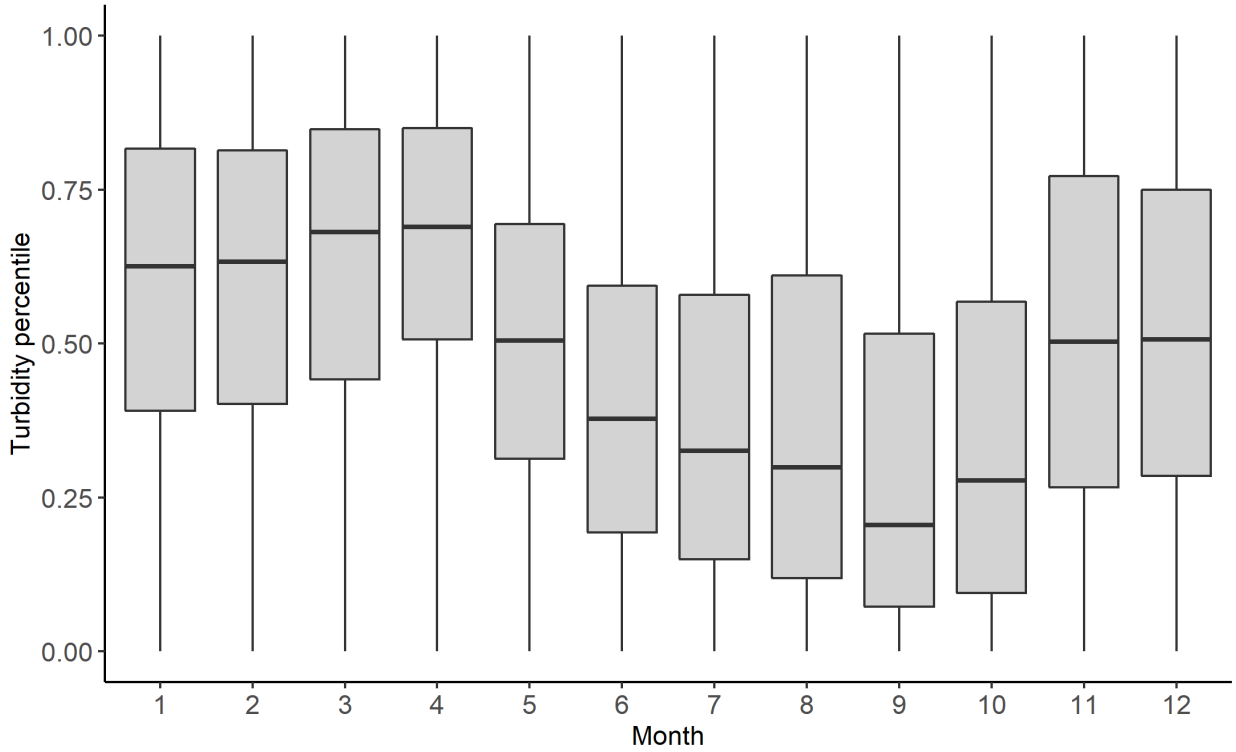

Figure 13. Percent ranks of turbidity by site and year combinations for each month in the data set (1 = January, 2 = February,…). The percent rank outputs a number between 0 and 1, which is computed by rescaling the minimum rank to 0.

The percent rank of turbidity can tell us how the turbidity at a given site in a given month and year compares to the turbidity of all the sites in the same year. A higher percent rank means higher turbidity, and a lower percent rank means lower turbidity. From Figure 13, April has the highest median turbidity and September has the lowest median turbidity across all months, which corresponds to the results from Table 9. Furthermore, there appears to be a seasonal trend in the percent rank of turbidity; January through April have higher turbidity, May through September have lower turbidity, and October through December have higher turbidity (Figure 13). These results make sense in the context of streamflow, which typically decreases during the summer. Additionally, the month with the greatest variation in turbidity appears to be August based on the width of the box plots across months.

3.3.4 Streamflow-Turbidity Relationship

For the last section of this chapter, I provide a brief overview of the streamflow-turbidity relationship in the Catskills, paying specific attention to how this relationship varies spatially and temporally. Examining the streamflow-turbidity relationship is important because streamflow is one of the key drivers of turbidity (see Chapter 2). For the spatial variability in the streamflow-turbidity relationship, although turbidity tends to increase with normalized streamflow, the behavior of this relationship is not consistent across sites in the Catskills (Figure 14). The normalized streamflow does not always scale directly with turbidity at sites in the Catskills (Figure 14). For example, for several of the sites, such as Esopus at Big Indian (0136219503), Birch Creek at Big Indian (013621955), Woodland Creek (0136230002), and Beaver Kill (01362487), there appears to be a higher slope at higher normalized streamflow compared to lower flows (Figure 14).

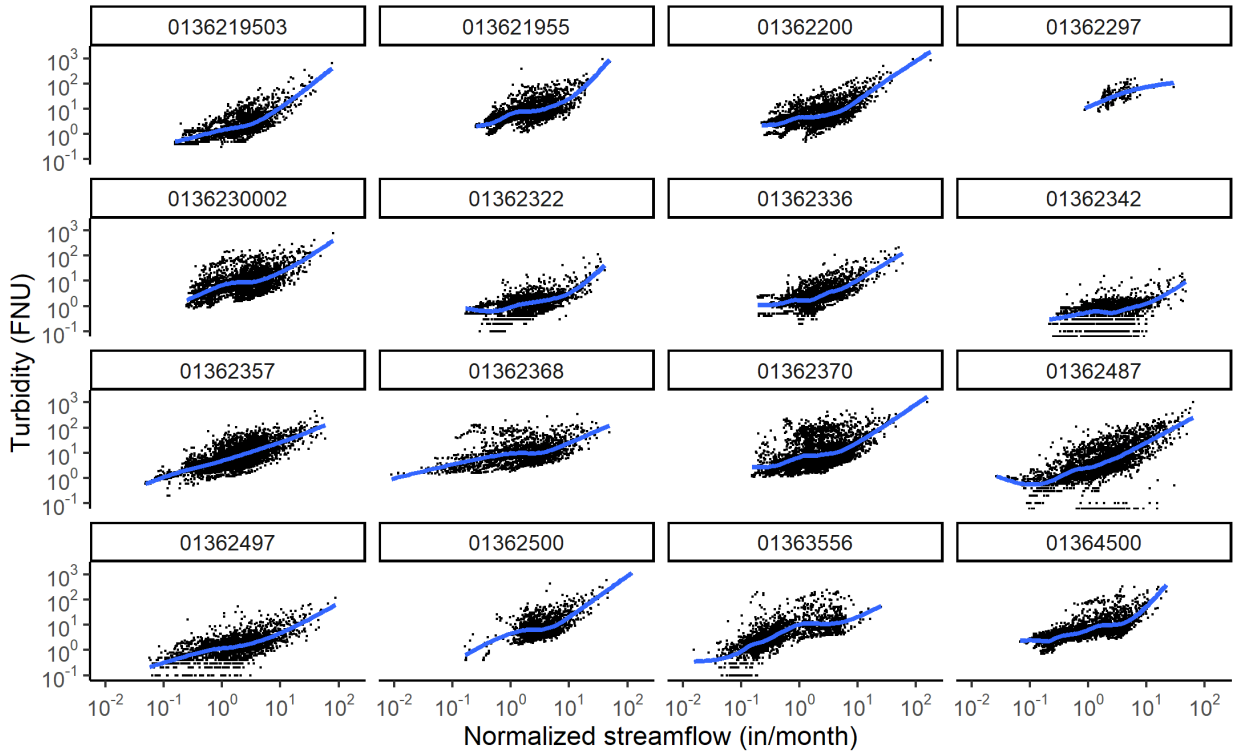

Figure 14. Streamflow-turbidity relationship across monitoring sites in the study area. Method of smoothing is LOESS (locally weighted scatter plot smoothing). LOESS smoothing was chosen to avoid forcing a linear relationship between the two variables, as a linear relationship may not appropriately describe how streamflow and turbidity behave at each site. LOESS smoothing is a non-parametric approach that does not make underlying assumptions about the data. Both axes are plotted on logarithmic scale.

This is evidenced by a non-linear relationship between turbidity and streamflow at these sites. However, this observation may be affected by there being less data available at higher normalized streamflow values. Contrarily, Ox Clove (01362368) appears to have a more gradual increase in turbidity for a change in streamflow, compared to the rest of the sites (Figure 14). Perhaps there is more vegetative land cover at this site compared to sites that have a non-linear increase in the streamflow-turbidity relationship. This can be a possible explanation for the relationship at Ox Clove because more vegetative cover of the land surface means there is more vegetation available to stabilize the soil, which can provide a buffer against stream sediment

inputs after extreme flooding events (see Chapter 2). Another possible explanation is due to other watershed characteristics, such as land surface slope and sediment type.

Examination of the streamflow-turbidity relationship at a select number of sites can also provide insights into how this relationship varies spatially in the Catskills. Examining this relationship at three spatially-distinct sites – Esopus Creek at Allaben (01362200), Esopus Creek at Coldbrook (01362500), and Little Beaver Kill (01362497) – again reveals that the streamflow-turbidity relationship varies across sites (Figure 15). For the same normalized streamflow value, the Little Beaver Kill tends to have a smaller associated turbidity compared to the Esopus Creek sites (Figure 15). This relationship may be affected by the differences in the amount of variance at sites with smaller versus larger drainage areas. In this study, sites with smaller drainage areas tend to have greater variance in turbidity, which can be explained by sites with larger drainage areas averaging the turbidity over larger areas compared to smaller drainage areas. So, these differences can potentially explain why the Little Beaver Kill has a wider range of turbidity values for a given streamflow compared to the Esopus Creek sites. Moreover, although I am correcting for drainage area across sites by using the normalized streamflow, I am not correcting for variables that are correlated to drainage area, such as the slope of the watershed, which likely can explain some of the differences across sites in Figure 15 as well.

In addition to spatial differences, the streamflow-turbidity relationship varies temporally at sites in the Catskills (Figure 16). With the example of Stony Clove Creek at Chichester (01362370), there are differences in this relationship between 2019 and 2021. For the same streamflow, the average turbidity was generally higher in 2021 compared to 2019 at Stony Clove Creek (Figure 16). These results are likely due to the December 2020 flood, which caused chronically-elevated turbidity at several of the Catskill sites.

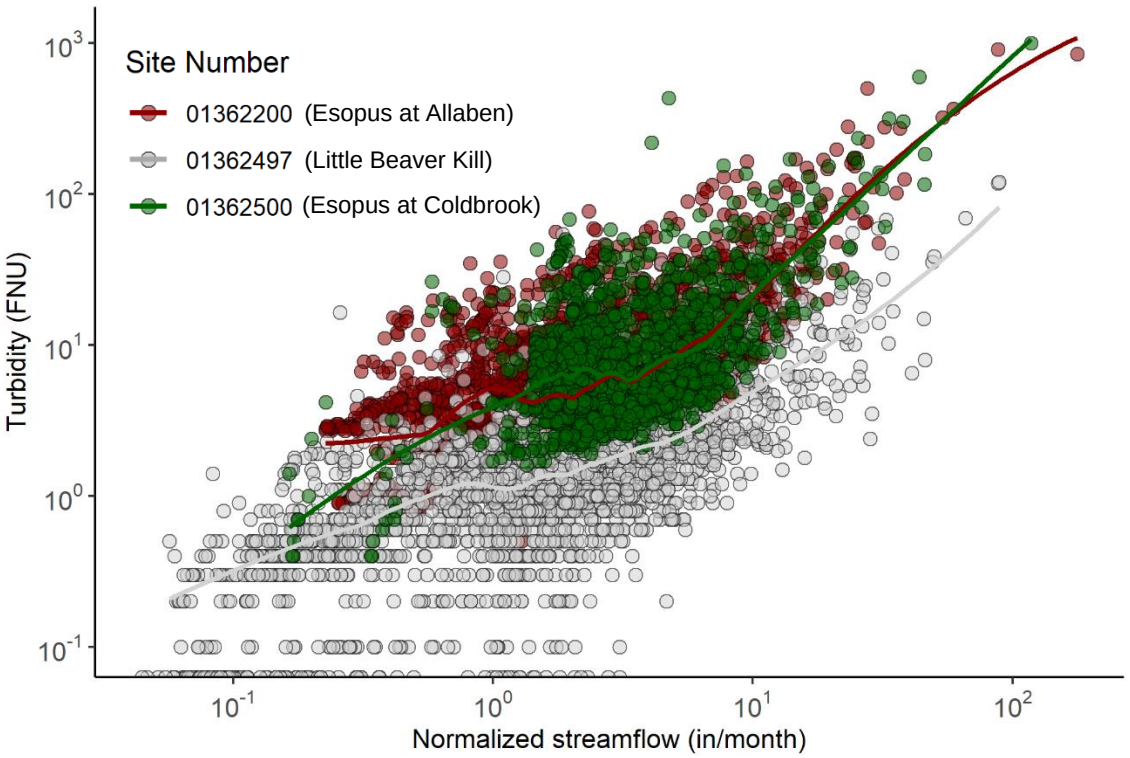

Figure 15. Streamflow-turbidity relationship for three sites in the Catskills. Smoothing method used is LOESS. Points are colored by site number. Both axes are plotted on logarithmic scale.

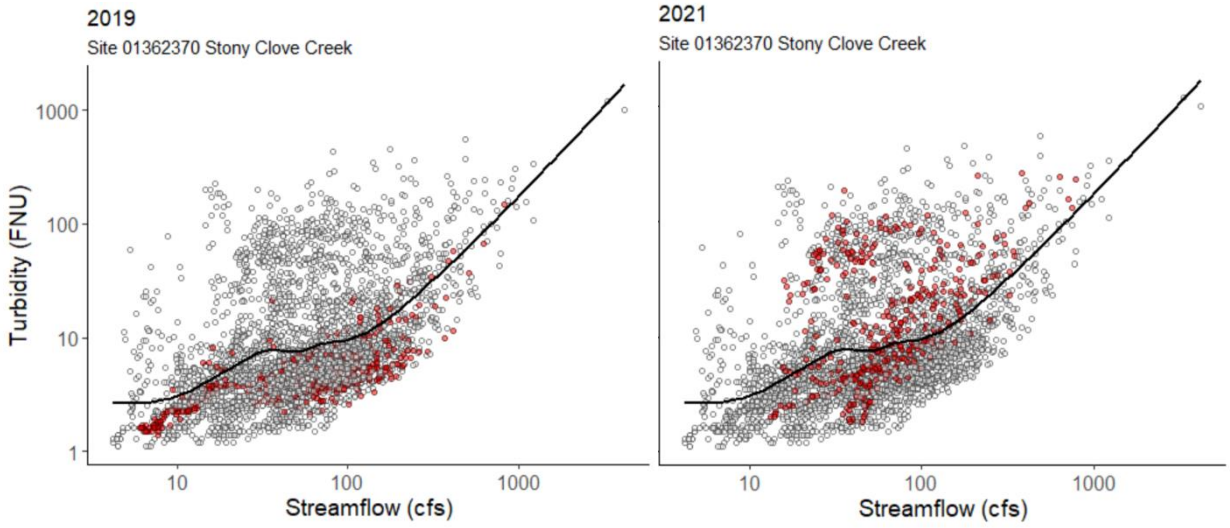

Figure 16. Differences in the streamflow-turbidity relationship between 2019 and 2021 at Stony Clove Creek at Chichester (01362370). The full record (2010 – 2022) is represented by grey circles, and data for each year (2019 and 2021, respectively) are colored in red. The LOESS fit to the full record is the solid black line. Both y-axes represent turbidity.

These results have important implications for how elevated turbidity should be managed after extreme flood events in the Catskills. Because the streamflow-turbidity relationship is dynamic in the Catskills, it is important to take these results into consideration when devising solutions to reducing turbidity throughout this region.

It is also useful to examine the seasonality of the streamflow-turbidity relationship, which is shown for the Esopus Creek at Allaben (01362200) during the study period (Figure 17). The summer points are from the months of May-October, and the winter points are from the months of November-April (after Mukundan et al., 2013). These groupings by month were chosen because the trends were difficult to discern using all four seasons of the year. The summer months tend to be associated with lower normalized streamflow and lower turbidity (Figure 17).

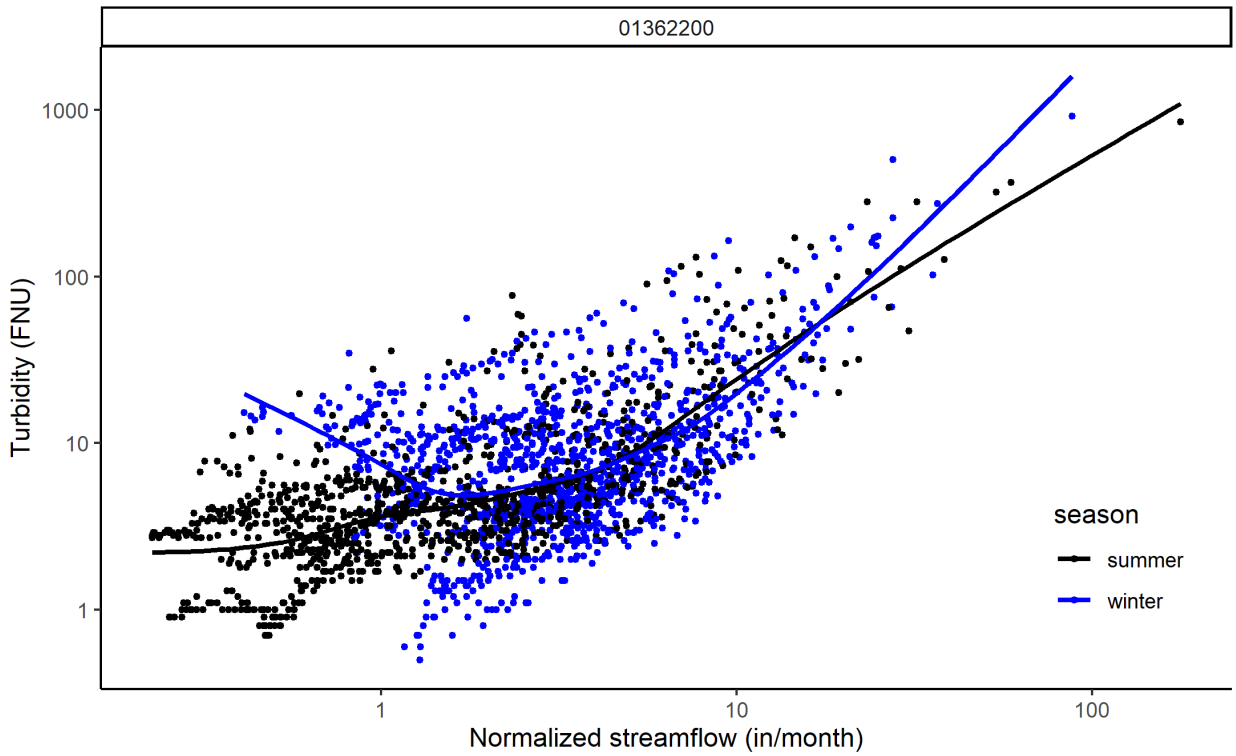

Figure 17. Streamflow-turbidity relationship at Esopus Creek at Allaben (01362200), showing the summer versus winter comparison. Points represent the paired daily average normalized streamflow and turbidity at this site. Both axes are plotted on logarithmic scale.

Furthermore, at higher values of normalized streamflow, higher turbidity values per unit streamflow were observed during the winter. Although the data is sparser at higher normalized streamflow conditions, this result can perhaps be explained by more frequent precipitation events occurring in the winter, which can cause an influx of sediment to the stream, elevating turbidity. However, this is only one possible explanation to explain this result, as more precipitation could have the opposite effect, reducing the sediment supply and thus turbidity (Mukundan et al., 2013). Further research is required to better understand the dynamics of the streamflow-turbidity relationship across monitoring sites in the Catskills.

Comparisons between the percentiles of turbidity and streamflow grouped by site and year combinations can provide information about the seasonal timings of turbidity for a given streamflow range; this information is shown across months for Woodland Creek (0136230002) and Esopus Creek at Big Indian (0136219503) in Figure 18. From Figure 18, it is apparent that the months differ in terms of the frequency of certain turbidity event types at these two sites. For example, January and February appear to have a low frequency of low-streamflow-low turbidity events, which represents the bottom-left quadrant in these months (Figure 18). Instead, January and February tend to have more frequent high streamflow-high turbidity events (upper-right quadrant). This result is expected because the winter months can undergo thawing events from snow melt, which can increase streamflow and hence turbidity. Another interesting observation from January and February is that they have low-streamflow-high-turbidity events (upper-left quadrant). We would expect low streamflow to generally be associated with low turbidity; here, in January and February, there are low streamflow events that are most often associated with high turbidity.

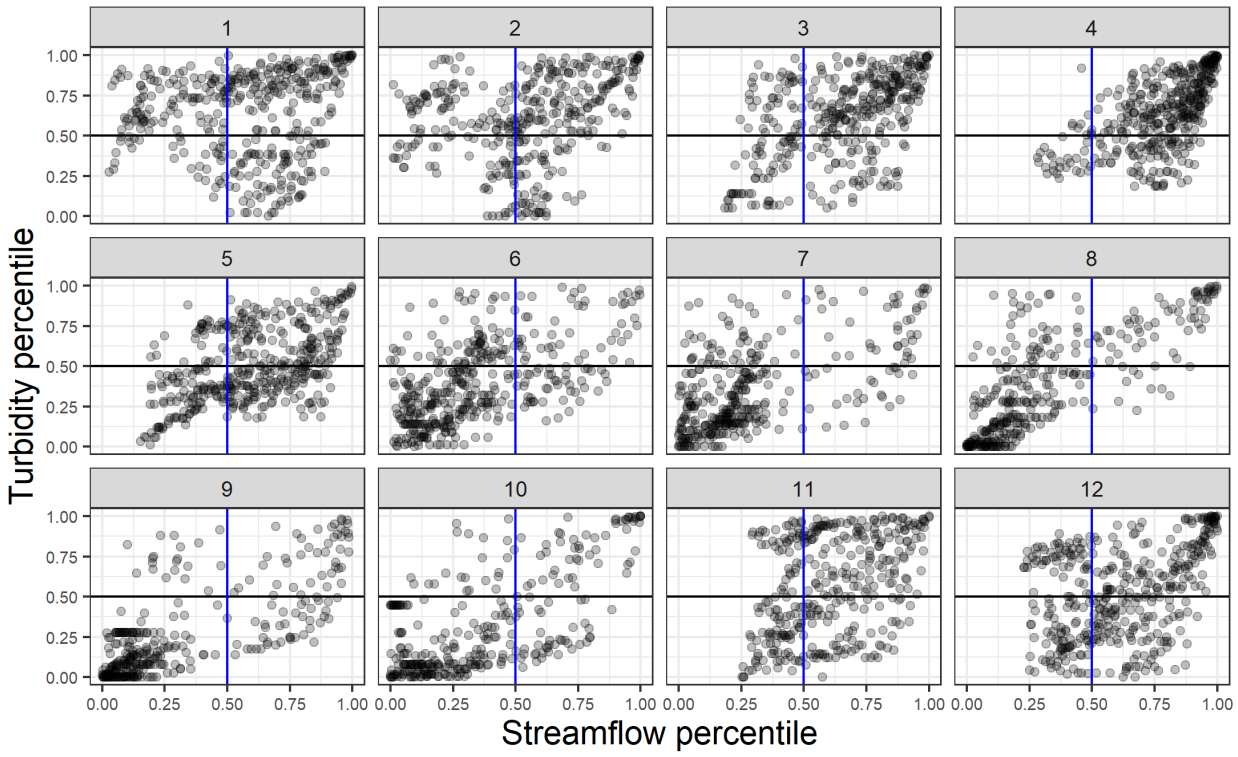

Figure 18. Scatter plots of the turbidity and streamflow percentiles across the 12 months of the year for Woodland Creek (0136230002) and Esopus Creek at Big Indian (0136219503). The vertical and horizontal lines show the 50th percentile for both turbidity and streamflow, which break the plots up into four quadrants. For example, the bottom-left quadrants show the frequency of low flow-low turbidity events in each month.

This result contrasts with September, which also has low streamflow events. However, these low streamflow events in September are almost always associated with low turbidity. Because these data shown are only for two sites, additional research is necessary to determine why these sites may behave in this manner. Furthermore, the month of April appears to have an extremely high concentration of high streamflow – high turbidity events, as evidenced by the high density of points in the upper-right quadrant of Figure 18. This result makes sense considering that the month of April experienced the highest median streamflow and turbidity across all monitoring sites and years in the data.

Lastly, we can understand the variation in turbidity that can be explained by the normalized streamflow by computing the R^2 for the streamflow-turbidity relationship (based on the LOESS approach) at each monitoring site in the Catskills. As the relationship used here to describe the relationship between turbidity and streamflow is computed with the LOESS approach, it is important to note that the smoothing window (the span) can affect the R^2 value. For instance, a span that does not smooth over the data very much (i.e., many points are hit by the smoothing), would correspond to a higher R^2 value because more of the systematic variation in turbidity caused by streamflow can be explained by the model. Therefore, it is important to consider the extent of smoothing when interpreting the R^2 values from the LOESS model. Nonetheless, as previously mentioned, the LOESS approach is advantageous here, say, to a linear model, because the LOESS approach does not make underlying assumptions about the data because it is a non-parametric approach.

Computing the R^2 values based on the LOESS approach at each monitoring site with available data shows that the Esopus Creek at Allaben and Esopus at Big Indian have R^2 values above 0.7 (Table 10). This means the normalized streamflow explains the variation in turbidity well (> 70%) at these sites. There are a total of eight sites that have an R^2 value greater than 0.5 (Table 10). The sites with the lowest R^2 values correspond to Esopus Creek at Mount Marion (01364500), Esopus Creek near Lomontville (01363556), and Ox Clove (01362368). These results suggest that there may be different mechanisms controlling differences in turbidity (e.g., streamflow) between the upstream and downstream sites of the Ashokan Reservoir. These results make sense considering the differences in the physical characteristics of the upper and lower Esopus Creek sites throughout the Catskills. These results on the variation in turbidity that can be explained by the normalized streamflow will be useful to inform future research in this study.

Table 10. List of the R^2 values corresponding to each monitoring site for the relationship between turbidity and normalized streamflow. The model used to compute the R^2 is based off a LOESS approach with a span value of 0.75. The same LOESS approach is shown in Figure 14.

USGS Station ID	R^2
01362200	0.74
0136219503	0.72
01362500	0.69
01362487	0.65
013621955	0.63
01362497	0.62
01357500	0.58
01362336	0.54
01362322	0.49
01349527	0.48
0136230002	0.47
01362357	0.44
01362370	0.43
01362297	0.32
01362342	0.31
01364500	0.30
01351500	0.24
01363556	0.14
01362368	0.14

3.4 CONCLUSIONS

Characterizing turbidity and streamflow in the Catskills has important watershed management implications, as the Catskill system supplies the majority of the water for NYC's daily water needs. Here, I characterized streamflow and turbidity in this region and examined the relationship between these two variables. For streamflow characterization, I found that there were several sites that ranked the highest for their mean area normalized streamflow, which includes Esopus at Coldbrook, Woodland Creek, one of the Hollow Tree Brook sites, and Stony Clove at Chichester. The results from Woodland Creek and Stony Clove found here correspond to the findings by the NYC DEP (2022). For seasonal trends, April, March, and December had the highest mean normalized streamflow in the Catskills. With the example of Birch Creek, the month of April has received greater mean normalized streamflow through time, which suggests

that earlier spring snow melt events may have impacted the streamflow regimes throughout the Catskills. Although it is difficult to predict whether this trend will continue in the future at all sites in the Catskills, it is nonetheless important to consider in the context of climate change.

For the turbidity characterization, the months of January through April had the highest median turbidity across sites during the period of record, which suggests that earlier timings of spring snow melt may have contributed to elevated turbidity during these months. Normalized streamflow can explain some of the variation in turbidity at sites in the Catskills, but it cannot explain all of this variation. For example, the top sites by their median turbidity were one of the Hollow Tree Brook sites, Stony Clove Creek, Woodland Creek, and Ox Clove. The rankings of these sites are not exactly the same as the streamflow rankings, which implies that other factors need to be considered that can affect turbidity (e.g., topography, land cover, et cetera). For these top sites by their median turbidity, Woodland Creek and Stony Clove Creek were also found to be sources of elevated turbidity in the Catskill system by McHale and Siemion (2014). But, here, I found there to be discrepancies between two of the Hollow Tree Brook sites for their median turbidity, which can potentially be explained by the differences in the frequency of bank failures at each of these sites.

The effects of the December 2020 flood were also apparent from the results. Several sites, including Woodland Creek, Stony Clove at Chichester, and Warner Creek, had elevated turbidity above baseline conditions for three months after the December 2020 flood. These results have important watershed management implications with respect to stream restoration and monitoring in the Catskills, particularly for after extreme hydrologic events. It is evident that STRPs were effective in the Catskills, such as at Stony Clove at Chichester, which is shown by the decline in normalized turbidity after 2012. However, continual monitoring is needed across

the sites in the Catskills to better understand how turbidity responds after high streamflow events.

Lastly, for the streamflow-turbidity relationship in the Catskills, although this relationship is positive, it differs spatially and temporally in this region. Spatially, some sites demonstrate a linear relationship, whereas others are non-linear. Turbidity does not always scale directly with normalized streamflow. Temporally, the streamflow-turbidity relationship can drastically change after severe flood events, such as at Stony Clove at Chichester after the December 2020 flood. Future work should further investigate the dynamics of this relationship in the Catskills to better inform water resources management and preserve the quality of the water in this supply system.

3.5 References

Anderson, C.W., 2005, Turbidity: v. 1, p. 699–704, doi:10.1016/B978-012370626-3.00075-2.

Burns, D.A., Klaus, J., and McHale, M.R., 2007, Recent climate trends and implications for water resources in the Catskill Mountain region, New York, USA: Journal of Hydrology, v. 336, p. 155–170, doi:10.1016/J.JHYDROL.2006.12.019.

De Cicco, L.A., Lorenz, D., Hirsch, R.M., Watkins, W., and Johnson, M., 2021, dataRetrieval: R packages for discovering and retrieving water data available from U.S. federal hydrologic web services:, doi:10.5066/P9X4L3GE.

Earle, S., 2015, Physical Geology: BCCampus.

EPA, 2020, Guidance Manual for Compliance with the Surface Water Treatment Rules: Turbidity Provisions.

Markham, C.G., 1970, Seasonality of Precipitation in the United States: Annals of the

Association of American Geographers, v. 3, p. 593–597.

McHale, M.R., and Siemion, J., 2014, Turbidity and Suspended Sediment in the Upper Esopus Creek Watershed, Ulster County, New York: p. 1–42.

Mukundan, R., Pierson, D.C., Wang, L., Matonse, A.H., Samal, N.R., Zion, M.S., and Schneiderman, E.M., 2013, Effect of projected changes in winter streamflow on stream turbidity, Esopus Creek watershed in New York, USA: Hydrological Processes, v. 27, p. 3014–3023, doi:10.1002/hyp.9824.

NYC DEP, 2008, Evaluation of Turbidity Reduction Potential through Watershed Management in the Ashokan Basin.

NYC DEP, 2020, Modification of the Catalum SPDES Permit EIS.

NYC DEP, 2021, Upper Esopus Creek Watershed Turbidity/Suspended Sediment Monitoring Study: Biennial Status Report.

NYC DEP, 2022, Upper Esopus Creek Watershed Turbidity and Suspended Sediment Monitoring Study: Mid-Term Report.

R Core Team, 2020, R: A Language and Environment for Statistical Computing:, https://www.r-project.org/.

Siemion, J., McHale, M.R., and Davis, D., 2016, Suspended-Sediment and Turbidity Responses to Sediment and Turbidity Reduction Projects in the Beaver Kill, Stony Clove Creek, and Warner Creek Watersheds, New York, 2010 – 14 Scientific Investigations Report 2016 – 5157:, http://dx.doi.org/10.3133/sir20165157.

Stahl, M., 2022, Seasonality indices: Environmental applications:, https://stahlm.github.io/ENS_215/Winter_2022/Lectures/case_study_seasonality_indices.html.

Wang, K., Davis, D., and Steinschneider, S., 2021, Evaluating suspended sediment and turbidity reduction projects in a glacially conditioned catchment through dynamic regression and fluvial process-based modelling: Hydrological Processes, v. 35, doi:10.1002/hyp.14351.

4. Conclusions

4.1 THESIS SUMMARY

Elevated turbidity in surface waters poses a health risk to people who consume this water, especially in unfiltered systems such as the Catskills water supply system. Therefore, it is imperative to understand the turbidity conditions in affected water supply systems as well as the factors affecting turbidity to better inform watershed management and stream remediation efforts. Here, I used a case study of the Catskills to explore the turbidity and streamflow dynamics in this region. Before conducting these characterization steps, I first presented a conceptual framework to provide an overview of the factors and processes that can affect turbidity generation, and then I applied this conceptual framework to a case study of the Catskills. This framework was useful to inform the characterization of streamflow and turbidity in the Catskills due to the multitude of variables besides streamflow that can affect turbidity.

Next, performing the streamflow and turbidity characterization steps allowed for a broader understanding of the typical streamflow and turbidity conditions in the Catskills, as well as how the relationship between these two variables differs spatially and temporally. The results from this work show that there is a statistical and practical difference in mean streamflow and turbidity across sites in the Catskills, suggesting that there are various mechanisms that may be responsible for controlling these differences, such as factors like topography, land use, and stream remediation efforts. The results from this work also reveal the timings of when turbidity peaked seasonally in the Catskills, which occurred during the months of January through April across sites. These results have important implications for future climate change scenarios, as climate change will affect the timing of streamflow and thus turbidity. However, the results from

this research also demonstrate that streamflow alone cannot explain all of the variation in turbidity across sites in the Catskills, which requires further research to better understand how different factors (e.g., land cover, channel slope) affect turbidity dynamics. Lastly, after examining the effects on turbidity after the severe December 2020 flood, I found that there is a characteristic process in the Catskills that can describe this response. This process starts with a severe flood event (the December 2020 flood), which elevates turbidity above baseline conditions. Turbidity remains elevated until there is an intermediate flood event that can flush the erodible sediment deposits generated during the severe flood, which was shown by the effects of the March 2021 flood at several Catskill sites. The results from this thesis have critical importance for how water resource managers should address the issue of elevated turbidity in streams, particularly after extreme flooding events.

4.2 RESEARCH LIMITATIONS

Addressing the limitations of this research is important to guide future work on turbidity characterization in the Catskills. Firstly, in my research, although I visited some of the Catskill monitoring sites (e.g., Panther Kill), I was unable to visit all of the sites. This aspect of the project affected my ability to fully understand the physical characteristics of the Catskill sites, such as the frequency of mass wasting events, the topography near the stream gage at each site, and so on. Visiting more of the sites would have been beneficial for me to better interpret the results obtained from this study. Another limitation of my research was that the data available for all of the 20 monitoring sites in the Catskills does not consistently overlap through time. The data on turbidity and streamflow was sparser during the earlier years examined during this study period, from around 2010 to 2015. Although I tried to account for the discrepancies in data

availability at each site by often constricting the data to only include more than 350 observations in a given year at each site, sometimes this approach was not feasible to implement at certain sites, such as at Panther Kill, which only has approximately two years of data. Gap filling the data on turbidity was beyond the scope of this study.

More broadly, another limitation of this research pertains to the complexity of the turbidity problem, which posed a significant challenge in this study. There are many variables that can affect turbidity (e.g., streamflow, channel geometry, basin slope, precipitation, air temperature, ice cover, human disturbance,…), so it was challenging to account for all of these variables when interpreting the turbidity data. Moreover, it was difficult to attribute variation in turbidity to specific variables, such as land cover change, channel slope, et cetera. Obtaining data on some of these variables (e.g., human disturbance) also poses a challenge as they cannot be easily or directly measured. Thus, this limitation of my research highlights the importance of encouraging collaboration among researchers actively addressing the turbidity problem in the Catskills in order to narrow some of these uncertainties in addressing the problem.

4.3 RECOMMENDATIONS AND FUTURE RESEARCH

4.3.1 Recommendations

Considering the results of this research, I will briefly discuss some of my recommendations for actions that should be taken to address the turbidity problem in the Catskills. Firstly, turbidity was shown to peak during the months of January through April in the Catskills, which suggests that earlier spring snow melt events may affect the streamflow and thus the turbidity dynamics in the Catskills. Therefore, continued and consistent monitoring of turbidity and streamflow at Catskill sites is necessary to understand how the timings of

streamflow and turbidity may change in the context of climate change. Although there has been significant work conducted to evaluate the effectiveness of STRPs in the Catskills (e.g., Wang et al., 2021), it is imperative to continue this type of work due to the uncertainties that currently exist (and which will likely persist into the future) in terms of turbidity conditions in the Catskills. Furthermore, to address the turbidity problem more holistically in the Catskills, there needs to be more collaboration among resource managers, researchers in academia, engineers conducting stream remediation efforts, and relevant stakeholders. Encouraging these types of collaboration will help to better address the issue because individuals and groups can share ideas on new findings related to the problem. I hope to have the opportunity to share this thesis with researchers and resource managers at the NYC DEP and the USGS so they can review these findings and see how we can try to fill some of these knowledge gaps. My results and their subject matter knowledge on the issue of turbidity in the Catskills may give rise to interesting findings that can help to further address this important issue.

4.3.2 Future Research

This study has investigated the turbidity and streamflow dynamics in the Catskills region, but future work is required to better understand the turbidity problem in this study area. The streamflow-turbidity relationship needs further examination, particularly for how this relationship changes spatially and temporally in the Catskills. A better understanding of the seasonality of the streamflow-turbidity relationship in the Catskills is also necessary in the context of climate change, which will likely affect this relationship.

I plan to continue this research to investigate the effects of other variables besides streamflow on turbidity generation. This work entails obtaining raster data on variables such as

land cover, source material, channel slope, precipitation, and temperature throughout the Catskills during the study period analyzed in this thesis. To accomplish this, I have begun to use the climateR package in R to access point and gridded climate data. This package has been useful to obtain these data, as I can simply construct a call to a particular data set of interest and obtain the parameters and dates of choice. Furthermore, I plan to use the whitebox package in R to conduct geospatial analysis. I can perform common GIS analysis operations, such as terrain analysis, which may help to explain the variation in turbidity in the Catskills. I can also use the elevatr package in R to obtain the DEMs for each site (Figure 1).

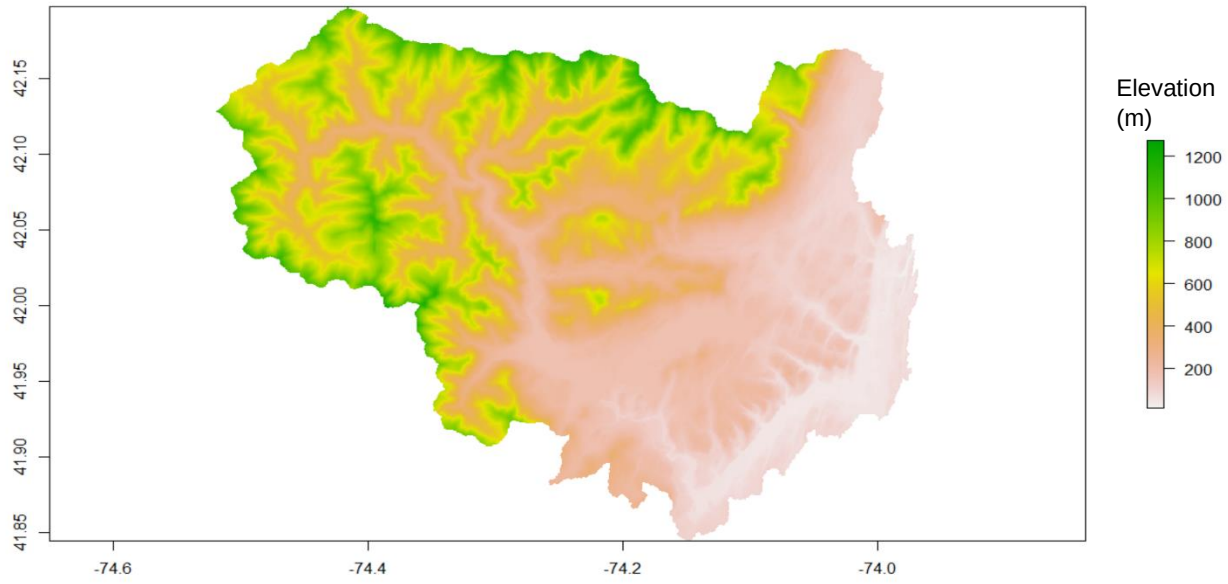

Figure 1. DEM of the Catskills region. Elevation units are in meters. Future work will involve obtaining the individual DEMs of the watersheds delineated for each site, as well as obtaining the river networks throughout the Catskills.

Other packages in R that may be useful to perform the spatial analysis include rivnet and nhdplusTools. Once I obtain the necessary data, I plan to address two research questions:

1. What environmental or climatic variables are most responsible for turbidity generation in the Catskills?

2. Are there certain monitoring sites that are similar to one another in terms of their turbidity characteristics? Why are they similar or dissimilar?

Addressing these questions will be imperative to better understand the results from my thesis thus far, particularly the turbidity dynamics. To answer these questions, I will use two machine learning (ML) approaches, which are Random Forest (RF) models and K-means clustering. The RF model can be used to address regression or classification problems (Boehmke, 2019). The RF model is a supervised ML algorithm (having a predefined target variable) that builds decision trees on different samples by taking the majority vote for the classification. RF models are created on subsets of the data, which are used to construct the decision trees. RF models use bagging as the ensemble method, which splits the data into training and test subsets. Each model is trained independently, which generates results. The final output is determined by majority voting from combining the results from all of the models. RF models are advantageous to decision trees because they address the problem of overfitting, which occurs when the ML model gives accurate predictions for the training data but not the test data set (Boehmke, 2019). The RF model here will be used to determine which environmental variables are most important in generating turbidity; this is possible because the RF model ranks the feature variables by their importance in determining the target variable, here, turbidity. I plan to use the following variables as feature/predictor variables in the RF model: streamflow, grain size/source material, land cover, stream channel slope, basin slope, precipitation, and temperature.

The second question can be addressed using clustering methods, specifically the method of *k*-means clustering. *K*-means clustering assigns each data point to a group, where data points slowly get clustered into *k* groups (clusters) based on similar features (Boehmke, 2019). This

approach will be useful to characterize which stream monitoring sites are similar to one another, such as which physical characteristics of the streams are generating similar results in turbidity.

Finally, I plan to investigate how stream power (one predictor of channel form and dynamics) differs at various reaches in the Catskills. This may provide insights into how the physical characteristics at each site differ from one another, which is important to consider in the context of turbidity characterization.

4.4 References

Boehmke B. Hands-On Machine Learning with R. Boca Raton, FL: CRC Press; 2019.

Wang, K., Davis, D., and Steinschneider, S., 2021, Evaluating suspended sediment and turbidity reduction projects in a glacially conditioned catchment through dynamic regression and fluvial process-based modelling: Hydrological Processes, v. 35, doi:10.1002/hyp.14351.